



Application de l'analyse quantitative des images au cyto-diagnostic des cancers du col de l'utérus

Anna Kulker

► To cite this version:

Anna Kulker. Application de l'analyse quantitative des images au cyto-diagnostic des cancers du col de l'utérus. Modélisation et simulation. Université Joseph-Fourier - Grenoble I, 1986. Français. NNT: . tel-00321543

HAL Id: tel-00321543

<https://theses.hal.science/tel-00321543>

Submitted on 15 Sep 2008

HAL is a multi-disciplinary open access archive for the deposit and dissemination of scientific research documents, whether they are published or not. The documents may come from teaching and research institutions in France or abroad, or from public or private research centers.

L'archive ouverte pluridisciplinaire **HAL**, est destinée au dépôt et à la diffusion de documents scientifiques de niveau recherche, publiés ou non, émanant des établissements d'enseignement et de recherche français ou étrangers, des laboratoires publics ou privés.

THESE

Présentée à

**L' UNIVERSITE SCIENTIFIQUE, TECHNOLOGIQUE
ET MEDICALE DE GRENOBLE**

pour obtenir le titre de
docteur de l' Université Scientifique, Technologique
et Médicale de Grenoble

BIOLOGIE

par

KULKER Anna épouse VAN DRIEL

o

**APPLICATION DE L' ANALYSE QUANTITATIVE DES IMAGES
AU CYTO-DIAGNOSTIC DES CANCERS DU COL DE L' UTERUS**

OOOOO

Thèse soutenue le 15 décembre 1986 devant la commission d' examen

J.S. PLOEM

Président

G. BRUGAL

J.M. CHASSERY

P. CHIBON

C. DA LAGE

F. MEYER

Examineurs

UNIVERSITE SCIENTIFIQUE ET MEDICALE DE GRENOBLE

Année universitaire 1986-1987

President de l'Université : M.Tanche

MEMBRES DU CORPS ENSEIGNANT DE SCIENCES ET DE GEOGRAPHIE

PROFESSEURS DE 1ère CLASSE

ARNOUD Paul	Chimie organique
ARVIEU Robert	Physique nucléaire I.S.N.
AUBERT Guy	Physique C.N.R.S.
AURIAULT Jean-Louis	Mécanique
AYANT Yves	Physique approfondie
BARBIER Marie-Jeanne	Electrochimie
BARBIER Jean-Claude	Physique expérimentale C.N.R.S.
BARJON Robert	Physique nucléaire I.S.N.
BARNOUD Fernand	Biochimie macromoléculaire végétale
BARRA Jean-René	Statistiques-Mathématiques appliquées
BELORISKY Elie	Physique C.E.N.G.-D.R.F.
BENZAKEN Claude	Mathématiques pures
BERNARD Alain	Mathématiques pures
BERTRANDIAS Françoise	Mathématiques pures
BERTRANDIAS Jean-Paul	Mathématiques pures
BILLET Jean	Géographie
BOEHLER Jean-Paul	Mécanique
BONNIER Jean-Marie	Chimie générale
BOUCHEZ Robert	Physique nucléaire I.S.N.
BRAVARD Yves	Géographie
CARLIER Georges	Biologie végétale
CAUQUIS Georges	Chimie organique
CHIBON Pierre	Biologie animale
COHEN ADDAD Jean-Pierre	Physique
COLIN DE VERDIERE Yves	Mathématiques pures
CYROT Michel	Physique du solide
DEBELMAS Jacques	Géologie générale
DEGRANGE Charles	Zoologie
DELOBEL Claude	Mathématiques appliquées
DEPORTES Charles	Chimie minérale
DESRE Pierre	Electrochimie
DOLIQUE Jean-Michel	Physique des plasmas
DOUCE Rolland	Physiologie végétale
DUCROS Pierre	Cristallographie
FONTAINE Jean-Marc	Mathématiques pures
GAGNAIRE Didier	Chimie physique
GERMAIN Jean-Pierre	Mécanique
GIRAUD Pierre	Géologie
HICTER Pierre	Chimie
IDELMAN Simon	Physiologie animale
JANIN Bernard	Géographie
JOLY Jean-René	Mathématiques pures
KAHANE André, détaché	Physique
KAHANE Josette	Physique

. IV .

KRAKOWIAK Sacha	Mathématiques appliquées
KUPKA Yvon	Mathématiques pures
LAJZEROWICZ Jeannine	Physique
LAJZEROWICZ Joseph	Physique
LAURENT Pierre-Jean	Mathématiques appliquées
DE LEIRIES Joël	Biologie
LLIBOUTRY Louis	Géophysique
LOISEAUX Jean-Marie	Sciences nucléaires I.S.N.
MACHE Régis	Physiologie végétale
MAYNARD Roger	Physique du solide
MICHEL Robert	Minéralogie et Pétrographie (Géologie)
OMONT Alain	Astrophysique
OZENDA Paul	Botanique (Biologie végétale)
PAYAN Jean-Jacques	Mathématiques pures
PEBAY PEYROULA J. Claude	Physique
PERRIAUX Jacques	Géologie
PERRIER Guy	Géophysique
PIERRARD Jean-Marie	Mécanique
PIERRE Jean-Louis	Chimie organique
RASSAT André	Chimie systématique
RENARD Michel	Thermodynamique
RINAUDO Marquerite	Chimie CERMAV
ROSSI André	Biologie
SAKAROVITCH Michel	Mathématiques appliquées
SAXOD Raimard	Biologie animale
SENGEL Philippe	Biologie animale
SERGERAERT Francis	Mathématiques pures
SOUCHIER Bernard	Biologie
SOUTIF Michel	Physique
STUTZ Pierre	Mécanique
VALENTIN Jacques	Physique nucléaire I.S.N.
VAN CUTSEN Bernard	Mathématiques appliquées
VIALON Pierre	Géologie

PROFESSEURS DE 2ème CLASSE

ADIBA Michel	Mathématiques pures
ANTOINE Pierre	Géologie
ARMAND Gilbert	Géographie
BARET Paul	Chimie
BECKER Pierre	Physique
BEGUIN Claude	Chimie organique
BLANCHI Jean-Pierre	STAPS
BOITET Christian	Mathématiques appliquées
BORNAREL Jean	Physique
BRUANDET Jean-François	Physique
BRUN Gilbert	Biologie
CASTAING Bernard	Physique
CERFF Rudiger	Biologie
CHARDON Michel	Géographie
CHIARAMELLA Yves	Mathématiques appliquées
COURT Jean	Chimie
DEMAILLY Jean-Pierre	Mathématiques pures
DENEUVILLE Alain	Physique
DEPASSEL Roger	Mécanique des fluides
DERRIEN Jacques	Physique
DUFRESNOY Alain	Mathématiques pures

GASPARD François	Physique
GAUTRON René	Chimie
GENIES Eugène	Chimie
GIDON Maurice	Géologie
GIGNOUX Claude	Sciences nucléaires
GILLARD Roland	Mathématiques pures
GIORNI Alain	Sciences nucléaires
GUIGO Maryse	Géographie
GUMUCHIAN Hervé	Géographie
GUITTON Jacques	Chimie
HACQUES Gérard	Mathématiques appliquées
HERBIN Jacky	Géographie
HERAULT Jeanny	Physique
JARDON Pierre	Chimie
JOSELEAU Jean-Paul	Biochimie
KERCKHOVE Claude	Géologie
LEBRETON Alain	Mathématiques appliquées
LONGEQUEUE Nicole	Sciences nucléaires I.S.N.
LUCAS Robert	Physique
LUNA Domingo	Mathématiques pures
MANDARON Paul	Biologie
MARTINEZ Francis	Mathématiques appliquées
MASCLE Georges	Géologie
NEMOZ Alain	Thermodynamique CNRS-CRTBT
OUDET Bruno	Mathématiques appliquées
PELMONT Jean	Biochimie
PERRIN Claude	Sciences nucléaires I.S.N.
PFISTER Jean-Claude	Physique du solide
PIBOULE Michel	Géologie
RAYNAUD Hervé	Mathématiques appliquées
RIEDTMANN Christine	Mathématiques pures
ROBERT Gilles	Mathématiques pures
ROBERT Jean-Bernard	Chimie physique
SARROT-REYNAULD Jean	Géologie
SAYETAT Françoise	Physique
SERVE Denis	Chimie
STOECKEL Frédéric	Physique
SOUTIF Jeanne	Physique
SCHOLL Pierre-Claude	Mathématiques appliquées
SUBRA Robert	Chimie
VALLADE Marcel	Physique
VIDAL Michel	Chimie organique
VIVIAN Robert	Géographie
VOTTERO Philippe	Chimie

MEMBRES DU CORPS ENSEIGNANT DE L'IUT 1

PROFESSEURS DE 1ère CLASSE

BUISSON Roger	Physique IUT 1
DODU Jacques	Mécanique appliquée IUT 1
NEGRE Robert	Génie Civil IUT 1

PROFESSEURS DE 2ème CLASSE

BOUTHINON Michel	EEA. IUT 1
------------------	------------

.VI.

CHAMBON René	Génie mécanique IUT 1
CHEHIKIAN Alain	EEA. IUT 1
CHENAVAS Jean	Physique IUT 1
CHOUTEAU Gérard	Physique IUT 1
CONTE René	Physique IUT 1
GOSSE Jean-Pierre	EEA UIT 1
GROS Yves	Physique IUT 1
KUHN Gérard, détaché	Physique IUT 1
MAZUER Jean	Physique IUT 1
MICHOULIER Jean	Physique IUT 1
MONLLOR Christian	EEA IUT 1
NOUGARET Marcel	Automatique IUT 1
PEFFEN René	Métallurgie IUT
PERARD Jacques	EEA IUT 1
PERRAUD Robert	Chimie IUT 1
TERRIEZ Jean-Michel	Génie mécanique IUT 1
TOUZAIN Philippe	Chimie IUT 1
VINCENDON Marc	CHIMIE IUT 1

MEMBRES DU CORPS ENSEIGNANT DE MEDECINE

PROFESSEURS CLASSE EXCEPTIONNELLE ET 1ère CLASSE

AMBLARD Pierre	Dermatologie	C.H.R.G.
AMBROISE-THOMAS Pierre	Parasitologie	C.H.R.G.
BEAUDOING André	Pédiatrie-Puériculture	C.H.R.G.
BEZEZ Henri	Orthopédie-Traumatologie	HOPITAL SUD
BONNET Jean-Louis	Ophtalmologie	C.H.R.G.
BOUCHET Yves	Anatomie	FACULTE LA MERCI
	Chirurgie générale et digestive	C.H.R.G.
BUTEL Jean	Orthopédie-Traumatologie	C.H.R.G.
CHAMPETIER Jean	Anatomie topographique et appliquée	C.H.R.G.
CHARACHON Robert	O.R.L.	C.H.R.G.
COUDERC Pierre	Anatomie pathologique	C.H.R.G.
DELORMAS Pierre	Pneumophtisiologie	C.H.R.G.
DENIS Bernard	Cardiologie	C.H.R.G.
GAVEND Michel	Pharmacologie	FACULTE LA MERCI
HOLLARD Daniel	Hématologie	C.H.R.G.
LATREILLE René	Chirurgie thoracique et cardiovasculaire	C.H.R.G.
LE NOC Pierre	Bactériologie-Virologie	FACULTE LA MERCI
MALINAS Yves	Gynécologie-Obstétrique	C.H.R.G.
MALLION Jean-Michel	Médecine du travail	C.H.R.G.
MICOUD Max	Clinique médicale et Maladies infectieuses	C.H.R.G.
MOURIQUAND Claude	Histologie	FACULTE LA MERCI
PARAMELLE Bernard	Pneumologie	C.H.R.G.
PERRET Jean	Neurologie	C.H.R.G.
RACHAIL Michel	Hépto-Gastro-Entérologie	C.H.R.G.
DE ROUGEMONT Jacques	Neurochirurgie	C.H.R.G.
SARRAZIN Roger	Clinique chirurgicale	C.H.R.G.
STIEGLITZ Paul	Anesthésiologie	C.H.R.G.

.VII.

TANCHE Maurice	Physiologie	FACULTE LA MERCI
VERAIN André	Biophysique	FACULTE LA MERCI
VIGNAIS Pierre	Biochimie	FACULTE LA MERCI

PROFESSEURS DE 2^{ème} CLASSE

BACHELOT Yvan	Endocrinologie	C.H.R.G.
BARGE Michel	Neurochirurgie	C.H.R.G.
BENABID Alim, Louis	Biophysique	FACULTE LA MERCI
BENSA Jean-Claude	Immunologie	HOPITAL SUD
BERNARD Pierre	Gynécologie-Obstétrique	C.H.R.G. Pavillon CANEL
BESSARD Germain	Pharmacologie	ABIDJAN
BOLLA Michel	Radiothérapie	C.H.R.G.
BOST Michel	Pédiatrie	C.H.R.G.
BOUCHARLAT Jacques	Psychiatrie adultes	HOPITAL SUD
BRAMBILLA Christian	Pneumologie	C.H.R.G.
CHAMBAZ Edmond	Biochimie	C.H.R.G.
CHIROUSSEL Jean-Paul	Anatomie-Neurochirurgie	C.H.R.G.
COLOMB Maurice	Immunologie	HOPITAL SUD
COMET Michel	Biophysique	FACULTE LA MERCI
CONTAMIN Charles	Chirurgie thoracique et cardiovasculaire	C.H.R.G.
CORDONNIER Daniel	Néphrologie	C.H.R.G.
COULOMB Max	Radiologie	C.H.R.G.
CROUZET Guy	Radiologie	C.H.R.G.
DEBRU Jean-Luc	Médecine interne et Toxicologie	C.H.R.G.
DEMONGEOT Jacques	Biostatistiques et Informatique médicale	FACULTE LA MERCI
DUPRE Alain	Chirurgie générale	C.H.R.G.
DYON Jean-François	Chirurgie infantile	C.H.R.G.
ETERRADOSSI Jacqueline	Physiologie	FACULTE LA MERCI
FAURE Claude	Anatomie et Organogénèse	C.H.R.G.
FAURE Gilbert	Urologie	C.H.R.G.
FOURNET Jacques	Hépto-Gastro-Entérologie	C.H.R.G.
FRANCO Alain	Médecine interne	C.H.R.G.
GIRARDET Pierre	Anesthésiologie	C.H.R.G.
GUIDICELLI Henri	Chirurgie générale et vasculaire	C.H.R.G.
GUIGNIER Michel	Thérapeutique et Réanimation médicale	C.H.R.G.
HADJIAN Arthur	Biochimie	FACULTE LA MERCI
HALAMI Serge	Endocrinologie et Maladies métaboliques	C.H.R.G.
HOSTEIN Jean	Hépto-Gastro-Entérologie	C.H.R.G.
HUGONOT Robert	Médecine interne	C.H.R.G.
JALBERT Pierre	Histologie-Cytogénétique	FACULTE LA MERCI
JUNIEN-LAVILLAULOY C.	O.R.L.	C.H.R.G.
KOLODIE Lucien	Hématologie biologique	C.H.R.G.
LETOUBLON Christian	Chirurgie générale	C.H.R.G.
MACHECOURT Jacques	Cardiologie et Maladies vasculaires	C.H.R.G.
MAGNIN Robert	Hygiène	C.H.R.G.
MASSOT Christian	Médecine interne	C.H.R.G.
MOUILLON Michel	Ophtalmologie	C.H.R.G.

.VIII.

PELLAT Jacques	Neurologie	C.H.R.G.
PHELIP Xavier	Rhumatologie	C.H.R.G.
RACINET Claude	Gynécologie	HOPITAL SUD
RAMBAUD Pierre	Pédiatrie	C.H.R.G.
RAPHAEL Bernard	Stomatologie	C.H.R.G.
SCHAEERER René	Cancérologie	C.H.R.G.
SEIGNEURIN Jean-Marie	Bactériologie-Virologie	FACULTE LA MERCI
SELE Bernard	Cytogénétique	FACULTE LA MERCI
SOTTO Jean-Jacques	Hématologie	C.H.R.G.
STOEBNER Pierre	Anatomie pathologique	C.H.R.G.
VROUSOS Constantin	Radiothérapie	C.H.R.G.

MEMBRES DU CORPS ENSEIGNANT PHARMACIE

AGNIUS-DELORE Claudine	Physique	FACULTE LA TRONCHE
ALARY Josette	Chimie analytique	FACULTE LA TRONCHE
BERIEL Hélène	Physiologie et Pharmacologie	FACULTE LA TRONCHE
BOUCHERLE André	Chimie et Toxicologie	FACULTE MEYLAN
CUSSAC Max	Chimie thérapeutique	FACULTE LA TRONCHE
DEMENGÉ Pierre	Pharmacodynamie	FACULTE LA TRONCHE
JEANNIN Charles	Pharmacie galénique	FACULTE MEYLAN
LATURAZE Jean	Biochimie	FACULTE LA TRONCHE
LUU DUC Cuong	Chimie générale	FACULTE LA TRONCHE
MARIOTTE Anne-Marie	Pharmacognosie	FACULTE LA TRONCHE
MARZIN Daniel	Toxicologie	FACULTE MEYLAN
RENAUDET Jacqueline	Bactériologie	FACULTE LA TRONCHE
ROCHAT Jacques	Hygiène en Hydrologie	FACULTE LA TRONCHE
SEIGLE-MURANDI F.	Botanique en Cryptochamie	FACULTE MEYLAN
VERAIN Alice	Pharmacie galénique	FACULTE MEYLAN

AVANT-PROPOS

Ce mémoire est le reflet des activités de recherche que j'ai conduites pendant les douze dernières années au sein du Département Cytochimie et Cytométrie à Leiden. Ces travaux sont le fruit d'une collaboration étroite avec mes collègues cytologistes, biologistes et informaticiens.

Ma reconnaissance la plus vive est adressée à J.S. PLOEM, qui m'a vraiment appris le métier de chercheur, pour la confiance qu'il m'a toujours témoignée et pour la création d'un cadre scientifique et matériel dans lequel il était très agréable de travailler et d'étudier. J'espère qu'il trouvera ici la concrétisation de nos réflexions communes. Sans sa forte stimulation avant et au cours de l'élaboration de ce mémoire, je n'aurais pu le conduire à son terme.

Qu'il me soit permis de dire combien j'ai apprécié de travailler avec G. BRUGAL. Je remercie très chaleureusement pour son enthousiasme et sa disponibilité pendant les périodes trop courtes où je pouvais travailler à Grenoble. Qu'il trouve ici l'expression de mon estime. Sa compétence et celle de son équipe ont certainement contribué à élargir mon point de vue sur le monde de la cytologie quantitative.

Je remercie très vivement F. MEYER de Fontainebleau qui n'a pas ménagé son temps pour m'apprendre les secrets de la morphologie mathématique. Sa compétence, dont il m'a fait souvent bénéficier, a fortement contribué au succès du projet. Pour la bonne coopération qu'on a eu pendant ces années, je lui adresse ma sincère reconnaissance.

Je remercie vivement C. DA LAGE et J.M. CHASSERY d'avoir accepté de s'intéresser à mon travail, de m'avoir fait profiter de leurs compétences et d'être membres de mon jury.

Je remercie P. CHIBON d'avoir consacré beaucoup de son temps pour faire accepter mon inscription au Nouveau Doctorat de l'Université de Grenoble et d'avoir accepté d'être membre du jury.

Je tiens à remercier très sincèrement J.J. PLOEM-ZAAYER pour sa grande disponibilité lors des nombreux entretiens qu'elle m'a accordés. Les conseils qu'elle m'a prodigués sans cesse au cours de ce travail m'ont été très précieux. Je la remercie très chaleureusement pour la coopération fructueuse et l'amitié qu'elle m'a témoignée pendant ces années.

De la même façon, je remercie L. GOYARTS-VELDSTRA. Grâce à son exactitude, grands nombres de cas ont pu être testés avec la machine. Sa présence à Grenoble pendant la soutenance est pour moi un grand honneur.

Il m'est très agréable de dire que j'ai travaillé avec beaucoup de plaisir durant ces années au Département de Cytochimie et Cytométrie. Que tous ceux qui ont contribué à créer cette bonne ambiance de travail soient sincèrement remerciés : W.E. MESKER, M.C.M. van VELZEN, C.F.H.M. KNEPFLE, M.J.M. van der BURG, H.J. TANKE, J.H. VROLIJK, N. VERWOERD, M. van der ZWAN, W.C.R. SLOOS, J. BONNET, J.C.M. SLATS. Je leur suis très reconnaissante pour toute l'aide qu'ils m'ont apportée lors de la réalisation de ce document.

.X.

Mes remerciements vont également à C.J. BAK et P. SOUILLARD (secrétariat) et Th. WAND (photographie) pour l'aide efficace qu'ils m'ont apportée dans la réalisation de ce document.

Finalement, je veux remercier mon mari P.J. van DRIEL pour l'intérêt qu'il a porté à mon travail et les encouragements qu'il m'a prodigués au cours de l'élaboration de ce mémoire. En plus de sa stimulation pendant la préparation de cette thèse, il a réalisé la partie statistique de cette étude.

SOMMAIRE / CONTENTS

Avant-propos.	
1. Preface.	1
2. Guidelines for automated cytology instruments.	5
2.1 An introduction.	7
3. Preparation and staining for automated cytology.	11
3.1 Introduction.	13
3.2 General aspects about preparation and staining.	14
3.3 Applied preparation methods.	19
3.4 Applied staining methods.	23
3.5 Quantitative evaluation of different staining procedures.	27
4. The Leyden Television Analysis System (LEYTAS).	31
4.1 Introduction.	33
4.2 Hardware.	34
4.2.1 The microscope system.	36
4.2.2 The image analysis system.	38
4.3 Software.	42
4.3.1 Selection of cells.	43
4.3.2 Rejection of artefacts.	47
4.3.3 Performance of different image analysis algorithms.	49
4.3.4 Total Cell Population Analysis (TCPA) program.	57
5. Automatically selected objects in cervical specimens.	59
5.1 Introduction.	61
5.2 Frequency of selected abnormal cells.	62
5.3 Frequency of selected alarms.	69
6. LEYTAS classification of cervical specimens.	75
6.1 Introduction.	77
6.2 Results in centrifuge preparations.	78
6.3 System reproducibility.	85
6.4 Results in conventional smears.	89
6.5 Classification results of TCPA program.	91
7. DNA measurements.	93
7.1 Introduction.	95
7.2 Measurement procedure with LEYTAS.	97
7.3 LEYTAS DNA histograms in cervical scrapes.	101
7.4 DNA as a parameter for screening in cervical cancer.	105
8. Nuclear texture information in automatically selected cervical cells.	109
8.1 Introduction.	111
8.2 Hardware of SAMBA.	112
8.3 Software of SAMBA.	113
8.4 Selection of cells.	114
8.5 Applied nuclear texture parameters.	116
8.6 Effect of nuclear parameters on specimen classification.	118
Literature.	123
Summary and conclusion.	137
Résumé et conclusions.	145

à mes parents
à Peter

Abstract.

In this thesis, a method will be presented to diagnose malignant and premalignant lesions of the cervix uteri on cervical scrape specimens using an automated screening device. The main aim was the development of a diagnostic method resulting in a higher sensitivity (lower false negative rate) than those reported by conventional cytodiagnosis (up to 25%). To enable automated image analysis, a centrifugation technique and a staining procedure (acriflavine-Feulgen-SITS, AFS) have been developed, to prepare cervical scrape specimens. This results in the separate visualization of nuclei and cytoplasm. The nuclear images are subsequently analyzed by the image analysis system.

The LEYden Television Analysis System (LEYTAS) is used for automated image analysis, which is performed using image transformations combined with conventional pixel processing. A total of 2063 cervical scrape specimens have been analyzed resulting in a false positive rate of 16% (or 11% when rapid human intervention is used) and a false negative rate (of specimens with a diagnosis of severe dysplasia or a more serious lesion) of 0.3% (1 out of 321). Furthermore 15.8% of the mildly dysplastic and 8.5% of the moderately dysplastic specimens have been negatively classified. A second program was tested for its screening capacities called the Total Cell Population Analysis (TCPA). With this program, a higher detection rate of dysplasia specimens was found when compared to the conventional screening program, thereby also decreasing the false positive rate. A pilot study of the automated analysis of conventional smears is also reported. The study encompasses 32 negative and 4 dysplastic smears and 1 positive smear. No overlap was found in the absolute and/or relative numbers of alarms when comparing the negative smears with the positive smear. One of the dysplasia smears showed numbers in the same range as the negative smear.

In the last two chapters, results are presented of the execution of measurements on LEYTAS preselected cell populations. Apart from DNA, several nuclear textural and densitometrical parameters have been applied using the SAMBA 200 system (SAMBA= System for Analytical Microscopy in Biomedical Applications). It could be demonstrated that cells selected in false positively classified (LEYTAS) preparations were significantly different from cells selected in true positively classified specimens regarding the investigated set of parameters. The parameter ranked first, proved to be the 'mean extinction'. It is concluded that application of nuclear parameters, as those incorporated in SAMBA, will result in a better separation between the positive and the negative specimens as presently obtained by LEYTAS.

keywords:

cervical cytology - image cytometry - automated image analysis - cervical cancer diagnosis - DNA measurements - nuclear texture.

Résumé

Ce mémoire de thèse présente une méthode de diagnostic des lésions pré-malignes du col de l'utérus, fondée sur l'utilisation d'un système automatique d'analyse des frottis cervico-vaginaux : le système LEYTAS (Leiden Television Analysis System). Afin de permettre l'analyse automatique, des méthodes de centrifugation et de coloration (acridine-Feulgen-SITS, AFS) ont été développées pour préparer des suspensions de cellules cervicales prélevées à l'aide d'un applicateur. L'utilisation de la coloration AFS permet la visualisation séparée des noyaux et des cytoplasmes grâce à la différence des propriétés spectrales de l'acridine-Feulgen et du SITS. Avec le système LEYTAS, seule l'image colorée par l'acridine est analysée. La plupart des méthodes d'analyse d'image utilisées dans cette étude sont fondées sur des transformations itératives. Une série de 2063 frottis a été analysée. Le taux de faux positifs dans cette série, incluant à la fois les négatifs et les spécimens inflammatoires, était de 16 %. La réduction de ce taux de faux positifs à 11 % a été possible par une interaction rapide entre un cytologiste et le système d'analyse. Le taux de faux négatifs, parmi les spécimens morphologiquement classés comme dysplasies sévères ou portant des lésions plus malignes, était de 0.3 %. Le taux des lames classées négatives dans le cas des dysplasies légères et modérées était 15.8 % et 8.5 % respectivement. Un deuxième programme a été testé comme programme de dépistage et désigné par le sigle TCPA (Total Cell Population Analysis). Dans une étude de faisabilité concernant 109 échantillons, un taux de détection plus élevé des dysplasies a été obtenu ainsi qu'un taux de faux positif plus bas. Une autre étude de faisabilité a été réalisée pour l'analyse automatique des frottis conventionnels. Au total, 37 cas ont été analysés et n'ont conduit à aucune confusion concernant le nombre absolu et le nombre relatif des alarmes entre les échantillons négatifs et 4 des 5 spécimens portant des dysplasies légères ou des lésions plus malignes. Les deux derniers chapitres présentent des résultats de mesures exécutées sur des cellules ayant un contenu élevé en ADN après sélection automatique par LEYTAS. En dehors de la mesure du contenu en ADN, plusieurs paramètres nucléaires ont été mesurés en utilisant le système SAMBA (System for Analytical Microscopy in Biomedical Applications). A l'aide de cet instrument, une étude a été entreprise pour tenter de discriminer, parmi les cellules ayant un contenu élevé en ADN, celles qui caractérisent les échantillons négatifs dysplasiques et positifs. Sur la base de cet apprentissage, tous les échantillons faux positifs obtenus après analyse par LEYTAS ont été correctement classés négatifs par SAMBA. En utilisant 7 paramètres, cette étude a permis de conclure que le taux actuel de faux positifs commis par le système LEYTAS peut être réduit fortement en utilisant des paramètres nucléaires tels que la densité optique moyenne et des paramètres de texture nucléaire.

Cytology de frottis cervico-vaginaux - cytométrie à balayage - analyse automatique d'images - diagnostic des cancers du col de l'utérus - mesure du contenu en ADN - texture nucléaire.

CHAPTER 1

PREFACE

Chapter 1

PREFACE

This thesis describes the application of an automated image analysis system (LEYden Television Analysis System, LEYTAS) to the diagnosis of cervical cancer in cervical scrape specimens.

In chapter 2, requirements for automated cytodiagnostic systems are described as they have been proposed by, among others, the International Academy of Cytology. During the past 10 years, priorities for automated systems changed, starting with a high demand for speed, towards the demand for a higher sensitivity of the screening test. Its rationales will be discussed.

One of the main problems for automated image analysis on cervical specimens proved to be the complex images as presented by the combination of the conventional smear technique with the Papanicolaou staining procedure. To overcome these difficulties, preparation and staining procedures have been developed, suited for automated image analysis. In chapter 3, some of these techniques, with their advantages and disadvantages, are discussed including a quantitative evaluation. The preparation and staining procedure developed for LEYTAS is described in detail.

In chapter 4, a description of LEYTAS is given as it has been optimized for cancer cell detection. First the hardware components and the applied image transformations and software algorithms are described. In chapter 4.3.3 the performance of these algorithms is evaluated with respect to their capability in selecting (abnormal) cells and rejecting artefacts. The remainder of this chapter describes the Total Cell Population Analysis (TCPA) program, which has been developed to categorize the entire cell population according to size and absorption.

Chapter 5 deals with the frequencies of LEYTAS selected cells using two different criteria and compares these frequencies to the number of visually counted abnormal cells as reported in the literature. It is shown that the frequency distributions obtained for the different diagnostic groups (negative, dysplasia and positive) are significantly different using the Kolmogorov Smirnov test. The last part of this chapter describes the frequencies of all selected objects (alarms) in the different diagnostic groups of specimens with regard to its suitability for final specimen classification.

Chapter 6 describes the classification results at the specimen level. The reproducibility of the system, when reanalyzing the same slide within different time intervals and when analyzing parallel slides of the same sample, is discussed in chapter 6.3. In chapter 6.4, a pilot study is reported of LEYTAS analysis of conventional smears. The remainder of this chapter describes specimen classification results which have been obtained using the TCPA program on centrifugation preparations.

Using the cell selection capacities of LEYTAS in combination with a measurement program for integrated optical densities (IOD), the nuclear DNA content of preselected cell populations can be estimated as shown in chapter 7. Apart from stemline determination of the tumor, LEYTAS DNA histograms can be used for the assessment of infrequently occurring cells with a high DNA content as shown in chapter 7.3. To estimate the representativity of the sample as well as the DNA parameter, a pilot study has been performed (chapter 7.4) on cell suspensions from cervical scrapes and from tumor biopsies from the same patient.

The last chapter, chapter 8, deals with the use of several nuclear textural and densitometric parameters on preselected cell populations. Since these types of measurements cannot be performed with LEYTAS so far, the System for Analytical Microscopy' in Biomedical Applications (SAMBA, Grenoble, France) has been used for this study. The influence of these nuclear

parameters on LEVTAS selected cells, is evaluated with respect to the specimen classification, using linear discriminant analysis.

CHAPTER 2

GUIDELINES FOR AUTOMATED CYTOLOGY INSTRUMENTS

Chapter 2.1 AN INTRODUCTION.

About 10 years ago, the desire to detect and treat all precancerous and cancerous lesions of the cervix uteri, was initiated by the western civilized world and stimulated by the upcoming women liberation societies. At that time unemployment was not yet considered a major economical problem, and the execution of a mass screening program was mainly hampered by the lack of sufficiently trained cytotechnicians. The quality of visual screening was not as well investigated as nowadays and the only demand was the development of a system which could do the screening with an equivalent accuracy as a cytotechnician but much faster.

In that period, developments in cytology automation often took place in large research laboratories where a high level of computer technology was already available, resulting from e.g. atomic energy research (Fowlkes et al, 1976; Jensen et al, 1977; Golden et al, 1979). Physicists and engineers decided to apply their knowledge to technology and computer science in biomedical applications such as the automatic recognition of cells, chromosomes and tissues. The lack of biomedical input in these projects, partly caused by the nature of the institutes and partly by the fact that cytopathologists then had little experience in quantitative cytology, constituted a severe drawback to success. Furthermore, the instruments in that period had a relatively bad price versus performance ratio. Based on the results of these early efforts and the quality control reports of conventional cytology screening in the literature (Husain et al, 1974; Evans et al, 1974), requirements for automated cytology systems became more exactly defined.

The quality of a screening test is expressed in terms of sensitivity, specificity and predictive value (Sturmans et al, 1976). The definitions of these terms are summarized in table 2.1.

Table 2.1: The explanation of terminology used to express the quality of a screening test.

	Abnormality present	Abnormality not present
test positive	a	b
test negative	c	d

test positives = $a+b$
 test negatives = $c+d$
 false positives = b
 false positive rate (FPR) = $b/(b+d) \times 100$
 false negatives = c
 false negative rate (FNR) = $c/(a+c) \times 100$
 sensitivity = $a/(a+c)$
 specificity = $d/(b+d)$
 predictive value = $a/(a+b) \times 100$

The sensitivity of a screening test is defined as the proportion of positive tests from all investigated abnormal cases. The specificity is the proportion of negative tests from all investigated cases without abnormality. The predictive value of a positive test is defined as the proportion of truly positive cases from all positively classified cases.

During the last fifteen years, several certified cytology laboratories investigated their false negative errors in conventional screening. A recent study carried out in the Mayo Clinic (Rochester, Minnesota, USA, Gay et al, 1984), shows a false negative rate of 19.4%. The majority of the false negative cases (62%) represented sample errors. The remainder of the false negatives were attributed to screening failure (15%) or interpretation error (23%). This means that in 7.5% of the positive cases (carcinoma in situ and more severe lesions), abnormal cells were present in the cervical smear but were either not found during the routine screening or not interpreted as such. Other studies report similar findings. Husain et al (Husain et al, 1974) publish a false negative rate (of severe dysplasia, carcinoma in situ and invasive carcinoma) of 14.9%; in 36% of these (total of 5.4%), abnormal cells could be found in the smear after rescreening. False negative rates from the cytological institute of BKG (Bayerischen Krebsgesellschaft, Munich, West Germany) are reported to amount to 15-20% in a population screening (Blomberg, 1979). The false negative rate in this institute has been subdivided in the following categories: 7-10% for the invasive carcinomas, 13-20% for the carcinoma in situ lesions and 20-34% for the mild and moderate dysplasias. False positive rates reported by this institute vary from 0.1% for invasive carcinoma diagnoses to 0.5% for carcinoma in situ and dysplasia specimens.

Recognition of these high false negative rates in certified cytology laboratories, caused a shift in the machine requirements; accuracy became more important than speed. In a report published in 1979 with support of the German government (Blomberg et al, 1979), the maximum false negative error of any machine is restricted to 2%. The International Academy of Cytology (IAC) even describes the false negative limits as: "the system shall not be designed or constructed as to pass as negative any sample which contains malignant tumor cells" (Rosenthal, 1984). Other mandatory conditions prescribed by the IAC for an automatic system are:

- the system shall not flag more 'false alarms' on normal cells than could readily be handled by visual manual review.
- the system shall not use up the entire sample or render the sample unusable for classical microscopic review. The pathologist must be able to examine the sample after routine staining.
- the system shall yield reproducible results on repeated scanings of the same sample (within appropriate confidence limits).
- the system shall have an internal calibration standard for quality control.

Striking in this list of requirements is the fact that no demands are put on the speed of the system as well as on the false positive rate but that a 0% missed positive rate is demanded. This confirms the previous statement that reduction of the false negative rate has become the major issue in automation of cervical screening. On the other hand, one of the 'highly desirable features' of the system as defined by the IAC is: the system should operate cost-effectively. This demand is strongly related to a limited false positive rate. In this respect it should be realised that, when using an automated system, all positively classified slides (including the false positively classified ones) must be re-examined by visual screening to ensure a correct diagnosis. Since the cytotechnologist will be alerted that the specimen may contain abnormal cells, the time needed to rescreen a false positively classified specimen, will be much longer than the time required in normal routine screening. Consequently, an automated system must give a relatively low false positive rate to be economically attractive. Furthermore, the demand for a 0% false negative rate will be unattainable when also a limited number of false positives is required. There will always be a trade-off between the false positive and the false negative rate on both the cell and

the specimen classifier, as has been demonstrated by Castleman and White (Castleman and White, 1980). Another problem which coincides with the demand for such extreme machine false negative rates will be the prove of such a performance, since there exists at present no other reference diagnosis than the cytological or the histological one. Both are reported to lack the necessary reliability (Evans et al, 1974; Ringsted et al, 1978).

In our opinion the machine false negative rate should be as low as possible, certainly less than those of high quality laboratories. These severe restrictions have been used as a guideline during the development of the Leyden Television Analysis System (LEYTAS) as will be demonstrated in this thesis.

The potential advantages of an automatic screening procedure for cervical cancer would be:

1. Improvement of the reproducibility of the diagnostic procedure.
2. No fatigue problems and therefore a lower false negative rate.
3. Additional data on diagnosis and prognosis. Possibly a better relation to the biological behaviour of the lesion (progression or regression) can be obtained.
4. Prevention of interchange of patients during cytological evaluation by computer control.
5. Possibility of integrating the cytometric diagnoses in the automatic administration of the hospital, which facilitates the management of patients with respect to therapy and follow up as far as those tasks are becoming computer assisted.
6. Save of labour and cost.

Fifteen years ago, saving labour was considered an important argument in health care. However, by the ever increasing unemployment in Europe, this type of argument is no longer appreciated as positive. An improvement of the diagnostic procedure with respect to missed positive diagnoses remains valid and is even considered more important nowadays, as should be clear from the IAC list of mandatory conditions. When it comes to public health care, the high costs of false negative diagnoses have been recognized. Therefore, an improvement in the diagnostic procedure indirectly saves costs. For the community, the macro-economical advantages of the cost reduction (of treatment of patients with invasive cancers as a result of false negative diagnoses) have the main importance. For the individual patient however, a correct diagnosis is of direct vital interest. The reduction of false negative diagnoses limits the chance that a potentially present cancer is overlooked in an early stage of the disease when adequate treatment can still cure the patient.

Another advantage is the possibility to transfer a classification made by computers, to administration computers without human intervention. This enables an automatic chain, starting with a patient specimen provided with a machine-coded label to a written diagnosis which can be sent to the physician. Protection of private information is an important item to consider when constructing this chain. By the use of machine-coded labels, interchange of patients can be prevented. Last but not least, cytometry can provide prognostic indicators which are difficult or even impossible to obtain using visual cytomorphology. The efficiency of the diagnostic procedure can therefore be increased by deriving a larger amount of relevant information from one and the same sample. Indirectly this is also a cost-saving procedure, since the sampling process, often a costly and time consuming work, might lead to more and better diagnostic and/or prognostic data.

The price versus performance relation of the presently existing automation systems has until now prevented their use in routine laboratories. However,

in the past ten years, the price/performance ratio of microcomputers and computer memories, to be inserted in image analysis systems, has drastically improved. Extrapolation of these developments to the future, combined with all heretofore mentioned information, lead to the conclusion that integration of automatic procedures in cytology will be inevitable. Automated image analysis will certainly take its share from the mass production of microcomputers and computer memories.

CHAPTER 3

PREPARATION AND STAINING FOR AUTOMATED CYTOLOGY

Chapter 3.1 INTRODUCTION.

Soon after many research groups started to attack the problem of automated screening for cervical cancer, subgroups were formed in most centers to work especially in the field of preparation and staining (Bartels et al, 1974; Wheelless and Onderdonk, 1974; Bahr et al, 1978; Husain et al, 1978; Eason and Tucker, 1979; Otto et al, 1979; Rosenthal et al, 1979; Tanke et al, 1979; Wittekind et al, 1979; van Driel-Kulker et al, 1980; Schenk et al, 1981; Montana et al, 1982; Oud et al, 1984). This was no coincidence. The level of image analysis in that starting period could certainly not cope with the problems of overlapping nuclei, dirty background, different focus levels etc that routine cervical smears normally contain. Also in Leiden, we developed a preparation and staining procedure. In the first part of this chapter (3.2), the general aspects of preparation and staining for automated cytology will be discussed, followed by the preparation methods (chapter 3.3) and staining methods (chapter 3.4) which have been applied for this study. Finally, in chapter 3.5, the different staining procedures which have been tested by our group, will be compared quantitatively. Changes in staining intensity (fading) after storage over longer periods of time were investigated as well.

Chapter 3.2 GENERAL ASPECTS ABOUT PREPARATION AND STAINING.

Since the presently available machines are not as capable in the recognition of different cellular constituents as the human eye, automated analysis of cells demands additional preparation procedures as compared to techniques used in conventional cytology. Therefore procedures have been developed to reduce the number of overlapping cells and the varying thickness of preparations (Wheless and Onderdonk, 1974; Leif et al, 1975; Bahr et al, 1978; Eason and Tucker, 1979; Otto et al, 1979; Rosenthal et al, 1979; van Driel-Kulker et al, 1980; Montana et al, 1982; Oud et al, 1984). Two types of material will be discussed separately: fresh and paraffin embedded material.

Preparation of fresh material.

Most procedures are based on bringing the cell sample into a preservative solution consisting of a buffered salt solution with low concentrations of fixatives, antibiotics, antifungicides and sometimes mucolytic agents. Fixatives are added to inactivate the lytic enzymes. Generally this occurs at an ethanol concentration of 50% or higher. Since this will result in severe aggregation of cells, a 10 - 25% ethanol concentration is generally chosen. Antibiotics and antifungicides are added to prevent the growth of bacteria and fungi in the solution. The role of mucolytic agents is to lyse the mucus which can be present in high amounts in cervical specimens. The characteristics of this preservative solution are especially important if the cell suspension cannot be processed immediately as is often the case in cervical cytology programs. If cellular material is sent in by mail, the official mailing regulations should be followed concerning e.g. the ethanol concentration and the solution should be composed such that the cells can remain in the solution for about 3 to 5 days at room temperature.

Further steps in the preparation procedure include washing by centrifugation to remove mucus and change solutions, filtration and sedimentation techniques (Otto et al, 1979; Rosenthal et al, 1979) to remove leucocytes and mechanical (Wheless and Onderdonk, 1974; van Driel-Kulker et al, 1980; Oud et al, 1984) or chemical methods (Wheless and Onderdonk, 1974) to promote single cell frequency. When selecting a procedure to separate attaching cells, one should keep in mind that shape of nuclei and cytoplasm are of considerable importance if conventional cytomorphology should still be possible on the same preparations. Gentle treatment of cells in suspension is therefore of great importance and preservation of morphology should have priority, even when resulting methods are only of limited use in obtaining single cell suspensions.

Preparation of paraffin embedded tissue.

Traditionally image cytometry has always been carried out on fresh material such as smears, aspirations, scrapings of the tumor etc. For research applications however, difficulties often arise in obtaining fresh material especially when the procedure requires extra work from the hospital personel and when the protocol deviates from the routine protocol in the hospital. Therefore it would be a great advantage if single cells could be isolated from routinely prepared paraffin-embedded histological sections. Furthermore such a method would enable a retrospective study of archival material where the clinical outcome is already known. In our laboratory we apply a relatively simple technique to prepare monolayer specimens suitable for image analysis, from 50 um sections of paraffin-embedded tissue (chapter 3.3). This technique has been developed for flow cytometry (Hedley et al, 1983) and image cytometry (Mikuz et al, 1985) and has been adapted by us for use in automated image cytometry using centrifugation techniques (van Driel-Kulker et al, 1985).

Cell deposition.

To obtain preparations with cellular monolayers containing a defined number of cells, a combination of cell-counting and cell-deposition procedures is generally used. Especially when the smears are analyzed automatically, the cell concentration has to remain within restricted levels. Too few cells per microscope field can introduce problems with the mechanical focussing procedure. It also slows down the automatic process unnecessarily. On the other hand, too many cells will easily overlap resulting in an increase in objects mimicking abnormal cells. Cell counting may be performed with a hemacytometer (Eason and Tucker, 1979), a Coulter counter (Oud et al, 1984) or by measuring the light scatter of the cell suspension 'in situ' (Bahr et al, 1978; van Driel-Kulker et al, 1980).

The deposition of exfoliative cells onto the glass slide can be accomplished by smearing (Zahniser, 1979; Tanaka et al, 1981), by spreading a droplet of the cell suspension onto the slide (using sponges) (Oud et al, 1984) or by using centrifugation methods (Leif et al, 1975; van Driel-Kulker et al, 1980). The permanent attachment of cells to the glass is of utmost importance. This holds especially for cell suspensions from the cervix where abnormal cells may be present in very low numbers and where many microscope slides are often stained simultaneously in one staining bath. Precautions should be taken to prevent cross contamination of cells. Besides the reason to enhance cell attachment, centrifugation can be used to flatten the cells and to deposit the cells on a fixed location. For the cell deposition method, as for the entire preparation procedure applies, that great care should be taken to avoid cell loss and cellular cross contamination. The binding of cells to the glass should be artificially enhanced especially if the cells are in a prefixed condition induced by an ethanol containing preservative solution. For unfixed cells usually lower G forces are used then for prefixed cells. The bucket by Leif (Leif et al, 1975) allows addition of the fixative to the cells during centrifugation. To intensify the cell binding, microscope slides can be charged positive by protein treatment (e.g. poly-L-lysine coating (Mazia et al, 1975; Watts et al, 1984)), so that the negatively charged cells will adhere better to the glass.

DNA reference cells.

To enable the measurement of DNA, a reference cell is needed which has a fixed and known DNA content. The most simple way which is also prescribed in literature (Hiddemann et al, 1984), is to use an internal standard cell e.g. a lymphocyte or a normal epithelial cell. In exfoliative cytology however, a large part of the sample often shows degenerative changes, which makes it difficult to use internal cells as DNA reference cells. In flow cytometry, the use of chicken and trout erythrocytes are generally used as external standard cells (Vindelov et al, 1983). These cells can also be used for image analysis. It should be realized however that these cells are relatively small and compact. For flow cytometry, where fluorescence is used, these factors do not disturb accurate measurements. For image analysis however, the accuracy is limited. It would be better to use cells which are comparable in size and compactness with normal intermediate cells e.g. rat liver cells. Although we are still working on this subject, we have not yet been able to develop a practical preparation procedure by which liver cells can be measured accurately and reproducibly. For that reason, trout erythrocytes have been used as the reference value for the results given in chapter 7. The theoretical relationship between the DNA content of the trout cell and of the human diploid cell is 8 : 10. Differences in the fixation and staining method can slightly alter this relation.

Staining procedures.

Concerning the choice of staining procedure for automated cytology, many different opinions and philosophies exist. Through the years this has resulted in the development of many different cytochemical and cytomorphological staining procedures (Papanicolaou, 1945; Husain et al, 1978; Tanke et al, 1979; Mayall, 1969; Husain and Watts, 1984; Zahniser et al, 1979, Feulgen and Rossenbeck, 1924). Basically 2 types of methods have been developed:

- those optimized for the machine
- those optimized for cytomorphology

Staining methods which have been developed to match machine requirements, generally are composed of cytochemical dyes with quantitative properties with respect to nucleic acids. Among these are the pararosaniline-Feulgen (Feulgen and Rossenbeck, 1924), thionine-Feulgen-Congo-red (Zahniser, 1979), acriflavine-Feulgen SITS (Tanke et al, 1979), and gallocyanine (Mayall, 1969; Husain and Watts, 1984).

The Feulgen reaction using pararosaniline-S02 is one of the most reliable methods in quantitative cytochemistry and has been studied in great detail (Duyndam, 1975). The absorption maximum for pararosaniline lies at 573 nm. For this reason the stain is often used for systems of which the input device is sensitive for green light, as is the case with some video cameras and photomultipliers (Brugal et al, in press).

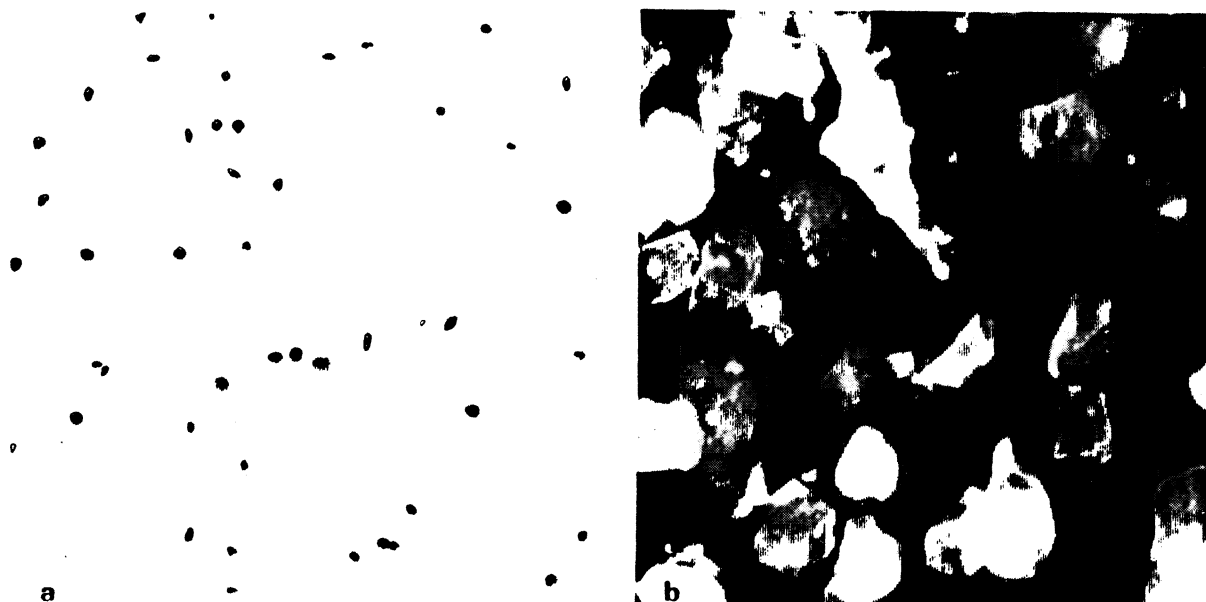


Figure 1a and b: Same microscopical image. Figure 1a displays the absorption image of acriflavine-Feulgen. Figure 1b displays the fluorescence of SITS after ultra violet excitation.

Thionine-Feulgen-Congo-red (TCR, Zahniser, 1979) and acriflavine-Feulgen SITS (AFS, Tanke et al, 1979) are examples of staining procedures which contain 2 different dyes; one quantitative dye which stains DNA according the Feulgen reaction, and a second dye for demonstrating cellular protein. In the AFS the two dyes can be visualized separately using the different spectral properties. (absorption maximum of acriflavine is 466 nm and of SITS is 365 nm). With LEYTAS (the system for which this staining has been developed) only the acriflavine image is analysed at its optimal wavelength of 466 nm. At this wavelength SITS absorbs no light and the quantitative properties of acriflavine can be fully explored (figure 1a and 1b). Acriflavine-Feulgen has

been preferred to pararosaniline-Feulgen for LEYTAS because the used Plumbicon TV camera is more sensitive for blue light than for green light. The TCR staining has been developed for the BioPEPR system (Zahniser, 1979) and consists of thionine-Feulgen, a quantitative DNA stain, and Congo-red which stains the cytoplasm. Thionine and Congo-red have absorption maxima at 600 and 500 nm respectively. Measurements are made between these two maxima at a wavelength of 545 nm. The advantage of this being the simultaneous analysis of nucleus and cytoplasm in one image. The disadvantage is that the stoichiometric properties of thionine are lost.

The galloxyaniline method is a cytochemical staining procedure suitable for DNA quantitation. It stains all nucleic acids (including DNA and RNA) (Pearse, 1980). When DNA should be demonstrated exclusively, the staining is preceded by RNase or HCL treatment to avoid unwanted staining of RNA. Spectral properties are similar to the Schiff.

All four staining procedures should be considered as machine-optimized stains of which the obtained image cannot be interpreted by cytotechnologists without more or less intensive retraining.

Since the staining procedure according to Papanicolaou is the only generally accepted staining in cervical cytology, procedures belonging to the second category should offer Papanicolaou resembling images. The advantage of these type of procedures is that the same slide as is used for image analysis, can be used for cytomorphology. The disadvantage is that the Pap is not a quantitative cytochemical staining procedure. Therefore the resulting images are not very reproducible; e.g. Bartels et al (Bartels et al, 1974) found that the cell to cell variation was about 20% under standardized staining conditions while measuring cyanophilic cells only. Efforts have been undertaken to improve the reproducibility of the stain by the use of purified dyes (Wittekind et al, 1979). Measurements of large numbers of cells and specimens should be carried out to show the increase in reproducibility compared to the conventional Papanicolaou.

By the same German group (Wittekind, 1985) a standardized Romanovsky Giemsa stain has been developed for application in analytical cytology. However, the use of a stain other than Papanicolaou in cervical cytomorphology is extremely limited (Koss, 1979). Furthermore, although based on standardized dyes, the stain is non-stoichiometric and main cell components such as nucleus and cytoplasm, can not be easily distinguished spectrally, therefore limiting its use in automated cell pattern recognition.

Another approach to obtain reproducible results on Papanicolaou resembling images is to use a stain that is spectrally similar to hematoxylin but also has quantitative properties, such as galloxyaniline (Mayall, 1969). In Leiden, galloxyaniline is used to stain conventional smears. Since no parallel slides can be made when a conventional smear is used, both cytomorphology and image analysis should analyze the same preparation. To optimize the procedure for both types of analysis, the following procedure is used. First the specimen is stained according to galloxyaniline and analysed with the machine. Following automated analysis, the slides are counterstained using the normal Papanicolaou dyes for staining of cytoplasm, as eosin and orange G. Resulting images are hardly distinguishable from Pap images using hematoxylin as the nuclear stain (figure 2a and 2b). Besides the advantage of a reproducible stain, the machine is able to analyse nuclear densities without disturbance from varying cytoplasmic staining intensities. With this method the machine as well as the cytologist can interpret images where they have been trained for. To overcome the disadvantage of counterstaining after machine analysis, the cytoplasm could be stained directly using a stain which absorbs all but green light (e.g. light green). This stain would not be visible at the wavelengths used for galloxyaniline (573 nm). Although a less time consuming staining procedure it would not fulfill the main requirement for these type of

staining namely to give Papanicolaou resembling images. This prerequisite does not include nuclear images only but also includes the information present in the PAP cytoplasmic image e.g. presence of keratin (Koss, 1979).



Figure 2a and b: Same microscopical image. Figure 2a displays the galloxyanine nuclear absorption image as it can be used for automated analysis. After counter staining of the cytoplasm (figure 2b), the cellular image highly resembles images as presented by the Papanicolaou procedure.

If, on the other hand, the cytoplasmic image is required during machine analysis, galloxyanine can be combined with FITC (fluoresceine isothiocyanate) to stain the protein (figure 3a and b). FITC is a fluorescent dye which emits green light after excitation with blue light. It is not visible at the absorption maximum of galloxyanine. Counterstaining can still be performed successfully after a galloxyanine-FITC staining. At present, no information is available on the reproducibility of the galloxyanine procedure as we apply it in our laboratory, with or without FITC counter staining.



Figure 3a and b: Same microscopical image. Figure 3a displays the galloxyanine absorption image. At the same time, the green fluorescent cytoplasm can be visualized using blue light to excite FITC (figure 3b).

Chapter 3.3 APPLIED PREPARATION TECHNIQUES.

Based on considerations discussed in the previous chapter, the following preparation procedure has been developed for cervical cytology specimens. It has been used for the LEYTAS system since 1979. Since then the procedure underwent only minor changes. Although the preparation is described here for cervical specimens, the procedure needs only minor adaptations to be applied to voided urine and aspirated cells.

Cell sampling and preservation.

Cervical cells are sampled with a cotton-wool-tipped applicator, after which the applicator is immersed in Polyonic buffered salt solution (0.09 M sodium chloride, 0.03 M sodium acetate, 0.03 M sodium gluconate, 6 mM potassium chloride, 1.5 mM magnesium chloride, 1.95 mM propyl 4-hydroxybenzoate and 4.25 mM methyl 4-hydroxybenzoate, pH=7.4) to which 96% ethanol is added until a final concentration of 25% ethanol is reached. In this preservative solution the cells can be kept for several days at room temperature which enables mailing (van Driel-Kulker, 1980). Although some cell samples were of reasonable quality after 2 weeks in the mail, others were extremely degenerated after 6 or 7 days. For that reason, only samples which arrive within 5 days are processed.

Cell preparation and fixation.

Upon arrival at the laboratory, the applicator is taken out of the solution and rinsed in a second tube with Polyonic solution. Both tubes are then centrifuged, the supernatants discarded and the two cell pellets combined. After washing the cells with Polyonic, 1 ml of carbowax (consisting of 2% (w/v) polyethylene glycol, MW=1500, in 50% ethanol) is added to the sediment.

The cell suspensions are then syringed automatically 20 times through 21 gauge needles. For syringing a special device has been constructed which can handle 4 suspensions simultaneously. The volume to be syringed can be varied. Syringing is executed directly before light scatter measurements.

Subsequently the concentration of the cell suspension is estimated by illuminating the suspension with a halogen lamp and by measuring the 90 degree light scatter. If the measured 90 degree light scatter is higher than a fixed arbitrary value, the suspension is further diluted with carbowax until reaching a value that concurs with the desired cell concentration of about 20,000 cells/ml. The intensity of the 90 degree light scatter is determined mainly by the epithelial cells. A large increase by the number of leukocytes e.g. does not influence the scatter signal significantly. Consequently, the scatter readings permit only a rough estimation of the total number of cells present in the suspension. For this reason an extra 1:1 dilution of each cell suspension has been made for several years to minimize the number of potentially unsuitable slides. However, a slide was never rejected by image analysis because the cell density was too high. For this reason the extra dilution has been abandoned.

Slide preparation.

For slide preparation the cells are centrifuged on the microscope slide using a centrifugation bucket (van Driel-Kulker et al, 1980). This newly developed centrifugation bucket, different from the already existing bucket according to Leif (Leif et al, 1975), has been developed to centrifuge prefixed cells. In our hands the preservation of the cells proved to be better when the cells are fixed before centrifugation. The adherence to the glass however, is less for prefixed cells than for unfixed cells. Therefore, high G forces must be used which puts high constraints on the bucket

concerning e.g. leakage. For the study described in this thesis, a bucket is used which has been developed in our laboratory. At the moment, a similar version is commercially available from Hettich (Hettich, Tuttlingen, West Germany).

The bucket constructed in our laboratory (figure 4), consists of two parts: a steel holder that fits into a commercially available centrifuge (Hettich Rotanta S, Hettich, Tuttlingen, West-Germany) and a plastic inner part containing 2 holes (cylindrical bores) of 1.5 cm in diameter each.

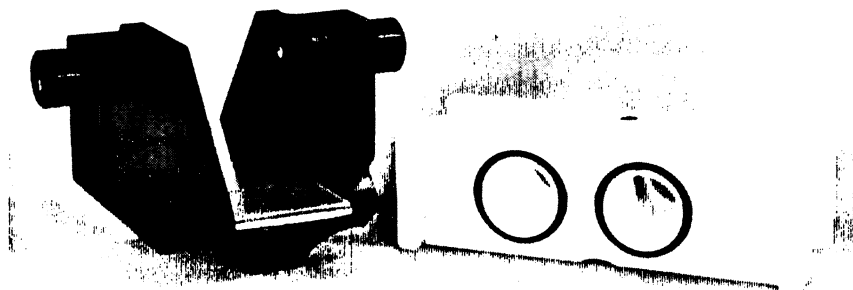


Figure 4: The Leiden centrifugation bucket for deposition of fixed cells at high G forces.

A poly-L-lysine coated slide (10 min 100 mg per 100 ml poly-L-lysine MW 500,000 Sigma Chemical Company, Saint Louis, USA) is put into the steel holder and the inner part is placed on top of the slide. The two parts of the bucket are held together by means of a spring lock. The cell suspension is then put into the holes. One milliliter of the cell suspension is placed in the first hole and one ml of rainbow trout erythrocytes (see end of this chapter) is placed in the second hole. Leakage is prevented by rubber rings at the bottom of the holes; they are pressed between the bucket and the slide by the springlock. Centrifugation is performed at 1,250 G for 15 minutes. The supernatant is then decanted and the bucket disassembled. The slides are dried at room temperature and stored for further fixation and staining.

Preparation of single cell suspensions from paraffin-embedded material.

Fifty μ m sections from paraffin blocks are cut using a microtome. Usually a single section is sufficient but from small tissue blocks two sections are required. The sections are placed in 10 ml glass centrifuge tubes and dewaxed using 2 changes of 3 ml xylene for 10 min at room temperature. The sections are rehydrated in a sequence of 3 ml of 100, 95, 70 and 50% ethanol for 10 min each at room temperature (Van Driel-Kulker et al, 1985). Replacement of all solutions is carried out by centrifugation and subsequent decantation of the supernatant. The tissue is then washed twice in PBS (buffered salt solution) and resuspended in 2 ml of 0.05% pronase (Sigma Chemical Company, Saint Louis, USA, 9.7 U/mg, type 7) in PBS. The tubes are placed in an incubator at 37°C for 30 min with intermittent vortex mixing. Following two times washing with PBS and syringing of the suspension through a capillary pipette, the sample is

filtrated through a 70 μ m nylon mesh filter. Cells which pass the filter are deposited onto a microscope glass by means of the centrifugation technique.

Selection technique for paraffin embedded tissue.

Sometimes the tumor compartment of the tissue block is so small in comparison to the normal tissue, that this can influence cytometric results (e.g. aneuploid cells are present but not detected in sufficient numbers in the histogram). For this reason, we have developed a preparation technique which enables the selection of certain areas in the tumor block, without destroying the remaining tissue (van Driel-Kulker et al, in press). The technique can be used either to enrich the sample to be analyzed with tumor cells or to analyze histopathologically different tumor compartments. The procedure is carried out as follows: The paraffin embedded tissue block is immersed in a petri dish containing a DAPI (4,6-diamidino-2-phenyl indol, SERVA, Heidelberg, West-Germany, 10 μ g/ml) solution in aqua dest. The block is placed such that the cut surface is in direct contact with the dye solution. After 5 minutes of immersion, the block is placed in a specially constructed holder on the stage of a fluorescence microscope with epi-illumination. The surface of the block can then be observed using low magnification (figure 5a, 6.3x).



Figure 5a and b: Figure 5a visualizes the tissue block surface after the block has been stained with DAPI and excited with ultra violet light. Figure 5b is a photograph taken from a HE stained section, cut prior to the DAPI staining of the block. Note the ressemblance between the morphological structures of the tissue in the two images.

Interpretation of the fluorescent image is facilitated when the HE stained diagnostic section, cut prior to the staining of the tissue block, is also inspected (figure 5b). If the desired area has been located by means of visual criteria, it can be selectively prepared by the following technique: A small holder for bores has been constructed to fit into the objective holder of the microscope. Small bores of varying sizes in diameter (from 2-5 mm) fit into this holder and are fixed using a screw. After turning away the objective, the boreholder with the selected bore is placed in position. Using the micrometer screw, the bore is pressed into the block. The depth of tissue infiltration can be controlled by registration of the micrometer screw movements. Then the bore is carefully withdrawn, which leaves all the tissue in the block. Verification that the desired area has been selected can easily

be done by turning the microscope objective again into position and check the incision lines made by the bore. If necessary, a second area can be visually identified and selected. A section is then cut at the desired thickness. Since sections tend to roll up during the cutting procedure with a microtome, tape is pressed against the tissue surface around the selected area before cutting. In this way, the section remains flat and the rolled up, selected area can easily be taken out. Further preparation is performed according the just described protocol.

Section thickness with respect to diameter bore.

Although the numbers of cell nuclei isolated from the sections may vary considerably between different types of tissue, at least 50 μm was needed for a 5 mm bore punch and at least 100 μm for a 2 mm bore punch. To avoid the use of too much tissue when the 2 mm bore is used, two or more areas may be selected instead of one. Then a 50 μm section will be sufficient. These findings are based on the results obtained with an image cytometer (LEYTAS) to generate histograms containing about 200 uncut nuclei. If histograms containing larger numbers of cells are necessary or wanted, e.g. for flow cytometry, larger cell numbers and more tissue will be needed (Stephenson et al, 1986).

DNA reference cells.

Erythrocytes from rainbow trouts are used as DNA reference cells. The preparation is as follows: 500 μl blood (to which heparine has been added as a coagulant) from a rainbow trout is added to 50 ml PBS. Fixation is performed by adding 5 x 4 ml 25% formaldehyde solution in PBS during a period of 15 min. The erythrocytes have to remain in this fixative (final concentration of formaldehyde = 7%) for at least 24 hours before use. For further storage, Eppendorf sample cups are filled with 100 μl fixed erythrocytes. The cups are kept at 4°C. Just before use of the reference cells, 900 μl carbowax is added to the Eppendorf cup. This solution is put into the second hole of the bucket just before centrifugation of the patients cell suspension.

Chapter 3.4 APPLIED STAINING METHODS.

Acriflavine-Feulgen-SITS staining procedure.

The AFS (acriflavine-Feulgen - Stilbene isothiocyanate sulfonic acid) staining has been developed to match machine requirements while also enabling cytomorphologic examination. The staining procedure starts with a carbowax fixed and air-dried specimen, and is carried out in a modified Shandon staining machine. The recipe is as follows:

- 60 min ethanol 100%
- 3 min distilled water
- 3 min running tap water
- 45 min 5N HCL at 28°C
- 3 min running tap water
- 30 min acriflavine (Chroma, Stuttgart, West-Germany) 0.1% at 28°C
- 5 min distilled water
- 5 min hydrochloric acid 1% in ethanol 70% ; 2x
- 5 min PBS
- 5 min citric acid phosphate buffer pH=5.5
- 15 min SITS (Polyscience Inc., Warrington, England) 0.01% in citric acid phosphate buffer pH=5.5 at 28°C
- 3 min citric acid phosphate buffer pH=5.5
- 3 min running tap water
- 5 min ethanol 100% ; 6x
- 5 min ethanol:xylene=1:1
- 5 min xylene; 2x
- mount with fluormount (Gurr, Poole, England)

Ethanol 100% is used for dissolving the wax layer introduced by the carbowax and serves as the final fixative for the preservation of nuclear chromatin.

Distilled water is used for rehydration of the specimens. Running tap water is included to make sure that cells, which have not been attached firmly to the glass, are washed away. In this way, cross contamination of cells is prevented as much as possible.

Hydrolysis of DNA is executed by HCL 5N; in a study performed by Tanke et al (Tanke et al, 1979), it was found that optimal stainability was obtained after 45 minutes. DNA staining is performed using an acriflavine solution to which $K_2S_2O_8$ is added (Tanke et al, 1979) to enhance the binding of acriflavine to DNA. The used concentration of acriflavine (0.1%) has been selected for morphological reasons. The obtained contrast between nucleus and background enabled both visual examination as well as automated nuclear segmentation. Tanke (Tanke et al, 1979) showed that the linearity of 0.1% acriflavine is acceptable provided absorption measurements are used and not fluorescence as was done in the beginning of the automation project (Al and Ploem, 1979).

Slides are washed with acid ethanol to remove noncovalently bound acriflavine. Rinsing with PBS is utilized to remove the acid ethanol and to neutralize the pH.

SITS serves as a fluorescent protein marker. Although there is a correlation between the amount of protein and the intensity of the stain, the binding is not proportional. Its use is mainly for cytomorphological reasons (recognition of amount and shape of cytoplasm, nucleoli). SITS is visualized using ultra violet exciting light.

Staining as well as hydrolysis is carried out at 28°C. This temperature was selected to avoid variations in room temperature, whereas a staining machine could still be used. The fixed temperature and the use of a staining machine both promote reproducibility in staining results which is especially

important in automated cytology.

After dehydrating with ethanol and finally with xylene, the slides are mounted in fluoromount. They remain under lead blocks to obtain a flat layer of mounting medium.

Acriflavine was preferred over pararosaniline, because the plumbicon TV camera used by LEYTAS is more sensitive in the blue region than in the green region of the spectrum. The absorption image of acriflavine is also preferred by cytologists if compared with the pararosaniline absorption image. SITS was selected because its blue fluorescent image can be spectrally separated from the acriflavine image and because its blue color is appreciated by the human eye. For more detailed information about the AFS procedure, the reader is referred to the following 2 publications: van Ingen et al, 1979 and Tanke et al, 1979.

Papanicolaou staining procedure.

With the knowledge that a high contrast between nucleus and cytoplasm would facilitate segmentation algorithms with LEYTAS, we selected a Papanicolaou procedure with these characteristics (figure 6a and b).

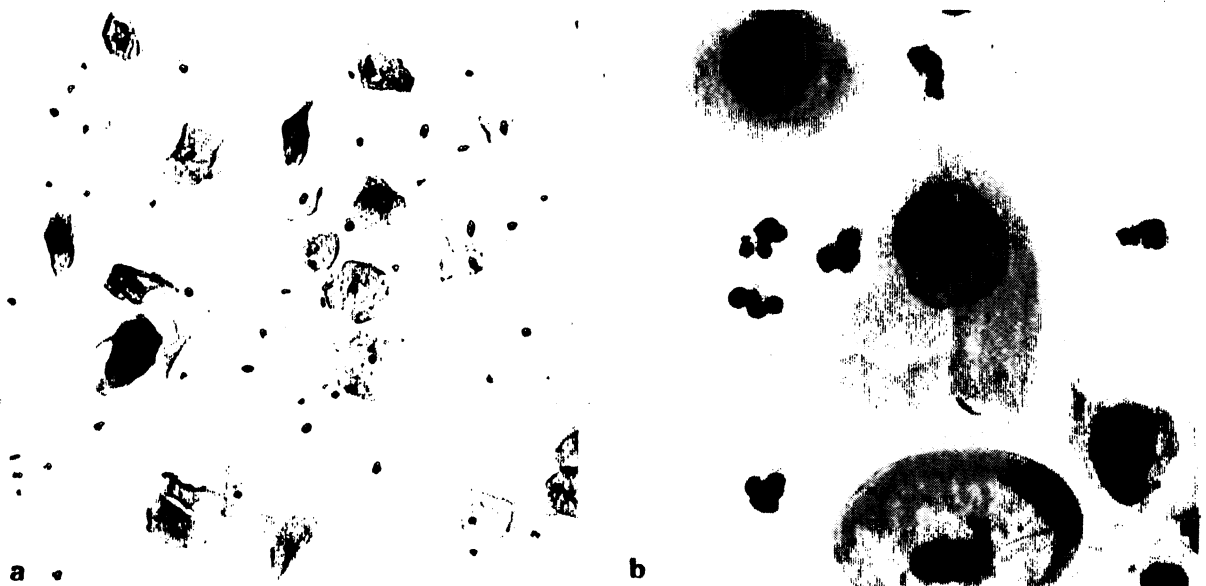


Figure 6a and b: Examples of the Papanicolaou staining procedure applied to centrifugation specimens of cervical cells. Figure 6a: low magnification (10x) of normal epithelial cells. Figure 6b: High magnification (50x) of dysplastic cells of metaplastic origin.

The protocol which had been specially adapted to be executed on centrifugal cytology specimens by the Research Cytology Unit of the University of California, San Francisco (UCSF, head Dr. Eileen King) fulfilled these criteria. The staining was optimized in such a way that nuclear texture was well presented for visual examination whereas the nuclear to cytoplasmic contrast was high enough to enable segmentation algorithms on the basis of greylevel images. At the time the staining procedure was selected, LEYTAS did not have any facilities for texture analysis. This means that when these type of parameters become available on the machine and the Papanicolaou staining is selected as the method to work on, the staining procedure to be used should be taken into reconsideration. In the study described in this thesis, the Papanicolaou staining is used for cytomorphology only. The protocol of the applied Papanicolaou is as follows:

- 60 min ethanol 100%
- 2 min distilled water
- 2 min Harris Hematoxylin (Papanicolaous solution 1a, Merck, Darmstadt, West-Germany)
- 20 sec distilled water
- 1 sec hydrochloric acid 0.1% in ethanol 70%
- 2 min running tap water
- 2 min Scott's tap water
- 5 min running tap water
- 20 sec ethanol 70%
- 20 sec ethanol 100%
- 20 sec orange G (Papanicolaous solution 2b, Merck, Darmstadt, West-Germany)
- 20 sec ethanol 100% ; 2x
- 8 min EA 65
- 20 sec ethanol 100% ; 3x
- 2 min isopropanol ; 2x
- 2 min isopropanol:xylene=1:1
- 5 min xylene; 2x
- slides are mounted with fluormount (Gurr, Poole, England).

Besides well known Papanicolaou ingredients, Scott's tap water (20 gms of magnesium sulphate and 2 gms of sodium hydrogen carbonate in 1000 ml distilled water, pH 8.2) is used to obtain the desired blue color for the nucleus.

Gallocyanine staining procedure.

In order to obtain a specific nuclear stain with a hematoxylin-resembling image, specimens are stained with gallocyanine. Varying staining protocols have been published of which we have selected a combination of two (Mayall, 1969; Husain and Watts, 1984), on the basis of cytomorphological criteria and reproducibility.

- 60 min ethanol 100%
- 5 min distilled water
- 5 min HCL 5N
- 5 min distilled water
- 30 min gallocyanine (Fluka, Buchs, Switzerland) 1% at 30°C
- 2 min distilled water
- 5 min running tap water
- 5 min ethanol 100% ; 3x
- 5 min isopropanol ; 2x
- 5 min isopropanol:xylene = 1:1
- 5 min xylene; 2x
- slides are mounted with fluormount

The treatment with 5N hydrochloric acid serves to destroy RNA. This way gallocyanine can be considered quantitative for DNA. The gallocyanine is stained at 30°C to speed up the staining reaction whereas the staining procedure can still be executed in a staining machine. After mounting, the slides can be analysed by LEYTAS using light of 573 nm. Subsequently the coverglass is removed in xylene and after replacing xylene by ethanol 100%, the slides are counterstained using the Pap protocol starting with the orange G. Following mounting, the slides can be analysed cytomorphologically; resulting images are hardly distinguishable from the conventional Papanicolaou.

Modified Papanicolaou staining according to Wittekind.

This staining procedure has been developed to obtain images, resembling those of the Papanicolaou (Wittekind et al, 1979). However, since pure dyes have been used, the results are expected to be more reproducible and therefore better suited for automated analysis. The protocol is as follows:

- 30 min distilled water
- 5 min ethanol 50%
- 5 min formamid 41% (Baker, Deventer, The Netherlands)
- 2 sec ethanol 50%; 2x
- 20 min thionine 0.32% (Merck, Darmstadt, West-Germany)
- 2 sec ethanol 100%; 3x
- 10 min eosin (0.04%, Gurr, Poole, England)-FCF (0.0058%, Allied, New York, USA) solution.
- 2 sec ethanol 100%; 2x
- 2 sec xylene
- 2 min xylene
- mount with fluormount (Gurr, Poole, England).

After formamid treatment, the cells are stained with thionine which serves as the nuclear stain. The staining with eosin-FCF (Fast Green) is carried out to stain the cytoplasm.

All staining procedures are carried out in an automatic staining machine (Shandon Special 24 Stainer, Shandon, Astmoor, England) which has been modified to enable rinsing in running tap water and heating of the different staining components. All functions of the machine are microprocessor controlled. The execution of the different staining protocols are preprogrammed. In this way, no more labour is needed to carry out a cytochemical Feulgen procedure than a Papanicolaou staining.

Chapter 3.5 QUANTITATIVE EVALUATION OF DIFFERENT STAINING PROCEDURES.

To evaluate the characteristics of certain staining procedures for automated cytology, we performed absorption measurements on 4 methods with potential use in automated image analysis using LEYTAS. The 4 methods are: the conventional Papanicolaou (PAP), the modified Papanicolaou according to Wittekind (MOD), the acriflavine-Feulgen-SITS (AFS) and the galloxyanine (GAL). All recipes are given in the previous chapter 3.4.

For the evaluation the following procedure was carried out: from the cervical scrape from one healthy individual, 12 preparations were made using the centrifugal cytology bucket procedure as described in chapter 3.2. Three preparations were stained in one staining bath according to any of the four procedures. In each of the preparations, 10 visually selected intermediate squamous cells were measured using a microdensitometer. Measurements were carried out at the absorption maximum for the nuclear stain being 466 nm for the acriflavin-Feulgen and 573 nm for all other staining procedures. Scanning was performed with 0.5 μ m steps and a 0.5 μ m diafragma using the HYDACSYS scanning program (van der Ploeg, 1977) and a 100x objective. We evaluated the integrated optical density (IOD) as it varied from one slide to another (interslide variation) and the variation within one slide (intraslide variation). The results are depicted in the following table.

Table 3.1: inter-and intraslide variation of IOD in different staining procedures.

staining procedures	average IOD value (A.U.)	^x interslide variation	^{xx} intraslide variation
PAP	64.2	10.3%	23.1%
MOD	65.3	30.0%	19.7%
AFS	103.0	1.8%	6.0%
GAL	74.9	3.9%	4.7%

x) The interslide variation has been calculated as the coefficient of variation (standard deviation x 100 / mean value) of the average IOD's per specimen.

xx) The intraslide variation has been calculated as the average coefficient of variation of the cells per specimen.

Both the inter-and the intraslide variation are relatively high for PAP and MOD whereas AFS and GAL show relatively low CV's. Although these experiments were carried out on limited numbers of cells and specimens, these numbers clearly demonstrate the preference for AFS and GAL as far as reproducible IOD measurements are concerned.

The characteristic of high reproducibility of the AFS is further supported by the results from the control measurements which have been performed on one negative preparation from each staining series. To control the AFS procedure on such a long term basis, microdensitometry measurements were carried out. Slides from 42 staining series in a three year period have been measured with the same measuring protocol as was applied for the evaluation of the different

staining procedures. The average CV per slide (intraslide variation) was 4.7%, whereas the interslide variation (CV of average IOD's per slide) amounts to 5.8%. As can be expected the interslide variation is somewhat higher in these 42 staining series than in the experiment of table 3.1, but remains relatively low. From the reproducibility point of view, the AFS procedure meets the requirements for automated cytology.

Besides the AFS, the conventional Papanicolaou has also been tested by our group during a long period. Although purely designed to match visual requirements, the PAP is often used for quantitative studies (Abmayr et al, 1979; Reinhardt et al, 1979; Tanaka et al, 1979; Meyer and van Driel-Kulker, 1980), the main reason being to facilitate final acceptance of any quantitative procedure in the medical community. There are many Papanicolaou protocols in use in the cytology laboratories. We selected a protocol directed towards a high contrast between nucleus and cytoplasm. This facilitates nuclear segmentation and therefore automated screening.

We performed microdensitometry measurements on PAP stained suspension preparations after 60 routinely executed staining series in a three year period and found an interslide variation of 9.2% (CV) and an intraslide variation of 9.4% (CV). The measured interslide variation correlates well with the experiment in table 3.1 (10.3%). The intraslide variation however, is considerably higher in table 3.1. Probably this is due to the low number of investigated preparations in table 1. None of the other staining procedures have been controlled for such a long period using measurements, neither by us or any other group.

As may be clear from these control studies, AFS is the preferred staining procedure for LEYTAS. However, AFS is not an accepted procedure for use in cytomorphology. This limits the use of AFS to cell suspensions only, since in that case several preparations can be made from one cell sample. A second preparation can then be Pap stained to serve as a morphological reference if needed. A disadvantage of cell suspensions is the labour of preparation; without automation the preparation procedure can hardly be considered as a practical proposition in a routine laboratory. Therefore we started to analyse conventional smears. Only one preparation is then available, demanding a staining procedure which allows both machine analysis and morphological diagnosis. That has been the reason for the introduction of another staining procedure, the gallocyanine. The method in use now, the recipe of which is given in chapter 3.4, still undergoes minor changes so that a quantitative evaluation of this staining procedure is not yet feasible.

Tenability of AFS stained specimens.

Another important characteristic of any procedure to be used for diagnostic purposes is its tenability after routine use. Some staining products suffer e.g. from sincere fading effects which occur already in several minutes. Preferably the staining product should remain approximately constant for several years. For this reason we performed IOD measurements on slides which had been stained according the routine AFS procedure, and had been stored for different periods of time, ranging from 6 months to two years. Normally during the first 4-6 weeks the slides are stored at room temperature in a special map to prevent exposure to daylight except during visual evaluation and LEYTAS analysis. After that period they are stored in the dark at 4°C. It turned out that the decrease in IOD ranged from 10 to 16% in the first 6 months but remained constant for the remaining test period (24 months). As will be demonstrated in chapter 6.3, this decrease in staining intensity does not influences classification results.

Trying to find the reason for this fading, we tested slides which had been split in 2 groups. One group was stored in the refrigerator in the dark immediately after staining and automated analysis and the other slides were

exposed to daylight at room temperature. After 2 months the average decrease in IOD amounted to 4.0% for the first group of slides and to 15.6% for the second group of slides. The decrease for slides exposed to direct sunlight mounted up to 84% in a 2 months period. The different results are given in table 3.2.

table 3.2: Fading of AFS stained cells under different circumstances.

storage of slides	average decrease of IOD in 2 months
4°C dark	4%
20°C dark	15%
20°C sun	84%

This large difference in fading between differently treated slides changed our routine procedure; within 2 weeks after staining the slide should be analysed and stored in the dark in the refrigerator, if possible. In that case the tenability of the AFS stained slides can be considered acceptable.

To check the potential loss of tumor cells in the proposed preparation technique for cervical scrapes, the cytological diagnosis of the conventional smear, if available, was compared with the cytological diagnosis of the Papanicolaou stained suspension preparation. We found that these did not always correlate. In 8 cases the cytological diagnosis of the suspension preparation was positive, whereas the diagnosis of the conventional smear was negative. On the other hand, we found 7 cases of which the suspension preparation did not contain abnormal cells, but where the diagnosis of the conventional smear was positive. Thus false negative samples are randomly distributed over conventional smears and suspension preparations. The literature also reports the presence of different cell types when two conventional smears are taken simultaneously (Sedlis et al, 1974). Therefore we conclude that a selective loss of abnormal cells induced by the applied preparation technique is highly unlikely.

CHAPTER 4

THE LEYDEN TELEVISION ANALYSIS SYSTEM (LEYTAS)

Chapter 4.1 INTRODUCTION.

A few years ago a project was started at the Department of Cytochemistry and Cytometry of the University of Leiden, for the automation of quantitative analysis of cervical specimens with the aid of an image processing system. Since the objects of interest represent only a small proportion of all objects to be examined, a hardwired image analyzer was chosen in which the data could be preselected without bringing them in a computer. The Texture Analysis System (TAS), developed by Ecole des Mines, Fontainebleau and manufactured by Leitz (Wetzlar, West Germany) was selected to form the basis of LEYTAS: the Leiden Television Analysis System.

LEYTAS resulted from a cooperative project between Leitz Wetzlar GmbH in Germany, the Department of Cytochemistry and Cytometry of the Leiden University in the Netherlands, and the Department of Mathematical Morphology of the Ecole des Mines of Fontainebleau, France. This European cooperation, sponsored by the German Ministry of Science and Technology, lasted from 1976 until 1986. During this period 2 versions of LEYTAS have been developed, being distinctive both in the optical system (at present the mainly used data acquisition set up) as well as in the structure of the image analysis computer.

As the first version of LEYTAS has been in our laboratory since 1975, a large number of clinical tests could be carried out of which some are described in this thesis. The first clinical programs for LEYTAS-2 only became available in the summer of 1985. Therefore, apart from small comparison trials between the 2 versions of the system, no large clinical series have yet been tested on this machine. In principle, all programs which run on LEYTAS-1, can be applied on LEYTAS-2.

The hardware components of both LEYTAS-1 and LEYTAS-2 will be discussed in chapter 4.2, whereas the applied image analysis programs are presented in chapter 4.3.

Chapter 4.2 HARDWARE.

The miniaturization and large scale integration of electronic components during the last decade has contributed significantly to the development of hardware image processing systems suited for analytical and quantitative cytology. In principle, presently available instruments carry out light absorption measurements of different cellular constituents at a certain resolution. Different type of input devices are presently in use, which can be subdivided in source scanners, image plane scanners and specimen scanners (van der Ploeg et al, 1974). Examples of source scanners used in prescreening instruments are the flying spot scanner which has been incorporated in CYBEST (Tanaka, 1979), and the cathode ray tube of the BioPEPR system (Zahniser, 1979). Measurements are performed by the projection of a light spot on the object and by moving the spot, thereby measuring one spot at a time. A photomultiplier tube combined with a mirror scanning as used in (the high resolution channel of) the SAMBA system (Brugal and Adelh, 1982) also belongs to this category. Television camera's are typical examples of image plane scanners; they perform measurements in the image plane of the microscope. They have been incorporated e.g. in LEYTAS (Vrolijk et al, 1980) and in FAZYTAN (Reinhardt et al, 1979). Another example of an image plane scanner is the linear photodiode array scanner which has been used in CERVIFIP (Tucker and Shippey, 1983) and in (the low resolution channel of) SAMBA (Brugal and Adelh, 1982). Specimen scanners use a microscope scanning stage to move the slide while the object of interest is illuminated by a light beam. An example of this is the Zeiss AXIOMAT system (Taylor et al, 1978).

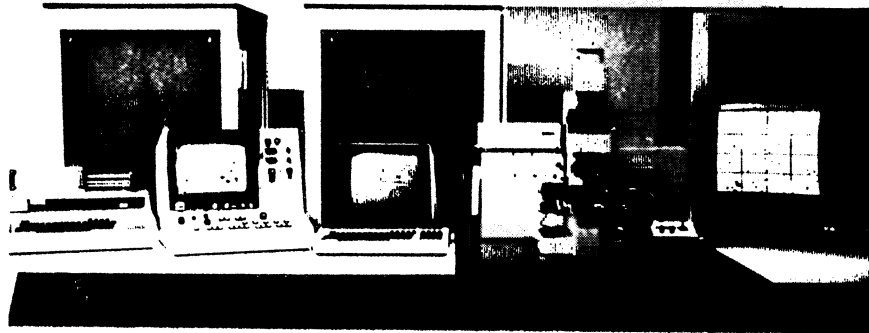


Figure 7: A photograph of LEYTAS-1. From left to right: a printer, the Texture Analysis System (TAS), a computer terminal, the microscope and the monitor for display of selected objects.

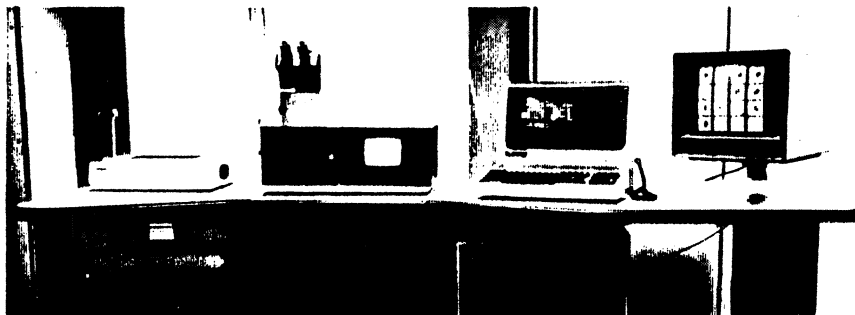


Figure 8: A photograph of LEYTAS-2. From left to right: a printer, the newly developed microscope, a computer terminal and the monitor for display of selected objects.

All present screening systems analyze the microscopical image, except BioPEPR. This system is basically different from the others in that it uses photonegatives of microscope fields rather than the microscope image itself. The resolution (pixel distance) for screening of objects is $1\text{ }\mu\text{m}$ for BioPEPR, CERVIFIP as well as LEYTAS, whereas CYBEST uses first a coarse scan of $4\text{ }\mu\text{m}$ to select a limited number of cells (300) and a fine scan of $1\text{ }\mu\text{m}$ to perform measurements of these cells. FAZYTAN scans at $0.5\text{ }\mu\text{m}$ pixel resolution.

For LEYTAS a Plumbicon television camera was selected to serve as the scanning device because of the adequate density and spatial resolution offered which is necessary for cytology quantification, and because current memories are capable of storing data at television speed. Although finally charge coupled device cameras (CCD) will be preferable because of their geometrical and spectral characteristics, they were not available for large arrays (e.g. 512×512 pixels) at the time of development. The interactive facilities of the TAS (image transformations are visualized on the TV monitor during execution) in combination with the fast response time of a hardwired image processor and a flexible control program using a minicomputer, leads to a system suited for human observer interaction with the results of the image processing.

Characteristics about the microscope system and the television camera will be given in chapter 4.2.1, whereas the image analysis system (TAS for LEYTAS-1 and MIAC for LEYTAS-2) will be discussed in chapter 4.2.2.

Chapter 4.2.1 THE MICROSCOPE SYSTEM.

First an outline will be given of the microscope system including its functioning, which is used for LEYTAS-1, followed by a description of the LEYTAS-2 microscope. The microscope of LEYTAS-1 features a modified Leitz Orthoplan stand (figure 9). A halogen lamp is used as a light source for bright field illumination of the entire field. The microscope can be equipped with an automated vertical illuminator and a high power Xenon lamp to enable incident light fluorescence microscopy (Ploem et al, 1979), but these facilities have not been used in the subjects under study in this thesis. The instrument is provided with a special, measuring type, Plumbicon television camera. A photometer unit can be added for scanning cytophotometry. A Leitz scanning stage is used with a step size of 5 μm and a range of 9 cm in the two orthogonal directions with a maximum speed of 300 steps/sec. During the screening procedure the stage is under computer control, whereas, if desired, the operator can take over using the keyboard of the computer terminal. To start the screening procedure, the area to be scanned is located without operator control, since the cells are on a fixed location of the microscope slide. The scanning area for screening is about 1 square cm, being 40 fields in the x direction and 40 in the y direction using low magnification. A projective rotor in front of the television camera is used to change magnification. Two different projectives in combination with one 40x objective of high numerical aperture (N.A. 1.30) allow imaging at any of these two magnifications. The images projected on the television camera are sized 250 x 250 and 80 x 80 μm respectively. The rotor to change projectives is driven by a stepping motor. They can be analyzed directly or simultaneously viewed at the television monitor. The flexibility of the microscope system is such that it can be modified and expanded, depending on the application. The description as it has been given here, serves the application of the system in automated cytology. Microscope modifications for different applications (such as the addition of a photometer unit for high resolution scanning cytophotometry and the combined use of fluorescence and absorbance in automated immunology) are described elsewhere (Ploem et al, 1979; Ploem, 1986).

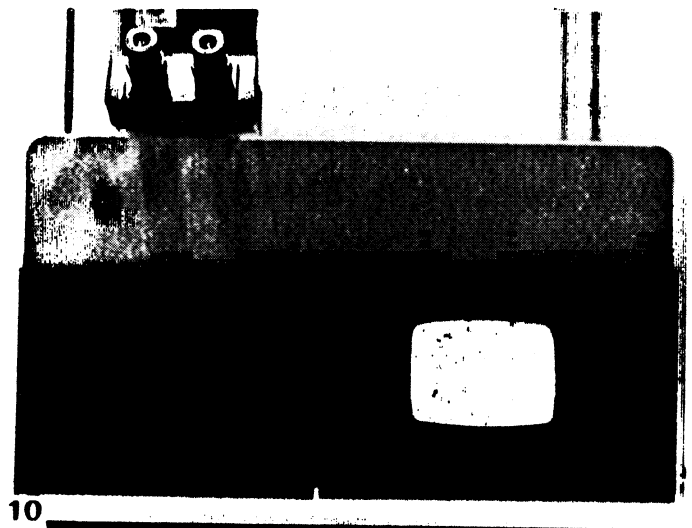
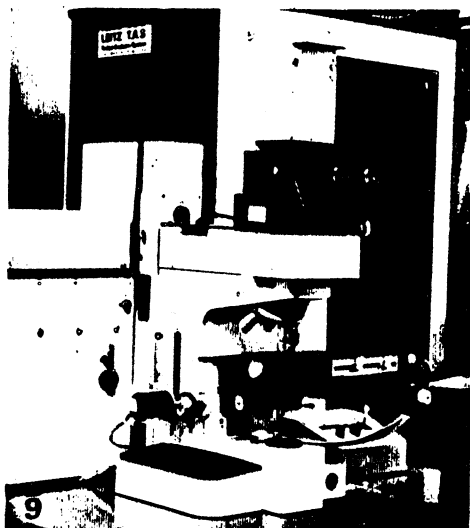


Figure 9 and 10: Examples of two generations of automated microscopes. Figure 9 displays the LEYTAS-1 microscope, which is based on a modified Leitz Orthoplan stand. All functions are under computer control. Figure 10 displays the newly developed automated microscope (Leitz) of LEYTAS-2. The computer controlled stage and two TV cameras are included.

Focusing.

To provide automatic as well as manual focus control, the fine focus knob of the Orthoplan stand is driven by means of a stepping motor through an anti-backlash gear. Automatic focusing is achieved by means of a special focus algorithm for use in conjunction with the image analyzing processor of LEYTAS. The algorithm is based on the optimization of the gradient at different greylevels. With the magnification conditions required for automated cytology, this algorithm takes about 0.1 sec, and it appeared to be necessary to use the algorithm every fifth microscope field during the screening procedure.

Concerning the optical system, LEYTAS-1 is composed of a, although completely automated, conventional microscope, whereas the microscope system for LEYTAS-2 is specially constructed for image analysis. This has been realized by the projection of the microscope image directly on the television camera. No intermediate oculars have been used, thereby abandoning the limitations caused by an acceptable observation angle of the ocular for the human eye. This permits the use of wide field objectives, offering high spatial resolution and a considerable focal depth at low magnification. Simultaneously the external complexity of the first automated microscope - LEYTAS-1 - could be reduced (figure 10).

A newly developed 40x objective with a numerical aperture of 1.30 enables the analysis of microscope fields of $512 \times 512 \mu\text{m}$ with a pixel separation of $1 \mu\text{m}$. Due to demagnification, the total microscope magnification is only 20x at this resolution, resulting in very bright images with a high depth of focus. At the same time, a high resolution image is available of $128 \times 128 \mu\text{m}$ with a pixel separation of $0.25 \mu\text{m}$. Two TV cameras are built in the microscope, both working simultaneously at a different magnification. For instance, rapid cell selection can be done with the low magnification TV camera; once an object is detected and centered, the high magnification camera can be used to analyze the high resolution image (figure 11 a and b).

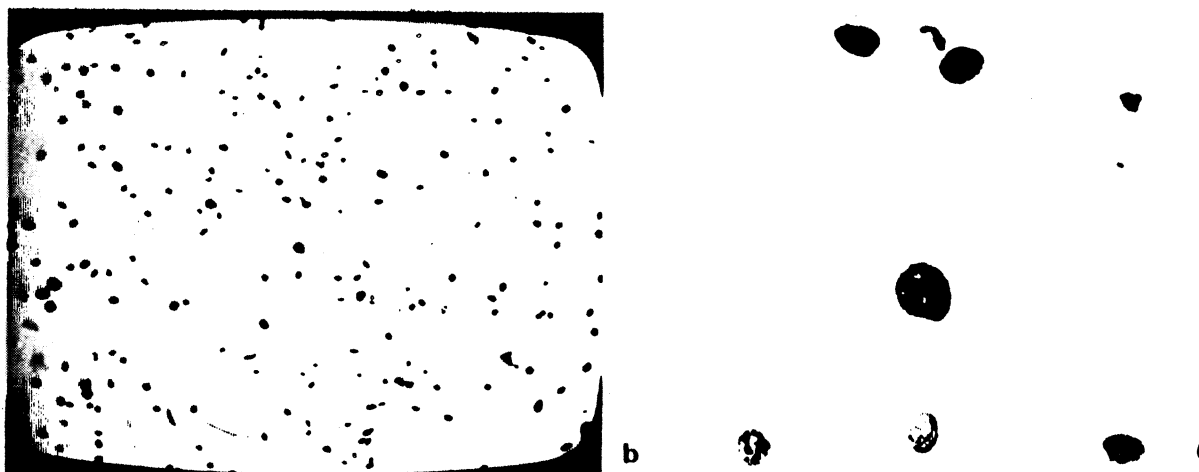


Figure 11a and b: Two TV images of the LEYTAS-2 microscope. Figure 11a shows the result of the low magnification image consisting of 512×512 pixels. Figure 11b shows the result of the high magnification image ($128 \times 128 \mu\text{m}$) of the same microscope field. Both images are simultaneously available.

Furthermore this microscope offers automatic focusing via movement of objective, an automatic slide changer, a slide code interpreter, an automatic supply of immersion oil and an additional light path for visual observation. All microscope components and functions are under microprocessor control.

Chapter 4.2.2 THE IMAGE ANALYSIS SYSTEM.

Again, first the image analysis system of LEYTAS-1 will be outlined; then the hardware components of LEYTAS-2 will be given. The LEYTAS-1 hardware consists of the microscope with Plumbicon camera (high quality measuring camera (Bosch, West Germany), a PDP 11/23 minicomputer and the TAS (Leitz, West Germany). The computer is equipped with 2 RK05 diskdrives, a VT100 display terminal and a printer.

The Plumbicon television camera is used as an input device. One full image consists of four frames positioned on either every second pixel or line relative to each other. Simultaneously with scanning, an image can be stored in a four bit buffer memory using a 10-MHz, eight-bit, analog-to-digital convertor; the necessary compression from eight to four bits is fully programmable. This enables the digitization of a selected intensity range within which objects of interest are located without losing information in the background range. Because four memories of $256 \times 256 \times 4$ bits are available, eight bits of grey value information can also be obtained by storing two consecutive frames and adjusting the conversion table for the AD convertor between the frames. However, the storage of four consecutive frames normally leads to a full image of $512 \times 512 \times 4$ bits, so it is possible to exchange spatial or density resolution. Each pixel is fully adressable. This part of LEYTAS, consisting of the AD convertor and the buffer memory, is special to LEYTAS and not commercially available.

Besides the storage of video frames in the buffer memory, images can be analyzed by the TAS. The TAS consists of the following commercially available components: two thresholding channels to perform the necessary compression to one bit (only one bit memories are available on the TAS), the erosion/dilation module of larger sizes (up to 16), which transforms the images on the basis of a structuring element, the ring logic which permits the programming of various structuring elements and the measuring logic. The TAS is also provided with eight bitplanes, a hardware contour follower and a lightpen unit. Shading compensation is carried out by the camera, which has an analog shading compensation implemented. The analog shading corrector present in the TAS is not used. Furthermore, since only the middle of the frame can be stored in a bitplane, the effects of the shading of the camera are relatively small on the images within a bitplane. Using the deformation module, images can be transformed by a shrinking algorithm (erosion), by the complementary expansion algorithm (dilation) or by a combination of both. Each pixel point of the image is thereby intersected with a structuring element. A transformation or a combination of transformations is usually followed by a measurement to obtain information about the result and to decide what should be the next processing step. Some of the possible measurements are the area, the number of objects (particle count) and the perimeter.

The TAS is provided with eight bitplanes of 256×256 pixels. The stored binary images can be combined logically and can subsequently be stored in a new bitplane, can be processed again by the hardwired modules of the TAS or can serve as a mask for new threshold settings. By combining the bitplane storage and image transformations, sophisticated iterative procedures can be developed, such as skeletonization.

Using the hardware contour follower, each object can be analyzed separately. Since the computer has access to the contour points of each object, it is possible to select objects on the basis of image analysis procedures and to consecutively read from the buffer memory only those grey values which are located within the object. In this way, data reduction is performed by the TAS while sophisticated pattern recognition algorithms can be carried out by software procedures.

LEYTAS has been constructed in such a way that the user has easy insight

in the performance of the image analysis routines. The TAS by itself offers the possibility to follow each image analysis program on the monitor, which is of considerable advantage during development of new programs. Furthermore, the grey value buffer memory in which selected objects can be stored, allows direct visualization of the results of the cell selection during and after the entire screening procedure (figure 12).

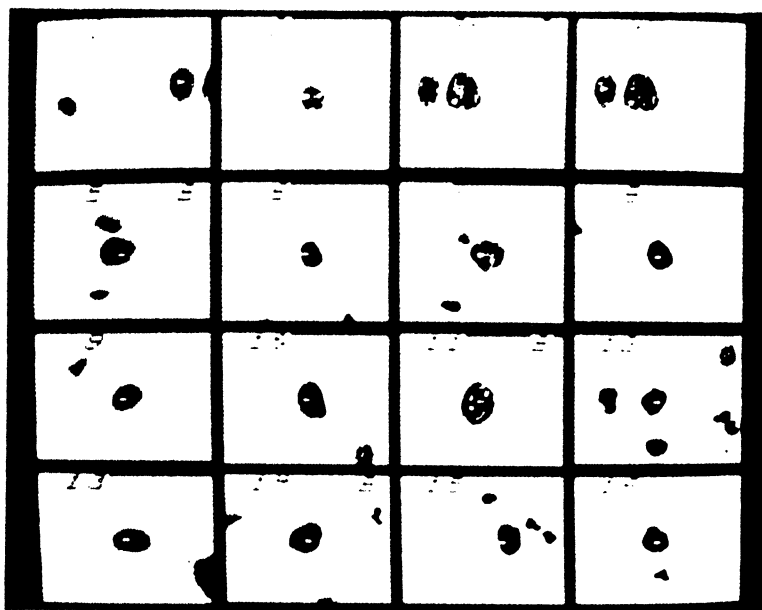


Figure 12: Photograph of monitor displaying 16 objects selected using LEYTAS-1.

When the analysis has finished, all alarms (selected objects) can be displayed on the TV monitor, 16 per TV screen (fig 12). Each alarm can then be classified visually. The quality of the display is sufficient to enable differentiation between 'single nuclei', 'overlapping nuclei' and 'dirt'.

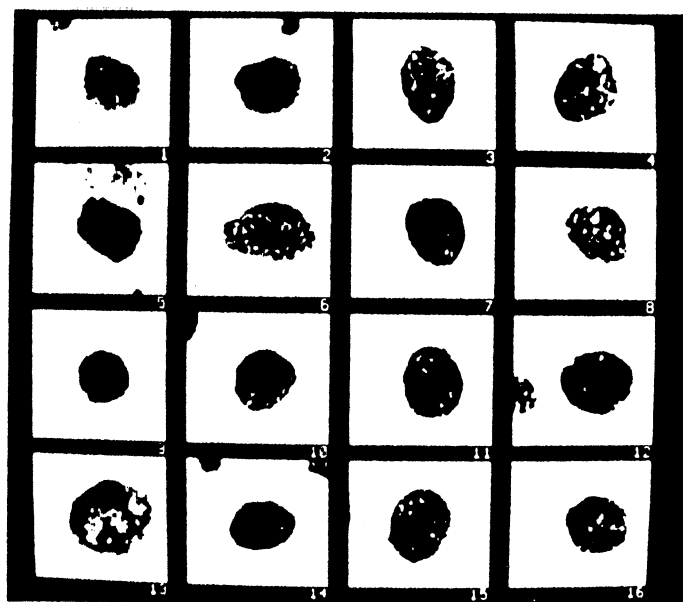


Figure 13: Photograph of monitor displaying 16 objects selected using LEYTAS-2.

However, the modulation transfer function (MTF, Castleman, 1979) of LEYTAS-1 is insufficient to differentiate easily between nuclei from benign and from malignant cells on the basis of stored images. LEYTAS-2 however, is provided with a much better MTF, which highly facilitates the visual recognition of abnormal cells on the basis of stored greyvalue images (figure 13).

For both systems, visual inspection of one TV screen displaying 16 alarms takes less than a minute and offers possibilities to add rapid human interaction to automated screening. This facility can be used to eliminate visually the few remaining artefacts and, especially with LEYTAS-2, to investigate quickly whether possibly abnormal cells are present.

Besides this way to interact with the screening results, a relocation of alarms in the microscope is also possible. This is executed with the computer operated stage using the stored x and y coordinates. Either all alarms, or a preselection of interesting alarms can be relocated. Since LEYTAS examines the original slide, the cytologist can in this way inspect all those fields which contain the selected suspect nuclei and give an evaluation of the morphology of the cells in the normal microscope image. At present this visual morphological evaluation is performed on the LEYTAS automated microscope. In the near future it will be possible to relocate the alarms on a separate routine-type laboratory microscope. The few extra components added to this stand will be a motor driven stage, a miniature TV monitor (size e.g. 6x8 cm) and a drawing prism which mirrors an image, displayed on this monitor, into the microscope image. This will result in an original microscope image superimposed by a simple line drawing of the contour of the by LEYTAS detected object in that field. If necessary, contours of other objects in the same microscope field can be superimposed as well to facilitate location of the detected cell. The measurements and diagnostic results obtained by LEYTAS, the x and y coordinates of the field in which LEYTAS found alarms, and the contours of these objects will be transferred on floppy disk to the microprocessor that is connected to the routine microscope. Relocation in the original slide of all alarms detected by the LEYTAS machine using a relatively simple microscope is thus available for visual inspection by a cytologist. Furthermore, this procedure offers the obvious advantage that (expensive) machine time is not used for the visual cytomorphological interpretation of cells.

Modular Image Analysis Computer (MIAC).

The Modular Image Analysis Computer (MIAC, Leitz) of LEYTAS-2 is constructed around a VME bus and a high speed video bus.

Table 4.1: Basic configuration of the Modular Image Analysis Computer (MIAC).

- | |
|---|
| 1. Analog to digital convertor |
| 2. Memory adress processor |
| 3. Memory board for storage of images |
| 4. Memory board for storage of images |
| 5. Memory adress processor |
| 6. Memory board for storage of images |
| 7. Memory board for storage of images |
| 8. Grey value processor for mathematical morphology |
| 9. Motorola microcomputer board + 1 megabyte memory |
| 10. Binary processor (mathematical morphology) |
| 11. Binary processor (mathematical morphology) |
| 12. Second Motorola microprocessor board for a slave processor +
1 megabyte memory |

The instrument can contain 14 triple slot eurocards and two double slot cards for interfacing a microscope, a terminal and a printer. A Motorola 68000 microprocessor serves as control processor for this instrument of which the basic idea is to combine rapid image analysis based on mathematical morphology (Meyer, 1979; Serra, 1982) with conventional pattern recognition analysis; the latter being carried out in slave processors (Motorola 68000). The basic configuration of the instrument is depicted in table 4.1. In the near future a DNA measuring card and a card for individual analysis of objects will be added. The binary processor and the grey value processor, using mathematical morphology algorithms, take care of rapid scene segmentation and analysis of particles in the microscope field. The basic time cycle for this type of operation in the MIAC is 20 milliseconds.

With the MIAC 512 x 512 pixels, as generated by the Plumbicon TV tube, are stored directly in the computer memory, using a high speed analog to digital conversion. Although these systems suffer from the limited signal to noise ratio of TV based systems, they are extremely fast for biomedical work, since basic morphology transformations can be carried out on an image of 512 x 512 pixels in 20 milliseconds, once the system has loaded the TV signal (40 msec).

Chapter 4.3 SOFTWARE.

The present generation of prescreening instruments uses either nuclear parameters only (LEYTAS, van Driel-Kulker and Ploem, 1982; CERVIFIP, Tucker and Husain, 1981) or a combination of nuclear and cytoplasmic parameters (BioPEPR, Zahniser et al, 1979; FAZYTAN, Reinhardt et al, 1979; CYBEST, Tanaka et al, 1979). Both LEYTAS and CERVIFIP use derivatives from the nuclear DNA content to select abnormal nuclei ('top hat' transformation for LEYTAS, integrated optical density (IOD) of haematoxylin stained nuclei for CERVIFIP) followed by the application of shape parameters for artefact rejection. BioPEPR as well as LEYTAS use a hierarchical tree structure for classification of objects. On the other hand, FAZYTAN uses a feature set of 360 parameters to describe each of the cells.

The study which formed the basis for the automated prescreening using LEYTAS is an interactive study performed by Ploem-Zaayer et al (Ploem-Zaayer et al, 1979). They showed a high correlation between the presence of cells with strongly elevated DNA content ($>5C$) and the presence of a precancerous or cancerous lesion of the cervix. In this study, cells to be measured were visually selected during screening of an entire slide containing 30,000 to 60,000 cells. All cells on the slide with a visually expected elevated DNA content were measured, as opposed to other studies where only a limited number of randomly selected cells was measured (Atkin, 1959, Boehm et al, 1971). Based on this study, the DNA content of cell nuclei was selected to form the basic parameter in the automated screening for abnormal cells in cervical specimens.

Since the TAS has been specially developed for the execution of image transformations, they form the essential tools of which the program is constituted. The transformations described in this thesis are expressed as mathematical morphology. All image analysis programs applied in this study have been written by Meyer F. from the Institute of Mathematical Morphology in Fontainebleau, France. The applied transformations are extensively discussed in his thesis (Meyer, 1979). Although it is not the author's competency to discuss algorithms, a short description will be given with the emphasis on the optimization of the transformations for this specific application. If the reader wants more detail about mathematical morphology, he or she is referred to the following publications: Matheron, 1967; Matheron, 1975; Meyer, 1978; Meyer, 1979; Serra, 1982.

Chapter 4.3.1 SELECTION OF CELLS.

Segmentation.

In contrast to visual selection of abnormal cells, by which the eye/brain combination works efficiently enough to distinguish nuclei from cytoplasm, background and artefacts in only one glance, image analysis systems need several segmentation and imaging routines to render comparable information. At first a segmentation algorithm is used to separate nuclei from background.

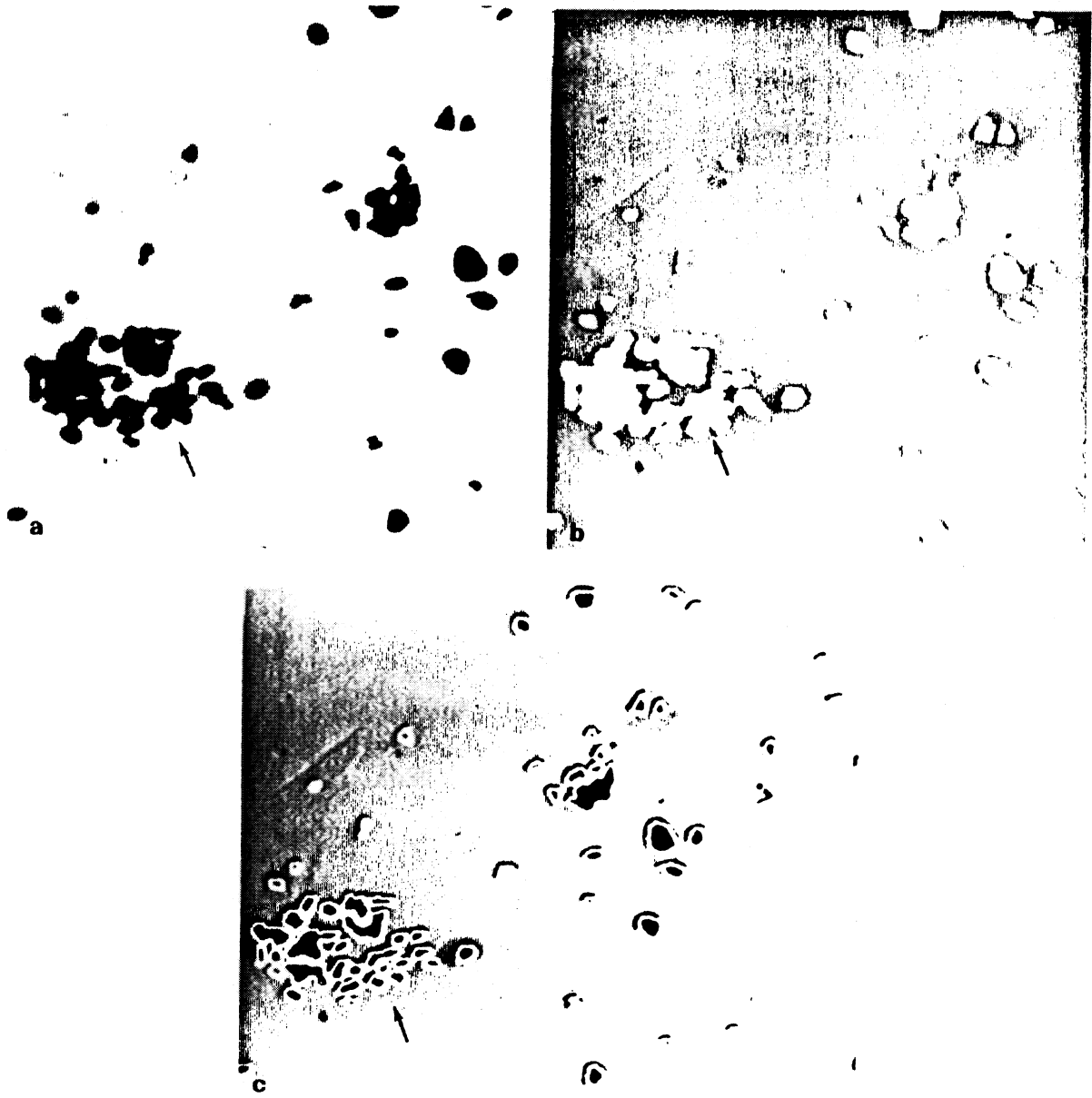


Figure 14a,b and c: Photographs taken from the TAS monitor (LEYTAS-1). Figure 14a displays the analogue image of a microscope field to be analyzed. Nuclear segmentation using thresholding (figure 14b) results in the connection of almost touching nuclei (see arrow). In figure 14c, the result is displayed when segmentation is performed using gradient detection. Many of the nuclei have been detected separately.

The type of segmentation algorithm is highly dependent upon the used staining procedure. If cells have been stained with e.g. a Feulgen procedure or galloxyaniline, only the nuclei will be visualized, resulting in relatively simple scene segmentation algorithms. On the other hand, most staining procedures used for visual interpretation of cells, e.g. the Papanicolaou staining, are characterized by the simultaneous visualization of nucleus and cytoplasm. In most cases, the nuclear image can be distinguished from the cytoplasmic image by a color difference as well as by an intensity difference, the absolute values of both being rather irreproducible from cell to cell and from specimen to specimen.

As AFS staining results in separate images of nuclei and cytoplasms, segmentation of nuclei can be based on thresholding only. However, problems arise when nuclei are almost touching. Using thresholding only, nuclei which almost touch are easily connected during segmentation as can be seen in figure 14b. As a result they will be rejected as an artefact in a later phase of the analysis. For this reason, a nuclear segmentation algorithm originally applied for Papanicolaou stained images, has also been implemented in the program which analyses AFS stained specimens (figure 14c). This segmentation algorithm is based on the detection of zones with high gradient and has been described by Meyer and Van Driel (Meyer and Van Driel, 1986). Since LEYTAS-1 has no grey value but only binary image processors, the detection of zones with high gradient is performed using the rather time-consuming procedure of combining thresholds, erosions and dilatations. To reduce the use of these time-consuming algorithms, they are activated exclusively, once a rapid test (to be explained later in this paragraph) has indicated the presence of any objects of interest in the microscope field under examination. If not, nuclear segmentation takes place every 20th microscope field to render information about the number of epithelial cells. All objects which remain after a predetermined size threshold on the segmented image and after the artefact rejection transformations, are counted as epithelial cells. This number should be appreciated as a very rough (and often under-) estimation of all epithelial cells present, since only intermediate cell nuclei are counted by this procedure. Because of the similarity between superficial cell nuclei and contaminating leukocytes in terms of image analysis, most of the superficial cells are not counted.

Cell selection.

The rapid test which is performed on every microscope field consists of deformations at predetermined grey value settings, which leads to the indication of the presence of any objects passing a certain size and/or intensity threshold. If no objects pass this algorithm, the next microscope field will be analyzed. If any object passes, gradient detection is activated. Once the nuclear contours have been detected, a test is activated to select only those nuclei which have an elevated DNA content. This test ('top hat' transformation, Meyer, 1979) consists of combinations of grey value thresholds and deformations and includes the elimination of most nuclei displaying normal DNA content as well as the elimination of large size artefacts.

The top hat transformation as it is executed using mathematical morphology, has been described by Meyer (Meyer, 1979). It has been developed to select cells with an increased DNA content rapidly. Roughly spoken, the transformation combines different greyvalue thresholds with size estimations in order to select cells on the basis of nuclear contrast and size (figure 15b). Two fixed combinations are used at present differing both in contrast and size requirements.

The variable settings of sizes and grey value thresholds used in the 'top hat' transformation were determined using a sequential method of testing.

Sequential testing of parameters on a slide basis can easily be performed by LEYTAS since thousands of cells per slide can be analyzed and tested for a certain parameter in a relatively short time. Testing of the different selection criteria for the 'top hat' transformation takes only a few minutes owing to the hardwired logic of the TAS. During the testing period, artefact elimination was performed visually.

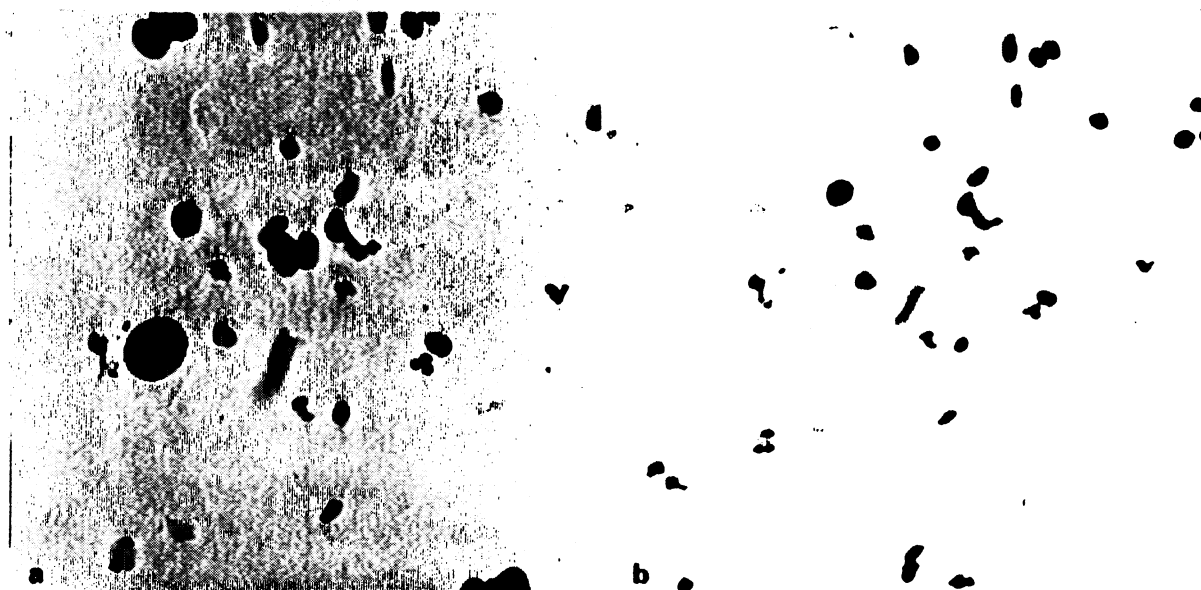


Figure 15a and b: Figure 15a is a microphotograph of AFS stained cervical cells. Apart from single small nuclei, several overlapping nuclei as well as one single enlarged nucleus is present. Figure 15b is a photograph taken from the TAS monitor, after execution of the 'top hat' transformation. The single enlarged nucleus as well as the overlapping nuclei have been detected. These objects will subsequently be tested by several artefact rejection routines (see figure 15c,d and e).

To serve as a learning set about 150 preparations were selected. About 70% consisted of negative samples (normal or inflammatory lesions). The remaining number were positive specimens consisting of cases with severe dysplasia, carcinoma in situ or invasive carcinoma. Using alternate testing of the positive and negative specimens, selection criteria were selected which detected no or almost no nuclei in negative specimens but detected some single nuclei in almost all positive specimens. As will be shown in the results, the specificity of this criterium, called 'high level' (HL), is high; the average number of HL nuclei selected in positive specimens proved to be 1600 x higher than the average number of nuclei detected in negative specimens. However, the absolute number of cells selected per positive specimen is relatively low, being an average of 32 per positive specimen.

To enhance the sensitivity of the cell selection, a 'low level' (LL) criterium was determined to select more cells in the positive specimens. A small number of cells selected in the negative specimens was now accepted. To determine the LL settings, the same method of alternate testing of positive and negative specimens was used. Although the number of cells detected per specimen varied considerably, the average number of LL cells selected per positive specimen (-270) is 68x more than the average number detected in the negative specimens (-4) as will be shown in chapter 5.2. For a better insight in the results of the image analysis programs, one should understand that HL cells are always a subset of the LL cells. The screening procedure runs using

the LL settings. Only after an object has been detected by the LL settings, the HL criteria are activated to test that nucleus.

The fact that fixed greyvalue thresholds are used for cell selection explains why so much effort has been put in the development of a reproducible staining procedure. Finally, a more sophisticated procedure will be desired, including an internal correction for slight staining alterations (a potential solution is given in chapter 4.3.4 by using the TCPA program) as well as a more accurate estimation of the 'top hat' transformation. The latter can easily be obtained by applying a more extensive set of threshold combinations. With LEYTAS-1, containing only one bit memories, this would result in a delay in the screening time. Since LEYTAS-2 is equipped with a grey value processor, a more accurate assessment of the 'top hat' transformation can be obtained in one basic cycle time.

Chapter 4.3.2 REJECTION OF ARTEFACTS.

Only those objects which pass the 'top hat' transformation are tested with several artefact rejection routines using a hierarchical tree structure. This means that objects continue into the tree only when previously applied artefact rejection algorithms classified the objects as a potential single nucleus. The application of the used artefact rejection algorithms have been published by Meyer (Meyer, 1979), and are tested in the following sequence:

1. a 'top hat' transformation with limited size and high contrast settings recognizes all condense objects of small size, where upon they are eliminated. The objective of this transformation is to eliminate overlapping lymphocytes and intensely stained dirt particles.
2. the inverted 'top hat' transformation recognizes highly contrasted areas that can occur when highly condensed cells (leucocytes) are grouped together, by detecting background between some of the cells.

These types of transformations can be executed relatively rapidly. Once objects pass these routines, relatively slow transformations will be executed based on the shape of the objects. First, shape is measured using image transformations executed on entire microscope fields; subsequently the bending energy (implemented by Smeulders (Smeulders, 1983)) is measured of the contours of individually passing objects.

Shape by image transformations.

The used shape measure is called the conditional bisectrix (CB) and should be considered as a derivative from a skeleton operation. The main difference between a conditional bisectrix and the skeleton is its connectivity; whereas the connectivity is always maintained in a skeleton operation, it can be lost using the conditional bisectrix.

Assuming the shape of a cell resembles that of a circle, the following requirements are set for passing the transformation after construction of the conditional bisectrix:

1. The CB should remain connected (figure 15c).
2. The skeleton of the CB should consist of one line without side branches. (If side branches have been formed, points can be detected having neighbours at three sides, whereas the maximum of neighbours in an unbranched line is 2.
3. The skeleton of the CB should not be longer than a predetermined size (if the CB does not vanish after the subtraction of a predetermined number of points, it is considered too long (figure 15d)).

If the object is not eliminated by any of the criteria set for the conditional bisectrix, another shape routine related to the bending energy, which is executed in software, is activated.

Bending Energy.

A shape feature widely used in biomedical analysis is the mean bending energy normalized to perimeter, according to Bowie and Young (Bowie and Young, 1977) The name has been derived from the physical energy needed to bend a rod into the shape of the object. It can be demonstrated that a circle has the minimum average bending energy of all closed objects. In a study performed by Smeulders (Smeulders, 1983) in our laboratory, it was found that the bending energy, plus parameters derived from the most concave and convex parts of the objects, was suited to differentiate between remaining artefacts and single nuclei.



Figure 15c and d: Objects selected by the 'top hat' transformation (see figure 15b) are tested by several shape parameters. In figure 15c the conditional bisectrix (CB) has been constructed. The CB of the two overlapping nuclei (arrows) becomes disconnected. As a consequence, they will be rejected. The skeleton of remaining objects is tested for its length. Objects with a skeleton longer than a predetermined size (see arrow in figure 15d) will be rejected as well.



Figure 15e: Of all cells present in the microscope field under investigation (figure 15a,b,c,d), only the enlarged nucleus remains detected after artefact rejection (indicated by the white rim around the object).

Chapter 4.3.3 PERFORMANCE OF DIFFERENT IMAGE ANALYSIS ALGORITHMS.

In this chapter the performance of the different image analysis transformations on the object level will be discussed. First the results of the individual transformations will be given followed by results of the combined transformations.

One of the consequences of using iterative transformations in image analysis is that comparison of the individual performances of the different algorithms should be done with care. This is caused by the iterative character, which includes that each transformation is carried out on an image resulting from a previous transformation and therefore all transformations are dependent upon all previously applied ones. An alteration in one of the transformations, can drastically change the performance of all following ones. This should be kept in mind when interpreting the performance results of all individual transformations.

For the screening results, two counts are of particular importance: the number of alarms and the epithelial cell count; the LEYTAS classification is based on these two counts. For that reason we have evaluated the performance of the different transformations which lead to these numbers. The epithelial cell count is carried out on intermediate epithelial cells, together with basal, parabasal and endocervical cells but excludes superficial epithelial cells on the basis of size. A practical argument for not counting superficial epithelial cells is that, based on nuclear information at a low magnification, the cell is hardly distinguishable from leucocytes. Malcounting of only relatively low numbers of leucocytes will result in an enormous increase of the reference cell population as soon as inflammatory conditions arise. To prevent this, the superficial cells are not included in the counted number of epithelial cells. As the epithelial cell count serves as a reference value for the number of alarms, it should as closely as possible, reflect the biologically relevant cell population. This cell population is better estimated by excluding white blood cells and superficial cells than by including both these types.

The number of alarms refer to all objects selected by the 'low level' settings of the 'top hat' transformation. The performance at the object level of the 'high level' settings have not been investigated here, since HL selected objects will not be used for specimen classification.

In this study the number of 'atypical' cells were visually counted separately from the 'abnormal' cells. An 'atypical' cell was defined as an abnormal cell which could also be present under benign inflammatory conditions. An 'abnormal' cell is considered to be abnormal to such an extent that they occur exclusively under (pre)malignant conditions.

Information about effect of individual transformations on the different cell types cannot be obtained during the routine screening; only the final result, after the application of all transformations is stored. Therefore a small study was performed on 50 slides, where the number of visually identifiable epithelial cells were counted in 5 microscope fields per slide and compared with the numbers counted by LEYTAS. The presence of atypical and/or abnormal cells was evaluated in 32 microscope fields of 250 x 250 μm per slide. The results of all intermediate transformations have been evaluated separately.

Selection of preparations.

Since these types of studies are extremely time-consuming, we decided to investigate only a limited number of microscope fields. Either a limited number of slides, or a limited number of microscope fields per slide was necessary to achieve that. Since the variation of cell types between different specimens is usually much larger than the variation found when

comparing different parts of one specimens, especially in suspension preparations, we have chosen for a relatively large number of slides ($n=50$) and only few microscope fields per slide ($n=5$). Both positive and negative samples should be equally present in the series. Dysplastic cases were left out because of the known difficulty of the cytomorphological diagnosis on the single cell level (Bacus, 1982). The positive and negative preparations were selected such that their total number of alarms exhibited a random representation over all slides from that diagnostic group. The distribution of the number of alarms in all diagnostic groups of specimens is given in chapter 5.3. Slides were selected with the following alarm counts per 1600 microscope fields:

Table 4.2: Number of specimens and corresponding alarm numbers, selected to test the performance of image transformations on the object level.

negative specimens		positive specimens	
alarm number	number of slides	alarm number	number of slides
0 - 5	12	0 - 50	3
5 - 10	6	50 - 100	4
10 - 15	3	100 - 200	6
15 - 20	1	200 - 300	4
20 - 40	2	300 - 400	1
40 - 60	1	400 - 500	1
60 - ~	1	500 - 600	1
		600 - 900	1
		900 - 1200	1
		1200 - 1500	1
		1500 - ~	1
total	26		24

The microscope fields to be investigated were selected randomly by the computer over the entire bucket area on the microscope glass.

In each microscope field to be investigated, a cytologist counted visually the number of intermediate epithelial cells, the number of 'atypical' cells and the number of 'abnormal' cells. Then the screening program was activated using a 'HALT' command after each transformation. In this way the result of each transformation can be observed on the TAS monitor. A total of 250 microscope fields have been examined, containing 14110 cells (= total cell count, including leucocytes). The areas in the negative specimens contained 6835 cells from 26 different specimens, whereas the investigated areas from the 24 positive specimens contained 7275 cells.

Evaluation of LEYTAS count of normal intermediate cell nuclei.

In table 4.3 the number of visually identified intermediate epithelial cells are given together with the effect of the transformations for selection and artefact rejection.

As can be seen in table 4.3, the largest number of objects selected by an erosion of size 3 on the segmented image are single epithelial cells. In fact 70.5% of all selected events, without any artefact elimination, are already epithelial cells (526 out of 746). After artefact elimination this ratio has increased to 83.7% (456 out of 545).

Table 4.3: Performance of the epithelial cell count transformations on a total of 540 visually counted epithelial cells.

type of object (visual ident)	* LEYTAS							
	visual count	total select	artef 1	artef 2	artef 3	artef 4	artef 5	remain
single epi	540	526	0.4%	2.3%	1.8%	7.6%	1.7%	86.7%=456
>= 2 epi		74	-	8.1	27.9	38.8	36.7	25.7%= 19
epi + leuco		27	-	-	18.5	31.8	13.3	48.1%= 13
>= 2 leuco		93	1.1	5.4	11.5	18.2	23.8	51.6%= 48
dirt		26	-	15.4	13.6	42.1	18.2	34.6%= 9
total number of epithelial cells counted by LEYTAS =								545

- * - total select is the number of objects which remain after an erosion of 3 on the segmented image.
- the numbers given under the artefact rejection (artef) procedures are the percentages of eliminated objects by that parameter. Remaining objects from the previous transformation serve as the reference number (=100%).
- artef 1 is the elimination of leucocytes using 'top hat' transformations.
- artef 2 is the elimination of objects touching the border.
- artef 3, 4 and 5 are parameters derived from the conditional bisectrix. 3 is the loss of connectivity, 4 is the formation of a triple point of the skelet and 5 is a skelet longer than a predetermined size.
- remain = the percentage of all selected objects which remain after the artefact elimination algorithms.

All separate transformations eliminate nuclei as well as artefacts. The higher the difference in performance between nuclei and artefacts, the better the transformation. Artef 3, 4 and 5, all three derivatives from the conditional bisectrix, perform well. On the other hand, the leucocyte elimination (artef 1) has hardly any effect both on nuclei as well as on artefacts. It should be considered to remove this algorithm or otherwise change it into one with a better performance. Artef 2, the elimination of objects touching the border of the field to be analyzed, is a practical solution and should not be considered a real artefact elimination algorithm. In fact it will remove more large sized objects since there is a higher chance that they will touch the border of the field.

The number of visually identified intermediate epithelial cells in this study is 540. The total number of LEYTAS counted epithelial cells is 545 (101%). This is a good correlation, although it should be realised that an average of 83.7% of this LEYTAS count is caused by visually confirmed epithelial cells. Remaining objects are groups of 2 or more leucocytes

(8.8%), groups of 2 or more epithelial cells (3.5%), epithelial cells overlapping with one or more leucocytes (2.4%) and dirt particles (1.6%). An overview of this distribution is given in table 4.4.

Table 4.4: Visual classification of LEYTAS counted reference cells.

single epithelial cells	83.7%
leucocyte overlaps	8.8%
epithelial cell overlaps	3.5%
leucocyte overlap with epithelial cell	2.4%
dirt particles	1.6%
LEYTAS epithelial cell count	<u>100.0%</u>

Evaluation of alarm count.

Detection of alarms is the most important process for LEYTAS in the automatic screening program. As explained in chapter 4.3.1. the selection is based on the 'top hat' transformation, whereas the artefact rejection transformations are similar to the ones used for the epithelial cell count. One artefact elimination routine is added, namely the one derived from the bending energy. In the fields under investigation the visual counts consisted of 159 single 'atypical' nuclei and 116 single 'abnormal' nuclei. In table 4.5 the effect of the image transformations on these nuclei as well as on other objects, are given. The parameter derived from the bending energy will be evaluated separately, later on in this chapter.

Regarding the 'top hat' procedure for selection of objects, we see that about half (53.5%) of all atypical cells and 84% of all visually abnormal cells have been selected. Of the 85 selected atypical cells, only 1 has been selected in a negative slide. No normal cells have been selected. This is no coincidence since the trimming of the LL settings of the 'top hat' transformation has been in such a way that it should select only few cells in negative specimens as was discussed in chapter 4.3.1. If we consider all single cells, visually identified as atypical or abnormal as objects to be selected, we see that the 'top hat' transformation succeeds in 66.5% (85+98 selected from 159+116 visually present). Regarding all objects selected by the 'top hat' transformation (395), the number of relevant objects (single cells) constitute 46.3% of these.

Considering the different artefact rejection routines applied in the screening program, we see wide variations between the 5 different algorithms (table 4.5). Also the performance of one algorithm can highly vary depending on the tested object, e.g. artef 5 (a measure of the nuclear shape by demanding a maximal skeleton length) is highly effective in eliminating groups of cells (line 3, 61.5%), groups of leucocytes (line 7, 60.0%) and dirt (line 8, 60.0%), whereas nuclei, either normal, atypical or abnormal, overlapping with one or more leucocytes (line 4 and 5) are not recognized by this procedure as an artefact. If we consider the performance of the different rejection procedures separately, we see that also for the alarm count, as was found for the epithelial cell count, artef 1 (leucocyte elimination) can be omitted or otherwise should be adapted into an effective algorithm. Artef 2 is necessary because it eliminates objects touching the border. It can be seen in table 4.5 that the larger the object, the higher the chance it reaches the edge of the field, resulting in elimination. It must be said here, that because of this elimination of border objects, subsequent microscope fields for screening, overlap 30 μ m in order not to lose any abnormal cells for that reason.

Table 4.5: Performance of the alarm detection transformations on visually identified objects.

type of objects (visual class)	* LEYTAS						
	total select	artef 1	artef 2	artef 3	artef 4	artef 5	remain
single atypical (n=159)	85 (53.5%)	0.0%	1.2%	2.4%	0.0%	6.1%	90.5% = 77
single abnormal (n=116)	98 (84.5%)	1.0	4.1	0.0	3.2	3.3	88.8% = 87
>=2 atyp or abnor (n=27)	19 (70.4%)	0.0	10.5	17.6	7.1	61.5	26.3% = 5
abn/atyp +leuko	17	0.0	5.9	12.5	35.7	0.0	52.9% = 9
epi norm + leuco	8	0.0	0.0	0.0	87.5	0.0	12.5% = 1
>=2 epi normal	63	1.6	4.8	13.6	48.9	33.3	25.3% = 16
>=2 leuco	35	0.0	20.0	35.7	44.4	60.0	11.4% = 4
dirt	70	1.4	10.1	25.0	10.5	60.0	14.3% = 10
total number of LEYTAS selected alarms=							209

- total select is the number of objects selected using the 'top hat' transformation. Between brackets: the ratio is given to the number of visually identified objects.
- the meaning of artef 1-5 are the same as given under table 4.3
- the numbers given under the artef procedures are the percentages of eliminated objects by that parameter. Remaining objects from the previous transformation serve as the reference number (=100%).
- remain = the percentage of all selected objects which remain after the artefact rejection transformations.

As was found with the epithelial cell count, artef 3,4 and 5 (derivatives from the conditional bisectrix) perform well: the percentage of single cells eliminated by the combined three transformations is 7.3 whereas this amounts to 75.5% for all non-single nuclei.

After the 'top hat' selection, single nuclei constituted 46.3% of all

selected objects. After artefact rejection, this ratio has increased to 78.5%. Regarding the total number of visually identified atypical and abnormal nuclei (table 4.6) 48.4% of atypical nuclei and 75.0% of abnormal nuclei were positively classified by LEYTAS. This results in a correct classification of 59.6% of all cytomorphologically relevant nuclei.

Table 4.6: Performance of LEYTAS image transformations in selecting visually abnormal cell nuclei.

visual classification	visual count	total select	eliminated	remain	% per visual count
atypical nuclei	159	85	8	77	48.4%
abnormal nuclei	116	98	11	87	75.0%
atypical + abnormal	275	183	19	164	59.6%

Discussion.

Results obtained in this study should be interpreted with caution. First of all because the study encompasses such a limited number of cells which prevents the use of statistics predicting the significance of the different tests. The reason why this study is so limited is mentioned in the beginning of this chapter. Although we have published several papers about the performance of LEYTAS on a slide basis, these are the first data obtained on the object level. Of course, any automated procedure for screening cervical cancer will be evaluated on its performance on the slide level and not on the object level. On the other hand, the acceptance of an automated procedure by the medical community ((cyto)pathologist) will be enhanced if the objects used for slide classification, are recognizable as relevant objects. For that reason a good correlation between machine selected cells and cytomorphologically abnormal cells is important.

The second reason to be cautious about these type of studies is because the cytomorphological diagnosis on the cellular level is known to vary highly among different cytologists (Bacus, 1982). The object classification in this study is based on the opinion of one (experienced) cytotechnologist. Of course the visual differentiation between single and non-single nuclei is quite evident in most cases. The cytomorphological evaluation of single nuclei, however, is something quite different. This has been the reason that none of the applied transformations have been 'tuned' on the object level, but on the preparation level. Although variation also exists on the slide level between cytopathologists (Evans et al, 1974) the consistency of the slide diagnosis is considerably higher than the cell classification.

Evaluation of parameter derived from the bending energy.

Since the bending energy parameter has been added several years later than the basic screening program consisting of image transformations, its performance has been evaluated on a relatively large number of objects before implementation. A total of 282 specimens have been analyzed with the basic screening program, while the performance of the bending energy was tested.

These specimens consisted of 143 negative specimens, 105 specimens with a cytological diagnosis of mild or moderate dysplasia (76 mild dysplasia and 29 moderate dysplasia) and 34 positive specimens. Preparations in none of the diagnostic groups have been selected randomly. The negative specimens in this series have been artificially enriched with inflammatory specimens, whereas dysplasia and positive specimens have been enriched with specimens of which the number of LEYTAS selected alarms (without the use of bending energy) fell just above the decision threshold (see chapter 5.3). This has been done to render as much insight as possible on a limited number of specimens, in the effect of the parameter in (false) positive and (false) negative classification results. In these 282 specimens, 21272 single nuclei have been selected (see table 4.7) using the image transformations described in the first part of this chapter. Of these 21272 single cells 598 (2.8%) were erroneously classified as artefacts by the bending energy parameter. Of the 3728 overlapping nuclei selected by the transformations, 1228 (=32.9%) were correctly classified as artefact, whereas 45.7% of the selected dirt particles (1014 out of 2220) could also be recognized as artefacts by the bending energy.

Table 4.7: Performance evaluation at the object level of parameter derived from the bending energy, in 282 specimens.

visual classification	number of selected objects by transformations.	number of objects classified as artefact using bending energy.
single cell nuclei	21272	598 (2.8%)
overlapping nuclei	3728	1228 (32.9%)
dirt	2220	1014 (45.7%)

Considering the fact that the parameter derived from the bending energy and from the most concave and convex part of the object, is only applied for objects which pass the image transformations for artefact rejection, it can be concluded that it is indeed a useful parameter in discriminating single nuclei from non-single nuclei.

In table 4.8, the effect of the bending energy parameter on the specimen level has been evaluated.

As can be seen in table 4.8, the implementation of the bending energy reduced the number of false positively classified specimens from 20 to 10 for the 85 negative specimens and from 38 to 30 for the 58 inflammatory specimens. A combination of these two diagnostic groups results in a reduction of false positively classified specimens of 12.6 % (from 40.6% to 28.0%). On the other hand 4 specimens with a diagnosis of mild dysplasia (out of 76) and 1 with a diagnosis of moderate dysplasia (out of 29) have additionally been classified negative using the bending energy parameter. There were no extra false negative classifications in the group of positive specimens (severe dysplasia or more serious lesions).

Based on these results, the parameter derived from the bending energy and the most concave and convex part of the object, has been implemented as an additional artefact rejection routine.

Table 4.8: Evaluation of the bending energy parameter on the specimen classification.

cytological diagnosis	* LEYTAS classification			
	without bending energy		with bending energy	
	neg	pos	neg	pos
negative n= 85	65	20	75	10
inflammatory n= 58	20	38	28	30
mild dysplasia n= 76	10	66	14	62
mod. dysplasia n= 29	1	28	2	27
positive n= 34	1	33	1	33

* Decision thresholds and their rationale are explained in chapter 5.3.

Chapter 4.3.4 TOTAL CELL POPULATION ANALYSIS.

Based on the experience gained with the screening program, a second program has been developed which describes the entire cell population concerning nuclear size and absorption. Although the screening program selects cell nuclei on the basis of size and absorption, no information is gained about the non-selected cells. When the total cell population is described, calculation of the abnormal cell population can be done once all data are stored in the computer, allowing a more flexible and statistically relevant treatment of the data. Furthermore slight changes in the staining intensity can be detected by analysis of the normal cell population, which enables correction in the greyvalue data of potentially abnormal cells.

Image analysis.

The basic image analysis algorithms are similar to those described for the screening program and, like the screening program, it has been written by Meyer. Segmentation is performed as explained in chapter 4.3.1 on each field in which any objects are present. No 'top hat' transformation is applied for cell selection. Artefact rejection algorithms by mathematical morphology, as explained in chapter 4.3.2 are executed on all segmented objects. Remaining objects are tested for their size and greyvalue density. The size of the objects is expressed in the maximal number of dodecagonal erosions which they survive, which proved to vary between 1 and 7. The greyvalue density is expressed in 15 levels, varying between 80% and 10% light absorption.

Results.

The results of the total cell population analysis are demonstrated in a matrix with the nuclear grey value density on the x-axis and the nuclear size on the y-axis. Examples of 2 matrices are given; figure 16 is derived from a typical negative specimen and figure 17 is from a typical positive specimen. The software of the program was constructed such that all cells belonging to predetermined size and/or greyvalue categories, could be relocated. Using this facility it was found that the first two rows consisted predominantly of epithelial cells and (degenerated) leukocytes. Most intact morphologically normal epithelial cells were found in the second row, which can therefore be used best as the reference row for normal cells. With regard to the greyvalue density distribution in the second row, a peak is almost always found in the fifth or sixth column. Relocation of all cells in the peak value in 10 negative preparations, demonstrated the following objects:

Table 4.9: Visual identification of objects causing peak values in the second row of the matrix.

Intermediate squamous cells	63%
Metaplastic/endocervical cells	25%
Leukocytes, degenerated cells, overlaps, dirt	12%
Total=	<u>100%</u>

As is demonstrated in table 4.9, intermediate squamous epithelial cells represent the largest proportion of all objects in the peak. This justifies the use of the peak position for correction of the staining intensity. Of all cases investigated up to date (109), only very few cases

demonstrated a peak shifted to the second or third column. In all these cases morphological examination of the investigated specimen indicated a large amount of degenerated intermediate cell nuclei often accompanying an inflammatory process. What is not clear yet is whether this inflammatory process also effects the abnormal cells. Another problem still under investigation is the question whether a distinction can be made between non-biological phenomena (e.g. caused by the preparation and staining procedure) and biological phenomena (e.g. degeneration of cells caused by inflammatory processes).

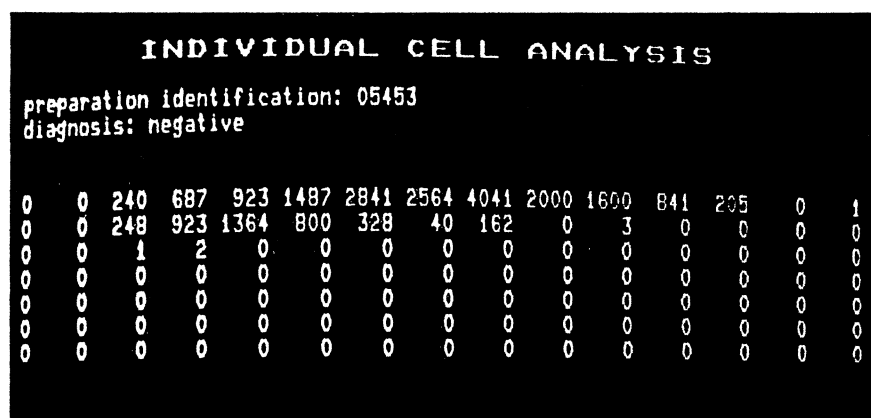


Figure 16: An example of a matrix, by which the data output of the TCPA program is presented. The x axis represents increasing grey values of nuclear densities. The y axis represents increasing values of nuclear size. This example is obtained from a negative specimen.

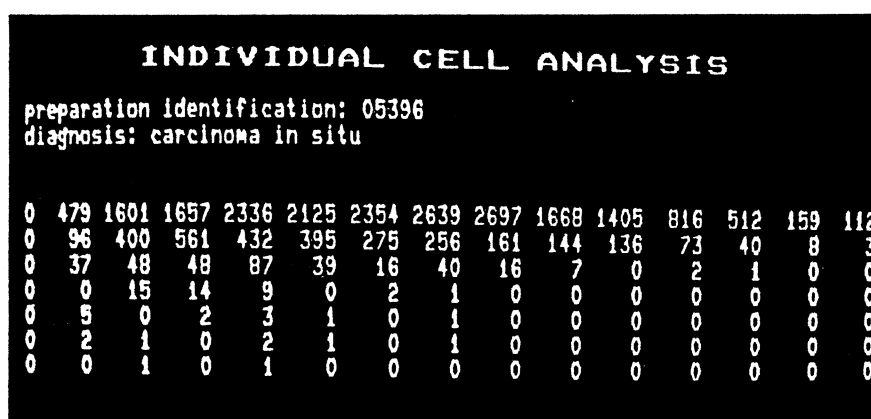


Figure 17: An example of data output from a positive specimen analyzed with the TCPA program. Note the shift of numbers to the right (higher nuclear densities) and downwards (larger nuclear sizes) when compared with the previous figure.

To test the capacity of this new program in the classification of cervical specimens, a pilot study has been carried out consisting of 109 specimens. The results are presented in chapter 6.5.

CHAPTER 5

AUTOMATICALLY SELECTED OBJECTS IN CERVICAL SPECIMENS

Chapter 5.1 INTRODUCTION.

As was explained in chapter 4.3.1, two sets of 'top hat' transformations have been determined using the method of sequential testing. One was named 'high level' ('HL') and had been adjusted such that cells were selected almost exclusively in positive preparations. The second was named 'low level' ('LL') and was adjusted such that more cells were selected in the positive preparations to enhance the sensitivity. The frequency of these cell types in negative, dysplasia and positive preparations will be discussed in chapter 5.2 including an evaluation of the reported frequencies of tumor cells in cervical specimens using visual cytodiagnosis. In chapter 5.3 the number of alarms (= selected cell nuclei + selected artefacts) in negative, dysplasia and positive specimens will be discussed with regard to automated classification of specimens.

Chapter 5.2 FREQUENCY OF SELECTED ABNORMAL CELLS.

After determination of the HL and LL settings their cell selection performances were tested on the learning set of 96 specimens with a cytological diagnosis of normal or inflammation ('negative') and 64 specimens with a cytological diagnosis of severe dysplasia, carcinoma in situ, squamous cell carcinoma or adenocarcinoma ('positive'). Specimens with a cytomorphological diagnosis of mild and moderate dysplasia were left out of this study in the learning phase of the project. The reason for this is the high uncertainty which is encountered in the cytological diagnosis of dysplasia, as has been reported in several studies (Ringsted et al, 1978; Bacus, 1982). First the results of the 'HL' and 'LL' settings on the 96 negative and 64 positive preparations will be discussed. These will be followed by the results of the HL and LL settings on the test set (total series). All LEYTAS results in this chapter have been obtained after visual elimination of remaining artefacts, so that only detected single nuclei are taken into consideration. Therefore these numbers cannot be extrapolated to automated screening. The next part of this chapter (chapter 5.3) will present the results as they have been obtained without visual interference. These data can then be extrapolated to automated specimen classification which will be discussed in chapter 6.

Number of cells selected by HL settings.

No single nuclei were selected in 94 of the 96 negative specimens after analysis of the entire bucket area on the microscope slide (1 square cm), containing on the average about 30,000 cells. In each of the two remaining specimens one nucleus was detected. Testing of the HL criteria on the 64 positive specimens resulted in the detection of single nuclei in 59 specimens. The average number of HL nuclei in all positive preparations was 32, varying from 0 to 490 selected nuclei per specimen (see table 5.1).

Number of cells selected by LL settings.

In 66 of the 96 negative specimens and in all positive specimens, cells were selected with the LL settings. The average number of LL nuclei selected in the negative specimens was 4, varying from 0 to 66 per specimen, whereas an average of 270 nuclei were selected per positive specimen showing a variation from 4 to 4290 selected nuclei per specimen (see table 5.1).

Table 5.1: average number of nuclei selected by 'high level' (HL) and 'low level' (LL) settings in negative and positive specimens.

	average number of HL nuclei	average number of LL nuclei
negative specimens (n=96)	0.02	4
positive specimens (n=64)	32	270

As can be concluded from these results, the detection of HL nuclei (cells) is a highly specific phenomenon which occurs almost exclusively in positive specimens. In fact HL nuclei occur 1600x (average) more often in positive

preparations than in negative preparations. The number of nuclei however is so low (32 as an average per positive specimen), that, from a statistical point of view, the chance of missing the rare cells is relatively high. A much more sensitive parameter is the LL criterium; cells are then found in all positive cases, but also in more than half of the negative preparations.

This study, in which only extreme diagnoses were used to test the screening capacity of the two cell selection settings, proves the fact that a clear correlation exists between a cytomorphological diagnosis, based on visually selected abnormal cells, and a potential machine diagnosis based on automatically selected cells. Nevertheless the number of HL cells of 5 positive specimens overlapped with those from 2 negative specimens whereas the number of LL cells from 6 positive specimens overlapped with the number found in 2 negative specimens.

Cell selection in a larger series.

First the image analysis algorithms were further optimized in an attempt to reduce the overlap between the negative and the positive preparations. This was achieved by an improvement in the nuclear segmentation. Nuclear segmentation using fixed thresholds (the method applied in the previous study) works sufficient if all objects are well separated. However, when nuclei lie close, they are easily connected by this algorithm, even when the nuclei are not touching. The developed gradient detection (chapter 4.3.1) proved to detect more nuclei, especially in crowded preparations. The cell selection criteria together with the gradient method for nuclear segmentation were then tested on a larger number of random cases including those with intermediate diagnoses (mild and moderate dysplasia).

Another remark that should be made before discussing the results, concerns the diagnostic groups. Since this chapter does not discuss automated screening, but primarily deals with objective determination of certain biological phenomena, the extensive cytomorphological description of each slide has been 'translated' into one of the following groups:

- normal ('NOR'): includes completely negative and inflammatory lesions.
- dysplasia ('DYS'): includes mild and moderate dysplasia of the squamous epithelium as well as mild and moderate atypia from the glandular epithelium.
- positive ('POS'): includes severe dysplasia and more severe lesions from the squamous epithelium as well as severe atypia and more serious lesions from the glandular epithelium.

Furthermore not all slides of the total series that will be presented in chapter 6.2, are represented here. This has been done for the following reason: In this study the group 'NOR' is composed exclusively of cellular material from healthy women without any complaints. These specimens have been taken from women visiting an anti conception clinic. Therefore the proportion of completely normal versus inflammatory specimens will be a good estimation of this distribution in a random female population. On the other hand, the total series mentioned in chapter 6.2, is mainly derived from hospital clinics from patients with complaints or specific problems. Thus the inflammatory specimens will be overrepresented in this group of hospital patients. The 'dysplasia' and 'positive' cases are represented by all cases with such diagnoses irrespective where they came from. Only those cases have been taken into account which have been analyzed with the optimized nuclear segmentation program.

Results.

In table 5.2 and 5.3, data of automatically selected HL and LL cells per diagnosis group are given.

Table 5.2: Automatically selected HL cells in a series of 972 specimens.

cytological diagnosis	number of HL cell nuclei per specimen				
	average	s.d.	min	max	median
NOR (n=554)	.13	.53	0	14	0
DYS (n=271)	11.2	30.2	0	378	5
POS (n=147)	42.7	115.4	0	988	18

Table 5.3: Automatically selected LL cells in a series of 972 specimens.

cytological diagnosis	number of LL cell nuclei per specimen				
	average	s.d.	min	max	median
NOR (n=554)	6.8	12.7	0	123	3
DYS (n=271)	84.8	165.4	1	2111	42
POS (n=147)	339.8	664.3	4	5846	146

As can be deduced from the statistical data given in table 5.2 and 5.3, the distribution of the parameters per specimen is not-Gaussian. This limits the use of statistics developed for normal distributions. For that reason, the average values as given in table 5.2 and 5.3 are of limited use in comparing the HL and LL parameters for the different groups of specimens. A better method to compare these type of distributions is to take e.g. the 90% value of the cumulative histograms; that is the cumulative parameter value which is not exceeded by 90% of the cases. The cumulative frequency histograms of both the HL and LL numbers are given in figure 18 and 19. A logarithmic scale is used to represent the numbers of selected cells on the y-axis, because of the large differences in cell numbers found between the different specimens. To enable a logarithmic representation, all 0 values have been changed into 1. This implies that specimens with 0 or with 1 selected cell cannot be differentiated on the basis of the graphical representation. The 90% values for the different diagnostic groups are summarized in table 5.4.

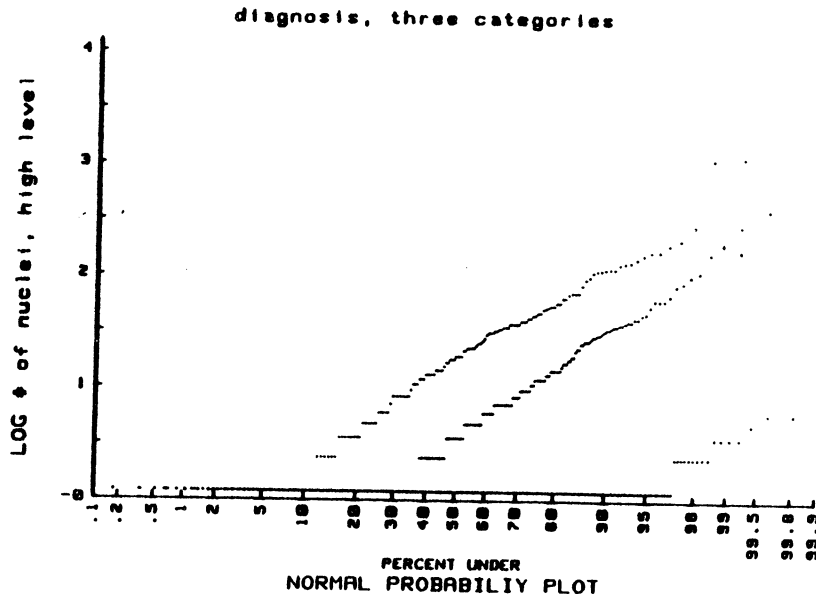


Figure 18: The cumulative frequency histogram of the number of 'high level' detected cells per specimen. The lowest line represents the negative specimens; the line in the middle, the dysplastic specimens and the upper line represents the positive specimens.

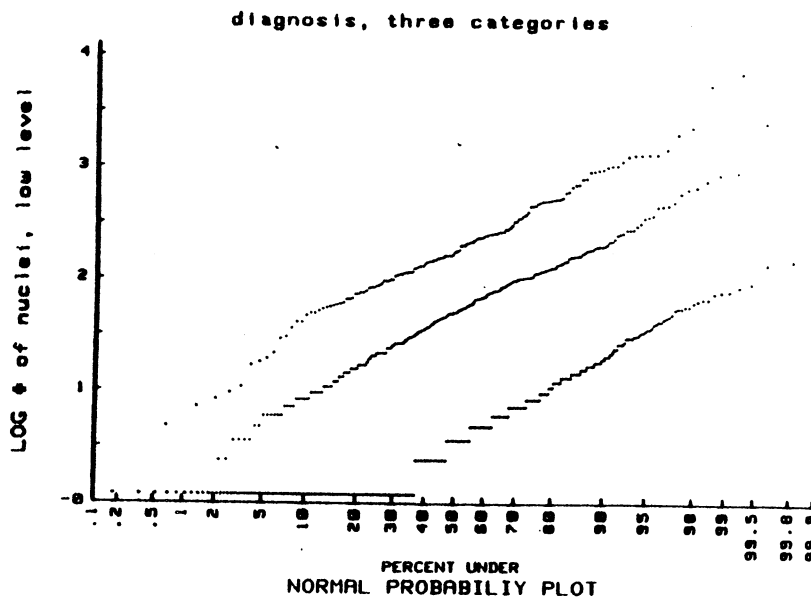


Figure 19: The cumulative frequency histogram of the number of 'low level' detected cells per specimen. The lower line represents the negative specimens; the line in the middle, the dysplastic specimens; the upper line represents the positive specimens.

Table 5.4: 90% values of 3 diagnostic groups for 2 parameters as calculated from the cumulative histogram.

cytological diagnosis	90% values	
	number of LL nuclei	number of HL nuclei
NEG	14	0/1
DYS	158	10
POS	708	100

The two independent sample test of Kolmogorov Smirnov (Kolmogorov, 1941) can be used to compare cumulative frequency histograms. In table 5.5 the Kolmogorov Smirnov (KS) distance is given for both parameters when comparing the different diagnostic groups (first and second column) followed by the minimal KS distance to obtain 99% significancy (third column).

Table 5.5. Kolmogorov Smirnov (KS) distances of both parameters when comparing different diagnostic groups.

	KS distance		
	LL nuclei	HL nuclei	critical region at 99% level
NEG/DYS	.6783	.5910	.1208
DYS/POS	.4498	.3938	.1670

When comparing the KS distances with the critical region for 99% significance, we see that all three diagnostic classes are significantly different from each other for both the HL and the LL nuclei (table 5.5). It can also be deducted from this table that the separation which is obtained with LL nuclei is better than for HL nuclei. Observation of the histograms shows that no HL nuclei have been detected in a high number of cases; about 97% of the negative and 10% of the positive specimens have no HL nuclei (or only 1, due to the log scale), indicating the highly specific character of the parameter. On the other hand LL nuclei occur more frequently namely in 99.5% of the positive specimens and in 37% of the negative specimens.

Discussion.

In this chapter results have been presented from automated cell selection. In fact two types of 'abnormal' cells have been defined, both highly correlated with the visual cytodiagnosis but differing both in sensitivity and in specificity. The literature contains some papers in which ratios of

abnormal cells are mentioned. Bibbo et al (Chicago) published three papers about the numerical composition of cervical samples. They found an average of three single abnormal cells per 2000 epithelial cells per smear (average of the vaginal, cervical and the endocervical smear which are in use by the Chicago group) in 25 cases of mild dysplasia (Bibbo et al, 1976). This number was seven in 25 cases with moderate dysplasia, 83 in cases with carcinoma in situ and 88 in cases with invasive carcinoma. By the Quebec automation group two papers have been published (Feldman et al, 1973; Louis et al, 1976) reporting an average of 121 (range 18-357) single abnormal cells in dysplastic smears, 183 in 70 carcinoma in situ smears and an average of 78 (range from 4-357) abnormal cells in routine smears diagnosed as invasive carcinoma. Neugebauer et al (Munich) reported an average of 69 (range 0 - 162) single abnormal cells per routine smear with a diagnosis of mild or moderate dysplasia (Neugebauer et al, 1981). This number was 125 (range 41-318) for dysplastic or CIS smears and 868 (range 444-4425) for invasive carcinoma smears. From the group of King (San Fransisco), Barrett et al reported abnormal cell frequencies varying from 0.049 to 1.52% in centrifugal cytology preparations from 15 cases of dysplasia to carcinoma in situ (Barrett et al, 1979). An overview of these results is given in table 5.6.

Table 5.6: Average numbers of isolated abnormal cells in cervical samples.

different laborato- ries	average numbers of abnormal cells in different diagnostic groups *						
	1	1/2	2	2/3	3/4	4	5
**	***						
Chicago	3 (25)		7 (25)			83 (25)	88 (25)
Quebec				121 (50)		183 (70)	78(120)
Munich		69 (6)			125 (9)		868 (6)
San Fransisco				0.049-1.52% (15)			
	average numbers of LEYTAS detected LL and HL cells for different groups of diagnoses.						
	1/2				3/4/5		
low level	85 (271)				340 (147)		
high level	11 (271)				43 (147)		

- * 1= mild dysplasia
 2= moderate dysplasia
 3= severe dysplasia
 4= carcinoma in situ
 5= invasive carcinoma

** in contrast to the other groups who counted the number of abnormal cells in the entire smear, these numbers are found per 2000 normal epithelial cells.

*** between brackets the number of investigated smears is given.

Care must be taken to evaluate these results since each group has used slightly different protocols. E.g. the Chicago group did not extrapolate their findings to the total smear as did the other groups. Other differences may be caused by sample taking. Bibbo et al showed that the number of abnormal cells varies highly between the type of smear (vaginal, cervical or endocervical). An important parameter is the definition of 'isolated cells'. For instance in the Chicago study, the total cell (including its cytoplasm) should lie isolated, whereas slight overlap of cytoplasm is permitted in the Quebec study. From most groups only the absolute numbers have been given in the table, partly because some groups did not give percentages, but also to prevent variations in the different results to be caused by the use of a different reference cell population e.g. epithelial cells can be used as reference cells for the Chicago study, whereas Barrett et al uses the total number of cells including leucocytes, as reference cells. Notwithstanding these drawbacks, there is a certain concurrence in these visual countings.

If we compare the cell numbers automatically selected by the LL and HL criteria with the visually counted numbers, we conclude that the numbers of automatically selected cells are not far outside the range of reported numbers of visually abnormal cells (table 5.6). The number of selected LL nuclei is somewhat higher, whereas the number of HL nuclei is somewhat lower than the visual counts of abnormal cells. The question can be asked which cell is really abnormal. The definition of an abnormal cell on a single cell basis on cytomorphological grounds have proved to be a big problem (Bacus, 1982). Also in our laboratory we have tried to classify single cells (Smeulders, 1983) but the consistency between two independent cytologists proved to be too low to allow any valid conclusions. Of course, the correlation of numbers itself does not prove the fact that HL and LL cells are indeed abnormal cells. But if additionally, as shown in chapter 4.3.3, most automatically selected nuclei are cytologically classified as 'atypical' or 'abnormal', it can only be concluded that the LEYTAS classification and the cytomorphological diagnosis in principle are based on the same type of information. There is however at least one big difference, which lies in the reproducibility. The reproducibility of machine selected cells can be considered high (see chapter 6.3). This is in contrast with the visual diagnosis of abnormal cells, either on a single cell basis (Bacus, 1982) or on a smear basis (Evans et al, 1974; Bacus, 1982) or on a histological section basis (Ringsted et al, 1978). This again proves the need for objectivation in cytology.

In the following part of this chapter, the data obtained with 'high level' settings will not be further explored. The reason for this is that in an early phase of the project it became clear, that the frequency of the HL nuclei could never contribute significantly to the completely automatic classification. Although a highly sensitive parameter, the number of selected nuclei is so low, that even the low number of artefacts as detected by LEYTAS, easily form the majority of alarms. Therefore the presence of HL alarms is not evaluated for its significance in the automated machine classification.

Chapter 5.3 FREQUENCY OF SELECTED ALARMS.

In this chapter the frequency of the alarms and the subdivision of these alarms per diagnostic group will be presented. Unlike in the first part of this chapter, the number of objects selected with the HL settings will no longer be discussed, because of considerations discussed in chapter 5.2. Besides the use of the absolute number of LL alarms, the relative number of LL alarms to the number of epithelial cells proved to be significant for classification purposes. This is due to the fact that an elevated number of LL alarms in negative specimens was often accompanied by a high number of epithelial cells. In those cases the relative number of LL alarms was not enlarged. The use of the relative number alone for classification purposes is limited by those negative cases where relatively few epithelial cells are present. It was found that the combination of the absolute with the relative number of alarms finally gives the best results. In the beginning, the relative number of alarms was calculated on the total cell count. This counting procedure however, offers only an approximation of the number of epithelial cells. Especially in preparations with many leukocytes, total cell counts can be extremely high ($> 100,000$), whereas the visual estimation of the number of epithelial cells showed that only a minority of this high number was caused by epithelial cells. Therefore, an epithelial cell count was developed (chapter 4.3) to be used as the reference cell population. It should be clear that the use of these two parameters (absolute and relative number of alarms) for classification is in fact an estimation of one parameter namely: the signal to noise ratio in selection of alarms in relation to the signal sensitivity of the system.

Because finally, both the absolute and the relative number of alarms will be used for specimen classification, data will be presented of both (correlated) parameters. If decision thresholds and alarm numbers are given in relation to specimen classification, they always refer to objects selected with the LL settings.

In table 5.7, the visual classification of all alarms in 'single nuclei', 'overlapping nuclei' and 'dirt' are given per diagnostic group.

Table 5.7: Visual classification of alarms in different diagnostic groups.

cytological diagnosis	average number of objects per specimen			
	total alarms	single nuclei	overlapping nuclei	dirt
NOR (n=554)	11.5	6.8	2.4	2.3
DYS (n=271)	98.2	84.8	9.6	3.8
POS (n=147)	374.9	339.8	24.6	10.5

It is clear from table 5.7 that the large differences in selected abnormal cells as presented in the previous chapter, are still present when we look at the total number of alarms; in other words, the number of selected artefacts could be kept sufficiently low. Striking is the fact that more artefacts (especially overlapping nuclei) have been selected in the positive specimens than in the negative specimens. Most of the overlapping nuclei in positive specimens have indeed been diagnosed as containing one or more abnormal

nuclei. Therefore further optimization studies for artefact rejection will be directed towards the elimination of dirt particles.

In table 5.8 and table 5.9 some basic statistical data is given of the number and the percentage of alarms respectively.

Table 5.8: Some statistical data on numbers of alarms per specimen.

cytological diagnosis	average	s.d.	min	max	median
NOR (554)	11.5	16.2	0	141	6
DYS (271)	98.2	174.6	1	2200	53
POS (147)	374.9	689.3	6	6092	164

Table 5.9: Some statistical data of the percentage of alarms per specimen.

cytological diagnosis	average	s.d.	min	max	median
NOR (554)	0.24	0.27	0	2.67	0.17
DYS (271)	1.45	1.60	0	9.83	0.90
POS (147)	3.02	2.12	0.25	9.84	2.31

For the same reasons as described in chapter 5.2, the use of cumulative frequency histograms with thereto belonging statistics has been applied. In figure 20 and 21, the cumulative frequency histograms are given of the absolute and relative numbers of alarms respectively. The values for both parameters at the 90% level are given in table 5.10.

Table 5.10: Parameters derived from the cumulative frequency histograms for the number and the percentage of alarms per diagnostic group.

cytological diagnosis	90% values	
	# alarms	% alarms
NOR (n=554)	25	0.447
DYS (n=271)	200	3.162
POS (n=147)	1259	5.623

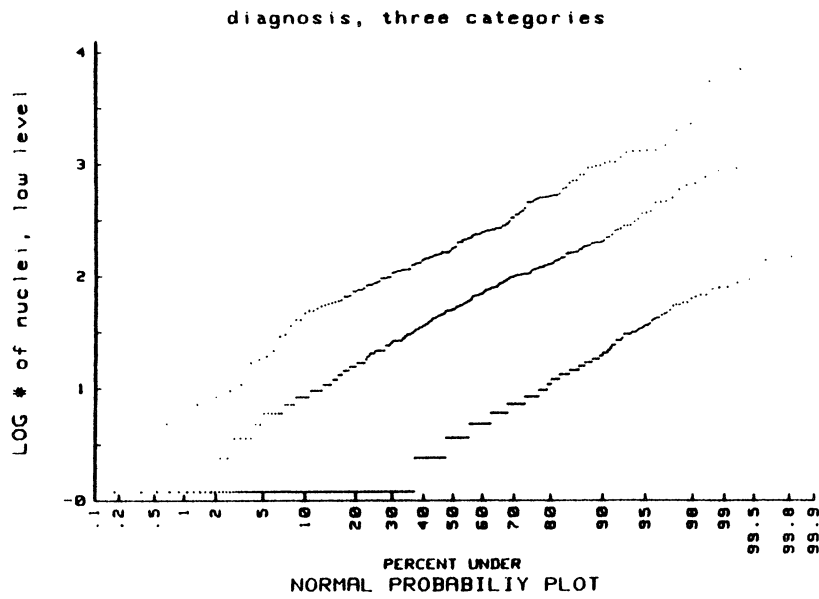


Figure 20: The cumulative frequency histogram of the total number of alarms per specimen. The lower line represents the negative specimens; the line in the middle, the dysplastic specimens; the upper line represents the positive specimens.

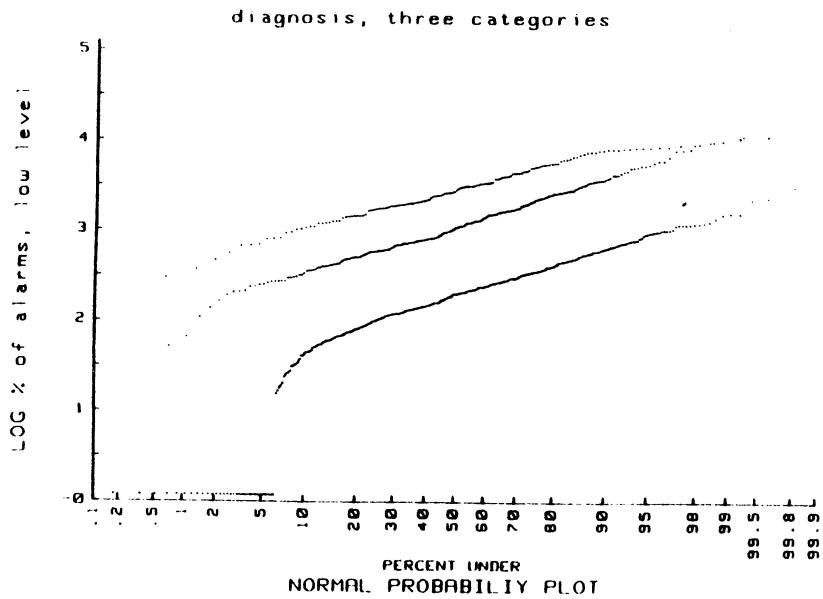


Figure 21: The cumulative frequency histogram of the percentage of alarms per epithelial cells ($\times 1000$). The lower line represents the negative specimens; the line in the middle, the dysplastic specimens; the upper line represents the positive specimens.

As in the previous part of this chapter the Kolmogorov Smirnov (KS) two sample test (Kolmogorov, 1941) has been used to compare the histograms of the different diagnostic groups. In table 5.11 the KS distance is given for both the absolute and the relative number of alarms when comparing the different diagnostic groups.

Table 5.11: Kolmogorov Smirnov (KS) distances of the absolute and the relative number of alarms, when 2 different diagnostic groups are compared.

cytological diagnosis	KS distance		
	# alarms	% alarms	critical region at 99% level
NEG/DYS	.6658	.6713	.1208
DYS/POS	.4682	.4488	.1670

When comparing the KS distances with the critical distance for 99% significance, we see that all three diagnostic classes are significantly different for both the relative as the absolute number of alarms (table 5.11). As is to be expected from the high correlation between the absolute and the relative number of alarms, the distance between the different diagnostic groups is similar for the two parameters.

Selected thresholds for specimen classification.

Since a false positive specimen error and a false negative specimen error do not carry equal weight, a decision threshold has been selected which gives as few missed positive classifications as possible, whereas the false positive rate is still within limits. These criteria were fulfilled at a minimal value of 10 alarms combined with a minimal value of 0.3% of alarms. The decision making involving these two parameters can also be represented according to figure 22. The number of analyzed epithelial cells is given on the x axis and the number of alarms is given on the y axis. Each point represents a specimen. The positive region is separated from the negative region by two lines: $A=10$ and $A=0.3C$. The combination of these lines can be regarded as an estimation of a logarithmic curve, which is well known in detection systems. It results from the lower limit of the system sensitivity combined with the signal to noise ratio.

A second representation of the data is given in figure 23. The axes represent the same units as figure 22. The average values as well as the 50% and 90% confidence limits are plotted for all investigated specimens in the three diagnostic groups. It can be seen that no overlap between the number of alarms in negative versus dysplasia and positive specimens occur for the 50% boundaries. Even the 90% boundaries of the negative specimens do not overlap with those of the positive specimens; the 90% boundaries of dysplasia specimens overlap with both the negative and the positive specimens.

Specimen classification results obtained with these decision thresholds are presented in chapter 6.

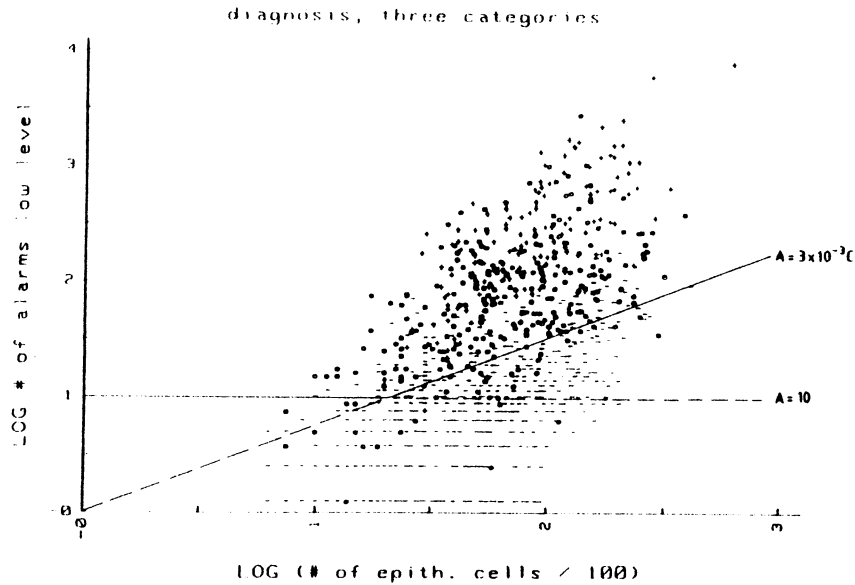


Figure 22: A scattergram including all specimens. The x axis represents the number of epithelial cells per specimen. The y axis represents the number of alarms per specimen. The decision thresholds used for classification of specimens are indicated by the two lines $A=10$ and $A=10^{-3}C$. All specimens falling above the undotted line, will be classified positive. The negative specimens are represented by -; the dysplastic specimens by o; the positive specimens by +.

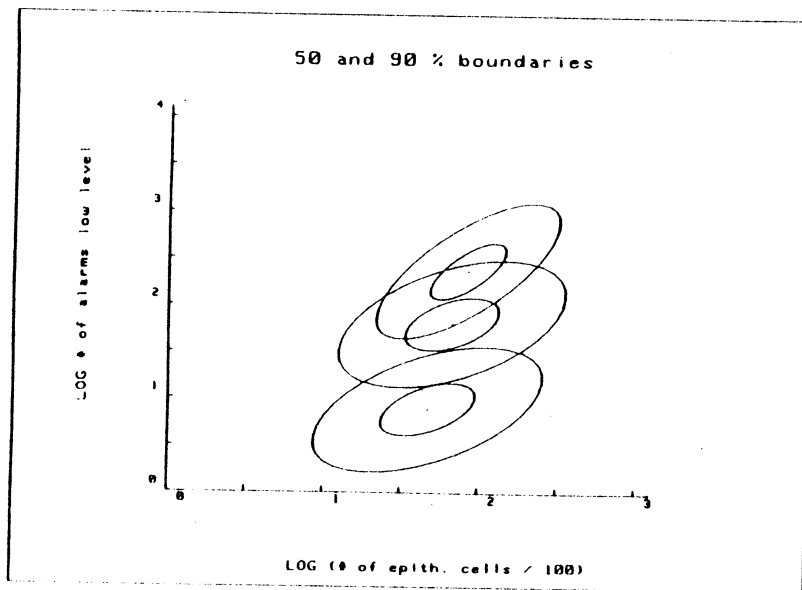


Figure 23: The x and y axis represent the same units as in the previous figure. The average values as well as the 50% and 90% confidence boundaries are plotted of the three diagnostic groups. Lower boundaries represent the negative specimens; the boundaries in the middle represent the dysplastic specimens; the upper boundaries represent the positive specimens.

CHAPTER 6

LEYTAS CLASSIFICATION OF CERVICAL SPECIMENS

Chapter 6.1 INTRODUCTION.

In this chapter, the classification of specimens based upon all LEYTAS selected alarms, consisting of abnormal cells and artefacts (as presented in chapter 5.3) will be discussed. After this machine diagnosis follows a second classification step, during which the alarms are displayed to allow visual interpretation of the selected objects. This will lead to a second interactive machine diagnosis. Results of both classification levels will be presented in chapter 6.2 and discussed together with the results obtained by comparable systems. In chapter 6.3 the reproducibility of the specimen classification will be discussed after a certain time period and when analyzing different preparations from the same cell sample. Chapter 6.4 and 6.5 both contain the results of pilot studies. In chapter 6.4 results are given of a first attempt to analyze conventional smears in stead of centrifugation preparations. In the last part of this chapter classification results are given as they can be obtained using the Total Cell Population Analysis (TCPA) program.

Chapter 6.2 RESULTS IN CENTRIFUGE PREPARATIONS.

A continuous series of 1500 AFS stained cervical preparations has been subjected to analysis with LEYTAS-1. The process of typing the slide identification into the terminal and putting the slide into the holder and in focus is followed by a completely automated screening procedure without interaction from the operator. Since centrifugal cytology warrants the deposition of cells on a specified location of the object glass, initialization of the stage is done by computer.

There was no visual selection of the preparations before LEYTAS analysis; each sample which arrived at our laboratory has been investigated. The only quality control was done by LEYTAS. If less than 500 epithelial cells were counted, the cellularity of the sample was considered too poor for a machine diagnosis. Using this limitation 41 preparations were disqualified, which amounts to 2.7% unsatisfactory specimens. The Papanicolaou stained parallel preparations of these 41 specimens were diagnosed negative in 39 cases and pointed to a dysplasia in 2 cases (one mild and one moderate dysplasia). The cellularity of these preparations was also poor.

The results from the remaining 1459 preparations are given in table 6.1

Table 6.1: Analysis of acriflavine-Feulgen-SITS stained cervical specimens using LEYTAS-I

Morphological diagnosis	Machine classification	
	negative	positive
Negative (663)	577	86
Inflammation (209)	106	103
Mild dysplasia (184)	29	155
Moderate dysplasia (82)	7	75
Positive (321)	1	320
Total 1459		

In the left column of table 6.1, the cytomorphological diagnosis of the parallel Papanicolaou stained preparation is given. This diagnosis represents the combined opinion of at least 2, but if necessary 3 experienced cytologists. Since these parallel preparations are derived from the same cell suspensions as the preparations analyzed with LEYTAS, both cell populations can be expected to be similar. The machine classification, that is a classification without operator interaction, discriminates the preparations into negative and positive on the basis of the detection of a minimal number of alarms ($n=10$) and a minimal ratio of alarms per counted epithelial cells ($=0.3\%$).

The number of false positively classified preparations is 86 on a total of 663 negative cervical specimens (13%, see Table 6.2) and 103 on a total of 209 specimens with cellular changes due to inflammation. In the group of mild and moderate dysplasia 29 (15.8%) and 7 (8.5%) cases respectively were not detected by the machine. Sometimes the misclassification could be explained by paucity of abnormal cells (mainly mild dysplasia) or by poor cellular

preservation. The group of moderate dysplasia also encompasses the diagnosis Papanicolaou class III, which is often given if atypical cells are seen of which the preservation is insufficient to give a more detailed diagnosis. The program for the total cell population analysis (TCPA) appears to be better suited for these cases (see chapter 6.5) From the large number of morphologically positive preparations (severe dysplasia and more serious lesions), only one preparation was missed by LEYTAS. This concerned a case of cervical adenocarcinoma, cytologically diagnosed as severe atypia of endocervical cells. Another parallel preparation from this cell sample was stained and analyzed resulting in a positive LEYTAS classification. This is not mentioned in the table since only the results of the first preparation of all cell samples have been given. A total of fourteen histologically proven adenocarcinomas were included in this analyzed series; all except the previously mentioned case were classified as positive by LEYTAS.

Table 6.2 displays the false positive and false negative rates for the machine diagnoses in the 1459 preparations.

Table 6.2: False Positive Rates (FPR) and False Negative Rates (FNR) of acriflavine-Feulgen-SITS stained cervical specimens using LEYTAS-I.

Morphological diagnosis	Machine Classification		Confidence limits for 95% confidence level	
	FNR	FPR	FNR	FPR
negative (663)		13.0%		10.5-15.9%
inflammation (209)		49.3%		41.7-56.3%
mild dysplasia (184)	15.8%		10.8-22.3%	
moderate dysplasia (82)	8.5%		3.5-16.9%	
positive (321)	0.3%		0.0- 1.7%	

The given confidence limits have been computed from a 95% confidence level. These numbers represent an estimation of the minimal and maximal errors that the system can make on the investigated set of specimens.

The preparations classified as positive by the machine can be evaluated further by including a human interaction step in the classification procedure. This has been realized by the storage of greyvalue images of selected events in the computer during the screening procedure. After the screening is terminated, these stored images are displayed to allow visual recognition and subsequent elimination of non-rejected artefacts (non-single nuclei). This type of interaction can be executed rapidly (less than a minute) because 16 of these stored images are displayed simultaneously on one TV screen. The operator/cytologist decides, on the basis of the stored images, whether there are any potentially abnormal cell nuclei among them. If not, the number of visually recognized false alarms (artefacts) is subtracted from the total number. The same decision criteria as used for the first machine classification (absolute number of 10 or 0.3%) are now applied to obtain a second interactive machine diagnosis. Using this procedure the FPR for negative specimens reduces from 13.0 to 8.0% whereas the FNR for positive specimens remains unchanged as can be seen in table 6.3.

Table 6.3: Analysis of AFS stained cervical specimens using LEYTAS-I; results after interaction.

morphological diagnosis	LEYTAS classification	
	FNR	FPR
negative (663)		8.0%
inflammation (209)		39.2%
mild dysplasia (184)	19.6%	
moderate dysplasia (82)	9.8%	
positive (321)	0.3%	

The false positive rate for inflammatory specimens is reduced with 10% to 39.2%. The impact of visual interaction for dysplasia specimens is limited; the FNR increases from 15.8 to 19.6% and from 8.5 to 9.8% for mild and moderate dysplasia respectively. The difference in positively classified specimens between a classification with and without interaction is caused by the fact that the human eye recognized artefacts which had not been automatically rejected by the machine.

For verification of the machine classification and for a final cytomorphological diagnosis, the selected cells can be relocated in the microscope. In this study, relocation has been carried out to enable a correct recognition of artefacts, since the stored greyvalue images, meant for this purpose, were of relatively low quality. An evaluation of the performance of a cytologist using machine selected cells was not possible in an accurate way since in many cases the LEYTAS operator was not trained in cytology.

Since the 1459 analyzed cervical samples were obtained in gynecologic clinics, atypical and abnormal samples constituted a relatively high proportion of all specimens. For that reason, the specimens with inflammation have been evaluated separately from the non-inflammatory specimens in the given total series (table 6.1, 6.2 and 6.3). Eventually, however, the system FPR will be calculated from all negative specimens in the population including those with inflammatory changes. To obtain information on the expected false positive rate in a population screening program, cervical samples from a birth control center were analyzed with LEYTAS. The proportion of inflammatory specimens can be expected to be similar to the frequency of such specimens in a population screening program. Table 6.4 shows the results in this consecutive series of specimens.

It is demonstrated that 16% of all normal preparations (negative + inflammation) are false positively classified by the LEYTAS machine classification. The addition of rapid visual interaction reduces the FPR to 11%. It is expected that these figures represent the FPR in a population screening program if analysis is to be carried out with LEYTAS.

Table 6.4: Results of LEYTAS analysis of AFS stained cervical specimens from a birth control center; machine diagnosis.

morphological diagnosis	machine classification		
	negative	positive	FPR
negative (471)	417	54	16% (11%)*
inflammation (92)	55	37	

* between brackets: FPR using rapid interaction.

Comparison between LEYTAS-1 and LEYTAS-2.

To evaluate the screening capabilities of LEYTAS-2 in comparison to LEYTAS-1 a limited series of preparations has been analyzed using both systems. While the time needed for machine analysis is reduced considerably, cell counts and numbers of selected cells using LEYTAS-1 and -2 show a high concurrence (table 6.5).

Table 6.5: Comparison of LEYTAS-1 and LEYTAS-2 analysis of 10 positive AFS stained cervical specimens.

	LEYTAS-1	LEYTAS-2
Epithelial cell count	8060	7840
Detected single cells	718	740

As with LEYTAS-1, the average number of selected cells is considerably higher in morphologically positive than in morphologically negative specimens as can be seen in table 6.6.

Table 6.6: LEYTAS-2 analysis of 10 AFS stained cervical specimens.

	average numbers of selected objects	
	negative	positive
alarms	17	732
single nuclei	6	619

The average number of alarms is 17 for the negative specimens and 732 for the positive specimens. The larger part of these alarms are caused by nuclei (6 out of 17 and 619 out of 732).

Discussion.

A practical study of cervical specimens has been described including results of a large number of investigated cases. Other automated screening systems which have published a high number of cases are CYBEST (n=9,010, Mukawa et al, 1983) and BioPEPR (n=3,444, Zahniser et al, 1980). Although the total amount of specimens in our study (n=1,459) is lower, it contains the highest number of abnormal cases (n= 587 versus 113 (CYBEST, Tanaka et al, 1979) and 57 (BioPEPR)).

Although reports of other systems have considered all specimens from abnormal lesions as one group, we deliberately separated those lesions which were diagnosed cytomorphologically as mild or moderate dysplasia from the positive lesions (severe dysplasia, carcinoma in situ and invasive carcinoma). The reasons for this are 1) the different therapeutic consequences for the patient and 2) the uncertainty involved in the cytomorphological and histopathological diagnosis of dysplasia (Ringsted et al, 1978). Therefore optimization of the screening program in the learning phase of the project has been performed exclusively on negative and positive specimens (van Driel and Ploem, 1982). It was only in the test phase that dysplastic cases entered the trial.

To compare classification of specimens with results obtained by other systems, we can evaluate the performance at two different levels. One is a specimen classification without any human intervention. Three systems have obtained these types of results on a sufficient number of specimens: CYBEST, BioPEPR and FAZYTAN. The false positive rate of CYBEST was 28.3% in a series of 9010 preparations (Mukawa et al, 1983). Two out of 113 cases with dysplasia or more serious lesions were erroneously classified as negative (1.8%). The system rejected 7.0% because of inadequate specimens. BioPEPR analyzed a series of 3387 negative specimens and 57 abnormal specimens (mild dysplasia and more serious lesions). This resulted in a false positive rate of 24.6%, a rejection rate of 5.2% and a missed positive rate of 3.5% (Zahniser et al, 1980). FAZYTAN reports a false positive rate of 13%, 30% missed positive classifications on mild or moderate dysplasia and 3% missed positives on a total of 180 specimens (Beer and Ostheimer, 1984). LEYTAS reports a false positive rate of 16% of 461 investigated cases, 15.8% of mild dysplasia (out of 184 cases), 8.5% of moderate dysplasia (out of 82 cases) and 0.3% of severe dysplasia and more serious lesions (out of 321 cases) have been false negatively classified. The rejection rate of LEYTAS is 2.7% (Ploem et al, 1986).

Thus the LEYTAS false positive rate is lower than the false positive rates obtained by CYBEST and BioPEPR. Besides a potentially better performance of LEYTAS, this might be caused by 2 facts: 1. The number of analyzed specimens with LEYTAS is insufficient. CYBEST and BioPEPR analyzed many more specimens. 2. The trade-off value for positive/negative was not chosen identical for the different systems. For BioPEPR and CYBEST, mild dysplasia was considered a lesion which should be detected, whereas LEYTAS was optimized to discriminate between negative lesions and severe dysplasia or more serious lesions. The latter reason also explains the difficulty in comparing false negative results. In the LEYTAS strategy, the negative classification of a specimen with a cytological diagnosis of mild dysplasia is considered less severe than the negative classification of e.g. a carcinoma in situ lesion. In the results of other systems, no difference is often made between these different cytological categories.

In contrast to CYBEST, FAZYTAN and BioPEPR, LEYTAS offers a second interactive classification. Results obtained at that level can e.g. be compared with CERVIFIP, which has been developed as a prescreener of potentially abnormal cells. The CERVIFIP classification is the cytology diagnosis given on CERVIFIP selected events. The latest CERVIFIP report

includes a false positive rate of 18% on a series of 79 negative preparations. Out of 50 positive slides (severe inflammation and more serious lesions) 4% was missed. The total rejection rate was 25% (Tucker and Husain, 1981). At this level the LEYTAS false positive rate = 11%, whereas 19.6% of the mild dysplasia, 9.8% of the moderate dysplasia and 0.3% of the positive specimens have been false negatively classified. As mentioned before the LEYTAS rejection rate is 2.7%

For CYBEST, BioPEPR and FAZYTAN holds that the morphological diagnosis of the conventional smear, which has been made simultaneously (directly before or after) with the suspension used for automated analysis, has been used as the reference diagnosis. CERVIFIP uses the cytological diagnosis of the suspension preparation used for automated analysis as the reference diagnosis. LEYTAS uses the cytological diagnosis of the Papanicolaou stained parallel preparation. Although all systems agree in the use of the morphological diagnosis as the reference diagnosis, it is not without drawbacks. Both the histological and the cytological diagnosis are known to vary from person to person (Evans et al, 1974; Ringsted et al, 1978). However, other reference diagnoses are not available.

If the diagnosis of a smear other than the one analyzed by the machine is taken as the reference, there is also a chance that different cell types are present, even when the samples have been taken with only several minutes interval (Sedlis et al). In our study we found that the diagnosis of the conventional smear taken simultaneously with the cell suspension did not always correlate. In 8 cases the cytological diagnosis of the suspension preparation was positive, whereas the diagnosis of the conventional smear was negative. On the other hand, we found 7 cases of which the suspension preparation did not contain abnormal cells, but where the diagnosis of the conventional smear was positive. Thus false negative samples are randomly distributed over conventional smears and suspension preparations. Therefore we conclude that a selective loss of abnormal cells induced by the applied preparation technique is highly unlikely.

If we compare the speed of the different systems, we find that CYBEST reports 3 minutes to analyze the entire slide (number of cells unknown). BioPEPR uses 4 minutes to analyze 6 photonegatives which are necessary to establish the diagnosis. An average of 5000 cells were analyzed this way. FAZYTAN needs about 2 hours for the analysis of 3000-4000 cells, but the new version of the system should run with considerably more speed. CERVIFIP needs less than 3 minutes to select the potentially abnormal cells in the entire slide. The system also stops when 20,000 cells have been analyzed. To arrive at a diagnosis, the time should be added that a cytologist need to diagnose the selected events. The time needed for analyzing an entire slide (average total cell count of 90,000 cells) with LEYTAS-1 is between 45 and 60 minutes. The present speed with LEYTAS-2 is between 5 and 10 minutes.

Besides the acceleration possibilities in the screening program of LEYTAS-2 due to the MIAC structure, the screening has been speeded up 4 times by enlargement of the microscope fields with this factor. This was made possible by the construction of an entire new microscope (Leitz, Wetzlar, West-Germany) designed specially to match image analysis requirements. Within this new microscope special options for automated processing of several microscope slides, such as automatic slide changer, slide code interpreter and an automatic supply of immersion oil, could be realized effectively.

The special characteristic of LEYTAS-1 to allow interaction at any desired phase during the screening has remained in LEYTAS-2. One of the most sophisticated and rapid ways of interacting with LEYTAS-1 has proved to be the display of stored alarms on a separate monitor. The use of this option has been extended in LEYTAS-2 by the improvement of the quality of the stored images. Not only can these images now be used for the elimination of

remaining alarms, also cytomorphological criteria, such as chromatin clumping and hyperchromasia, can be recognized. This offers new possibilities for those preparations in which abnormal cells have been selected by the system, but for which the number is too low to allow a correct automated classification. Cytologists can then rapidly screen the stored alarms to verify the machine diagnosis.

Although LEYTAS has proven to give satisfactory results in the screening of cervical samples, the relatively elaborate preparation procedures will limit its applicability in a population screening. Therefore we have started an investigation to analyze conventional smears. The results are presented in the chapter 6.4.

Chapter 6.3 SYSTEM REPRODUCIBILITY.

Several runs on the same preparation.

To test the reproducibility of the system in specimen classification, several slides have been analyzed repeatedly at specific time intervals. In table 6.7 the results of 4 runs of three different AFS stained specimens are given. The specimens have been selected in such a way (1 negative specimen, 1 specimen with a cytological diagnosis of mild dysplasia and 1 specimen with a diagnosis of invasive carcinoma) that the number of alarms vary widely.

Table 6.7: Reproducibility tests of LEYTAS counts.

	negative specimen		dysplastic specimen		carcinoma specimen	
total cells/1000	23/23	22/23	37/37	36/35	101/99	106/103
epith cells/100	24/27	25/32	33/31	36/26	55/48	64/58
alarms	2/4	1/3	56/49	53/41	282/245	370/296

The first two values at each column are obtained from subsequent runs carried out the same day. The second two runs were performed with about 1 week interval after the first two runs. This test was designed to test machine performance as purely as possible. Therefore longer time intervals have not been included to avoid eventual fading influences.

As can be deducted from table 6.7, different runs did not produce any different classification results. The number of alarms were always in the same order of magnitude in the four different runs. Slight increase or decrease of this number is paralleled by an increase or decrease of the number of epithelial cells and the total cell count. These differences might be due to changes in the regulation of the light intensity.

It should be noted that none of the 1500 slides in this series ever changed in classification result after re-analysis. Re-analysis has been carried out on every positive specimen of which the criteria fell close to the cut off point of 10 alarms or 0.3 %.

Several runs over a large time interval.

To test the reproducibility of the screening procedure over a longer time period, several slides have been rescreened during several months. This time fading influences can no longer be excluded, although care was taken to store the preparations in the dark at 4°C. In chapter 3.5, data is given about fading of the staining product in this time period. The results of LEYTAS screening are given in table 6.8.

The slides used for this experiment have been especially selected. Only those preparations were taken in which a slight alteration in the number of alarms could change the classification results. In none of the slides, the number of alarms (and/or selected nuclei) changed such that the classification was altered. Two similar versions of LEYTAS have been used for these experiments as indicated by the LEYTAS number (A or B). Although the average number of alarms and the average number of detected single nuclei are comparable for the two systems, it is striking that one of the systems (A) has a higher standard deviation for all these measurements than the other (LEYTAS B). Thus the modulation transfer function (MTF) is not identical for both

versions of the system. This is probably due to the slightly different microscope systems used since the image analysis hardware and software were identical. A satisfactory explanation for this variation could however, not be determined.

Table 6.8: Reproducibility tests of LEYTAS over several months interval.

slide nr	time period in weeks	nr of screenings	average nr of alarms \pm sd	average nr of nuclei \pm sd	LEYTAS set up
3735	59	14	33 \pm 9	30 \pm 8	A
3735	59	19	31 \pm 4	28 \pm 4	B
3530	40	14	46 \pm 8	38 \pm 8	A
3530	50	15	40 \pm 4	33 \pm 4	B
4540	16	11	41 \pm 7	37 \pm 6	A
4540	16	14	40 \pm 4	36 \pm 3	B

The time period during which a slide can still be analyzed has not yet been properly determined. As can be deduced from the previous results, the slides which have been rescreened for about a year, still gave reproducible results with respect to machine classification. As is shown in chapter 3.5, the fading of the staining product after one year varies between 10 and 16%. Obviously this has no direct consequences for the screening procedure.

The three slides used for table 6.8 have been rescreened 156, 156 and 116 weeks after the first screening. Results are printed in table 6.9.

Table 6.9: Results of rescreening of specimens after 2-3 years.

slide number	previous nr of alarms (nuclei)	time interval in weeks	present nr of alarms (nuclei)	relative decrease in alarms (nuclei)
3735	33 (30)	156	2 (1)	94% (97%)
3530	46 (38)	156	34 (29)	26% (24%)
4540	41 (37)	116	20 (18)	51% (51%)

As can be seen in table 6.9, the decrease in alarms after 2-3 years varies between 26% and 94%. It can be assumed that these changes will alter the classification results, as can readily be observed in one of the tested slides (3735). If we want to relate the decrease in the number of alarms with the decrease in staining intensity, IOD measurements of normal intermediate cells can be compared between the time of the first and of the last screening. Although we did not perform IOD measurements on these 3 slides at the time of the first screening, we have data available from negative specimens, which have been stained simultaneously with the three test slides. From the

relatively low interslide variation as mentioned in chapter 3.5 (5.8%) we conclude that another slide could well be used for this purpose. The relative decrease in IOD (table 6.10) amounted to 52% for slide number 3735, 32% for number 3530 and 74% for 4540.

Table 6.10: Comparison of change in LEYTAS results and staining intensity in a 2-3 year period.

slide number	time interval in weeks	decrease in LEYTAS alarms (nuclei)	decrease in IOD
3735	156	94% (97%)	52%
3530	156	26% (24%)	32%
4540	116	51% (51%)	74%

The decrease in IOD is much higher than the 10-16% which was known to occur after 2 years (chapter 3.5) and which did not lead to any measurable change in the LEYTAS results. On the other hand there exists no obvious linear correlation between the decrease in IOD and the decrease in LEYTAS alarms. Striking is the relatively high decrease in IOD of number 4540 (74%) after 'only' 116 weeks. From these results it can be concluded that LEYTAS analysis can not be carried out reproducibly (with the present program based on fixed thresholds) after 1- 2 years after staining. Results on such a limited series do not allow a more exact time interval. In any case it should be obvious that the variation from slide to slide can be so high that, to avoid any risks, rescreening of specimens should be performed only until about one year after staining.

Difference in parallel preparations from the same sample.

For LEYTAS analysis, only one centrifugation preparation has been used, although an average of 4 has been prepared from each specimen. Since the preparations are made from a well mixed cell sample, it can be assumed that all these slides are comparable concerning their cell composition. To test this hypothesis, two preparations of several samples have been analyzed and compared. For this study only those positive preparations are included of which the classification results were closest to the cut-off point. All other positive preparations analyzed by LEYTAS had higher alarms numbers and/or ratio's. The results are depicted in table 6.11.

Limited variation exists among the different cell samples concerning all counts. The only classification that changed when analyzing the parallel slide, is 4026, which is the only missed positive preparation mentioned in the total series in chapter 6.2. The parallel slide proved to be positively classified. One of the slides which came extremely close to the classification threshold is 4224. In the first slide 10 alarms resulting in a ratio of 0.31 alarms per epithelial cells had been detected. The second slide contained 11 alarms resulting in a ratio of 0.56%. Although the classification was positive in both preparations, it remained a 'borderline case'. Of course the presence of very few abnormal cells will always cause classification problems (Castleman and White, 1981). For this reason it will always be preferable to analyse all slides from a cell sample. Furthermore, the addition of extra parameters, e.g. those used by the SAMBA system as mentioned in chapter 8, can increase the validity of the cell classifier,

thereby improving the specimen classification results.

Table 6.11: Comparison of LEYTAS results after screening of two preparations from the same cell sample.

cytology number	LEYTAS data				
	total cell count/100	epithelial cells/100	alarms (nuclei)	alarms/epi x1000	classif result
4026-1	366	24	8 (6)	3.3	-
4026-2	599	43	26 (18)	6.2	+
4059-1	396	41	61 (57)	14	+
4059-2	225	29	57 (47)	16	+
4110-1	549	30	61 (50)	17	+
4110-2	1021	60	137 (115)	19	+
4163-1	404	77	89 (82)	11	+
4163-2	489	79	112 (95)	12	+
4172-1	521	39	69 (51)	13	+
4172-2	565	33	46 (41)	12	+
4224-1	137	32	10 (10)	3.1	+
4224-2	109	16	11 (9)	5.6	+
4272-1	811	37	44 (34)	9.4	+
4272-2	593	27	23 (18)	6.6	+
4331-1	450	40	68 (55)	14	+
4331-2	533	47	175 (166)	35	+
4334-1	904	30	45 (41)	14	+
4334-2	674	61	204 (175)	29	+
4347-1	3961	136	136 (92)	67	+
4347-2	3575	64	68 (39)	61	+
4380-1	2826	188	109 (70)	37	+
4380-2	2743	116	65 (49)	42	+
4413-1	1060	99	46 (34)	34	+
4413-2	1096	69	62 (48)	70	+

Chapter 6.4 RESULTS IN CONVENTIONAL SMEARS.

As has been demonstrated in the previous chapter, valuable results can be obtained if cervical specimens are screened for abnormal cells by LEYTAS provided specially prepared preparations are used. This prerequisite, the demand for centrifugation preparations, might limit the applicability of the method in every day clinical use. Due to the improvements made in image analysis during the last years, especially in the field of artefact recognition (Meyer, 1979; Smeulders, 1983) we decided to start an investigation on the attainability of screening conventional cervical smears. For this study the AFS staining procedure was found unsuitable because of its unfamiliarity by cytologists. Using centrifugation preparations, this was not considered a problem since parallel preparations, made from the same cell suspension, could be stained according to Papanicolaou. With direct smears, however, only one preparation is made from each sample. It would be preferable if a staining procedure was to be used which allows both visual and machine interpretation. For this purpose, gallocyanine was chosen as the nuclear stain because of its quantitative properties for DNA (Pearse, 1980) combined with its spectral similarity with haematoxylin (the nuclear stain in the conventional Papanicolaou). Following gallocyanine staining, the specimen is analyzed by the system, after which the staining is completed using the Papanicolaou counter staining ingredients eosin and orange G. The characteristics of this staining procedure are given in chapter 3. The final staining result is comparable with the conventional Papanicolaou and can easily be interpreted by the cytologist.

Table 6.12: LEYTAS analysis of gallocyanine stained conventional cervical smears.

morphological diagnosis	machine classification	
	negative	positive
negative (32)	32	0
dysplasia (4)	1	3
positive (1)	0	1

The results of LEYTAS-1 analysis of conventional smears are depicted in table 6.12. Using the same program as used for centrifugation preparations, as well as the same cut off threshold for classification, all negative and positive smears have been correctly interpreted. One of the four dysplasias, with a cytomorphological diagnosis of mild dysplasia, was negatively classified.

The results of this limited number of specimens are hopeful and justify the extension of the study to the point that investigated numbers will give valuable results which can be interpreted statistically. This extended study will be carried out on LEYTAS-2 with an optimized image analysis program which is under development at the moment. Although the first results as mentioned in table 6.12 look promising, one should realize that these have been selected specimens. Many of the slides which have been sent to our laboratory sofar, could not be analyzed with the present analysis program. Some of the problems

which are special to conventional smears and will have to get attention in the program to be developed, are:

- The cells are spread over large zones with many empty spaces in between. Hence the necessity to have a search strategy for interesting zones with sufficient numbers of epithelial cells. This also necessitates a computer controlled microscope stage which is not limited in its area under investigation.

- The fixation of smears is not standardized and differs from smear to smear. Whereas the crucial fixation step for the centrifugation preparations takes place in the laboratory under standardized conditions, the quality of the direct smear highly depends on the speed with which the cells are fixed, either using a cytospray or ethanol. The lack of standardization demands a considerable level of control from the system. If a large part of the smear is degenerated and suffers from air-drying - the most common cause of fixation errors in conventional smears - the system should be able to recognize this phenomenon and reject the specimen.

- The inhomogeneity of the background, presence of mucus or thick layers of cells brings the need for nuclear segmentation algorithms which are more or less independent of variations in the context. The 'top hat' detection of suspect cells also has to be corrected and adapted for the inhomogeneity of the background.

- When possible, the cells should be analyzed in relation to their neighbourhood. This includes:

- intensive search of other suspect events in the neighbourhood as soon as a first suspect event has been detected.

- study of groups of nuclei: degree of heterogeneity, overlapping of cells, thickness of the group etc.

- Information on the composition of the slide should be obtained. For instance presence of tissue fragments, leucocytosis, degree of degeneration, diathesis, bacteria etc. This information might be important to point at facts which are known to be indirectly related to malignancy (e.g. diathesis and leucocytosis). It can also be used for the rejection of slides or indicate the necessity of a repeat smear.

- Using the optical configuration of LEYTAS-1, several focal planes often occurred within one microscope field of a conventional smear. Since analysis is carried out on only one focal plane, many cells have been analyzed while out of focus. This problem will be minimized with LEYTAS-2 due to the high depth of focus available in the new microscope. Sometimes however, analysis will include the scanning of different focal planes of one microscope field.

Chapter 6.5 CLASSIFICATION RESULTS OF TOTAL CELL POPULATION ANALYSIS.

To test the diagnostic capacity of this new program (which will be referred to as TCPA = Total Cell Population Analysis) in relation to the already existing screening program, a set of 109 specimens has been analyzed with both image analysis programs. Selection of the specimens was random for about one quarter of this number. Remaining specimens were selected because they (almost) caused difficulties in the classification by the routinely applied screening program (that is relatively few alarms in the positive specimens or a relatively large number of alarms in the negative specimens). The results of this comparison are comprised in table 6.13.

Table 6.13: Comparison between conventional screening program and the total cell population analysis with regard to specimen classification.

cytological diagnosis	MACHINE CLASSIFICATION			
	screening program		TCPA program	
	neg	pos	neg	pos
negative (36)	16	20	18	18
inflammation (9)	3	6	6	3
mild dysplasia (18)	8	10	3	15
moderate dysplasia (15)	2	13	0	15
severe dysplasia (31) and more serious lesions	0	31	0	31
total ----- 109				

The decision thresholds for specimen classification with the conventional screening program have been given in chapter 5.3. The extraction of relevant parameters for the selection of abnormal cells using the total cell population analysis has been done in the following fashion: of all 109 specimens the total cell population was analyzed and measurement results (in the form of matrices) have been analyzed manually for the presence of relevant information concerning the discrimination between positive and negative specimens. It was found that the frequency of cells exceeding a certain absorption within a population of enlarged nuclei was much higher in the positive specimens than in the negative specimens. On the basis of these 109 specimens, which can be considered as a learning set, a threshold in this frequency was selected to give optimal discrimination. Results as given in the table have been obtained using this threshold. As can be seen in table 6.13, the number of false positives as well as the number of missed positives decreased which means an increase in sensitivity as well as in specificity of the TCPA program compared to the screening program.

The TCPA program is not essentially different from the screening program with regard to the cell selection procedure; both use nuclear size and intensity as cell descriptive parameters. The TCPA program however,

determines both the greyvalue and the size of the nuclei with more detail. Whereas the screening program uses a combination of 2 'top hat' transformations, the TCPA program recognizes 7 size classes and 15 grey value classes. At the moment we continue with this analysis program. It is not expected that results will worsen because the learning set of 109 specimens was selected in such a way that it was highly enriched with difficult specimens.

The main reason that the number of analyzed specimens is relatively low, is the speed of the program. At present it takes 7-9 hours to analyze one slide with LEYTAS-1. The program has not yet been implemented on LEYTAS-2 but once this has been done and the software has been rewritten to speed up the program, it will certainly result in a much shorter screening time (less than 30 minutes can be expected).

The program will probably be used as an addition to the presently used screening program by the execution of TCPA only every 10th or 20th microscope field. In that way the time needed for the final screening program with LEYTAS-2 will not exceed the demanded 5-10 minutes, whereas additional information is obtained on the composition of both the normal and the abnormal cell populations.

CHAPTER 7

DNA MEASUREMENTS

Chapter 7.1 INTRODUCTION.

Since the pioneer work on DNA cytometry by Caspersson in the third decade of this century (Caspersson, 1936), DNA and DNA-related measurements have become a widely applied technique in the present decade. From the literature, which has become far too vast to review, it becomes evident that two factors have contributed to this phenomenon. In the first place it was demonstrated that tumor cells often exhibit an increased amount of DNA (Sandritter et al, 1966; Atkin, 1959; Hrushovetz and Lauchlan, 1970), thereby implying its potential use for diagnosis and prognosis. Secondly instrumentation for DNA cytometry is now sufficiently sophisticated to permit its use in a clinical environment. Two main methods can be distinguished for measuring DNA: flow and slide based cytometry. Flow cytometry has the advantage that e.g. the DNA content of a large number of cells can be measured in a few seconds. This permits accurate determination of the DNA stemline of the tumor cells, provided adequate preparation and staining techniques have been applied and that the ratio of tumor cells in the sample is relatively high. Although a high proportion of cervical tumors has an aneuploid stemline (Boehm and Sandritter, 1975; Jakobsen et al, 1979), there are tumors with a diploid DNA stemline. With flow cytometry these tumors cannot be distinguished from benign lesions, which becomes evident in the following investigations. Using one parameter (DNA) flow cytometry on cervical biopsy specimens, Jakobsen et al (Jakobsen et al, 1979) found 0% false positive and 6% false negative cases. On the other hand, Sprenger and Witte (Sprenger and Witte, 1979) investigated cervical scrapes and reported 15% false negative and 39% false positive DNA histograms using flow cytometry. Causes which may contribute to this difference in results are a lower ratio of tumor cells and insufficient cellular preservation and dissociation in exfoliative cell scrapes compared to the cervical biopsy specimens.

To warrant detection of a certain cell subpopulation with a general flow cytometer, its frequency should be at least about 1%. In the case of cervical scrapes, often large numbers of normal epithelial cells and leucocytes are present in both benign and malignant conditions of the cervix uteri, the frequency of tumor cells might be as low as 0.049% (Barrett et al, 1979). Furthermore the detection of potentially present high DNA content cells is not only prevented by their low frequency, but also by the noise caused by artefacts such as doublets and triplets in the upper tetraploid region. This is caused by the insufficient artefact rejection of most flow instruments. Image cytometry has a much higher level of automated artefact rejection. Furthermore visual identification in the preparation warrants that only single cells are measured, whether they are manually (Auer, 1984) or machine selected (Cornelisse and van Driel-Kulker, 1985). On the other hand, until recently, slide based methods have been very time consuming. Therefore nearly all studies are based on the measurement of a restricted number, mostly 100, of randomly selected tumor cells. This results in a less accurate determination of the tumor stemline than using flow cytometry. Also the number of cells with high DNA content in the total cell sample will be underestimated due to the random cell selection.

In a study performed in our laboratory about 10 years ago (Ploem-Zaayer et al, 1979), we found the presence of cells with high DNA content ($> 5C$) to be a highly sensitive parameter for the diagnosis of severe dysplasia and more serious lesions. To establish the presence of such cells, whole preparations from cervical scrapes were visually screened for large and/or hyperchromatic cells, which were subsequently measured. Of course this method did not provide any information on the tumor stemline. Since the high DNA content cells as well as the tumor stemline are relevant parameters in regard to the patients diagnosis and prognosis (Atkin and Richards, 1956; Sandritter et al,

1966; Hrushovetz and Lauchlan, 1970; Boecking et al, 1984) , we presently use a method to obtain information on both parameters. To this purpose cells are selected at different cut-off levels using the LEYTAS-system. The most recent version of this system allows fast DNA measurements during cell selection, which enables DNA measurements of samples fulfilling the demands for adequate sample sizes (300 - 1000 cells) as defined by Weber et al (Weber et al, 1985).

Most often the ploidy pattern is used for either diagnostic or prognostic purposes. Next to the stemline, the number of cells with more than 5C DNA is used by our own group. A similar parameter has recently been used by Boecking, which he introduced as the 5C exceeding rate (Boecking et al, 1984). The advantage of using a parameter based on the number of cells above 5C DNA is its independance from visual, subjective evaluation of a histogram. For, although mathematical models have been developed for histogram analysis, usually the determination of a stemline is done visually.

In accordance with our own results in DNA measurements, most investigations using image cytometry report a diploid-tetraploid distribution in mild dysplasia, whereas the more serious lesions predominantly show aneuploidy (Evans and Monaghan; 1983; Bibbo et al, 1985). Bibbo et al (Bibbo et al, 1985) found clear distinctions between the ploidy patterns of normal and CIN I-III lesions using Feulgen-stained histopathologic sections. The distinctions between the different grades of CIN was not very clear, which the authors contribute to the large patient to patient variation. They found however, that aneuploidy - based on the measurement of 100 cells per sample - became only evident in CIN III cases. Aneuploidy in CIN has been reported to have higher rates of persistence or recurrence than euploidy or polyploidy (Fu and Hall, 1985). However there are contradictory results with regard to the possibility to differentiate between regressive and progressive dysplastic lesions on the basis of DNA measurements (Wagner et al, 1976; Nasiell et al, 1979). With regard to the prognosis of invasive squamous carcinoma, low ploidy cases are reported to be more radioresistant and more prone to develop lymph node metastasis than high ploidy carcinomas of comparable stage (Bibbo et al, 1985). The reverse has been reported for endocervical carcinomas (Bibbo et al, 1985). Our own study on the prognosis in ovarian cancer revealed that (near)diploid carcinomas have a better prognosis than aneuploid cases (Rodenburg et al, in press), thus supporting that adenocarcinomas generally have a better prognosis in case of low or diploidy.

Chapter 7.2 MEASUREMENT PROCEDURE WITH LEYTAS.

Provided that a dye has been used, which binds quantitatively to DNA, the DNA content can be assessed by measuring the integrated optical density (IOD). For IOD measurements LEYTAS can make use of a special card (DNS card which is part of the TAS) which integrates density values within a specified density scale. Making use of this card, a measuring program for LEYTAS-1 has been written by J.H. Vrolijk from the Department of Anthropogenetics in Leiden. Focusing at high magnification and determination of the contour are performed automatically to reduce differences caused by the operator as much as possible. To obtain accurate DNA measurements, special adaptations have been made to avoid errors caused by glare of light in the microscope and on the camera and to correct for background absorption. These include:

- fixed, small opening positions of the field diaphragm and the aperture diaphragm to reduce and stabilize glare influences.
- subtraction of the outer ring within the nuclear contour from IOD measurements, since this part of the nucleus proved to be highly influenced by the glare phenomenon.
- the cell to be measured is always centered to avoid as much as possible problems caused by lamp aberrations and shading, and because of the optimal correction of optics at this location.
- local background correction is obtained by assessing the mean IOD of a ring outside the nuclear contour, which is subtracted from the IOD values within the nucleus.

To verify the accuracy of the DNA measurements using the TAS, a comparison was made with measurements performed by a conventional scanning densitometric technique using a photomultiplier (PM). The applied software program was HYDACSIS (van der Ploeg et al, 1977). Final magnification for the photomultiplier, using a 100x objective is 500x, while the final magnification for measurement purposes of LEYTAS is 120x using a 40x objective. For these experiments, rainbow trout erythrocytes which have been added to each preparation as DNA reference cells, were measured with both systems. In 50 randomly selected preparations, 10 trout cells were visually selected and measured. It was found, as can be seen in table 7.1, that the intraslide variation (CV) was 5.1% (+ 1.3%) using PM and 8.8% (+3.8%) using the TAS. The interslide variation was 7.4% for both systems.

Table 7.1: Variations in IOD measurements (CV) using a photomultiplier (PM) and the television camera of the TAS.

	PM	TAS
intraslide variation	5.1%	8.8%
interslide variation	7.4%	7.4%

The variation in the TAS measurements is slightly higher than in the PM measurements. This difference will be largely due to the different magnifications used in combination with the size of the trout erythrocyte. LEYTAS DNA measurements in randomly selected cells from scrapings of benign tumors from the breast, showed coefficients of variations between 4.5 and 5.5%. Based on these results, we conclude that the nuclear DNA content can be estimated sufficiently accurate to perform ploidy analysis, but that a maximum error of 10% should be reckoned with. This means that cell lines with peak

values between 1.8 and 2.2 C are considered diploid.

Reference cells.

As has been mentioned before, rainbow trout erythrocytes are used as DNA reference cells. Their DNA content is 80% of the human diploid value. The ratio between the measured values can, however, be different due to applied fixation, staining and measurement procedure. The average ratio between the IOD of the trout erythrocyte nucleus and the cervical intermediate epithelial cell using the AFS staining procedure, is 0.88 for fresh material and 0.80 for deparaffinized cells. These factors are used to standardize the IOD values of measured cell populations. Although trout erythrocytes are relatively small and have a rather condensed nuclear structure, they are still being used as reference cells in our laboratory. This is caused by the fact that trout erythrocytes can be easily stored and put on a fixed location of the object glass to allow an automated measurement procedure for reference cells. Such an automated measurement procedure would not yet be possible with cells from the patient e.g. leucocytes or epithelial cells. Ideally two types of reference cells should be present: external reference cells to control the staining and internal reference cells to correct for variations in the sample. The trout erythrocytes as external reference cell may be replaced by another type of reference cell, preferably one of which the nuclear structure concurs with the structure from the normal epithelial cell e.g. rat liver cells. However, a practical protocol for storing rat liver cells is not yet available. With the more flexible LEYTAS-2 system, the use of normal epithelial cell nuclei as DNA reference values will be feasible without causing a severe time delay, due to the incorporation of greyvalue processors in the system as well as its possibility to carry out DNA measurements in parallel to the screening.

Since the standard cells have been centrifuged on a fixed location of the microscope glass, selection of trout erythrocytes as well as the measurement procedure is performed automatically. All objects within a certain size interval are counted as trout erythrocytes. A total of 50 per slide is selected and measured. In a series of 100 different specimens, an intraslide variation of 8.2% ($\pm 0.9\%$) and an interslide variation of 4.3% was found. The intraslide variation is similar as the one found with manually selected cells (8.8%) which indicates the accuracy of the automatic selection procedure. The interslide variation however is much lower being 7.4% for the manually selected cells and 4.3% for the automatically selected cells. This difference is probably due to the fact that cells which are selected visually represent the average typical cells in that population, whereas the automatically selected cells represent always the same subset of cells as they are defined by a certain size.

DNA histograms.

The DNA measuring protocol is applied to cells which have been selected automatically using the LEYTAS screening facilities (see chapter 4.3). It is executed in such a way that first cell selection and artefact elimination take place. Once sufficient cells have been selected (300), the stored greyvalue images (see chapter 4.2) are used to recognize visually all remaining artefacts which have not been eliminated automatically. The alarm numbers of these non-single cells can be fed into the computer terminal, whereafter they are removed from the data set. Then the microscope stage moves to another location on the glass slide for measurement of the reference cells which have been centrifuged on the same microscope glass but on a different fixed location. After measurement of the reference cells, the microscope stage moves to all individually stored objects. Each cell is measured and its IOD value is immediately correlated to the average trout value. In the case of

LEYTAS-2, DNA measurements can be performed simultaneously with the screening program, in one of the slave processors. Relocation will then no longer be necessary.

Different cell selection facilities of the screening program (e.g. 'low level' and 'high level' criteria) can be used for the selection of cells to be measured. Random cell selection can also be carried out by adjusting the 'top hat' settings such that all epithelial cells are selected. This will result in a DNA histogram representing the random DNA distribution of all cells, except lymphocytes and leucocytes which are discarded on the basis of nuclear size and contrast. A LEYTAS DNA histogram consists of a relatively low number of cell nuclei (about 200-300). Therefore the presence of cell nuclei with a high DNA content might be underestimated when cell nuclei have been selected randomly, especially since the frequency of these high DNA content cells can be extremely low (Cornelisse and van Driel-Kulker, 1985). For a better approximation of the presence of these rare cells, the DNA measurement procedure is applied to cells automatically selected using the LL or the HL settings. Results of DNA measurements in rat liver cell suspensions using the random cell selection as well as the LL and HL selection criteria are given in figure 24a, b and c respectively.

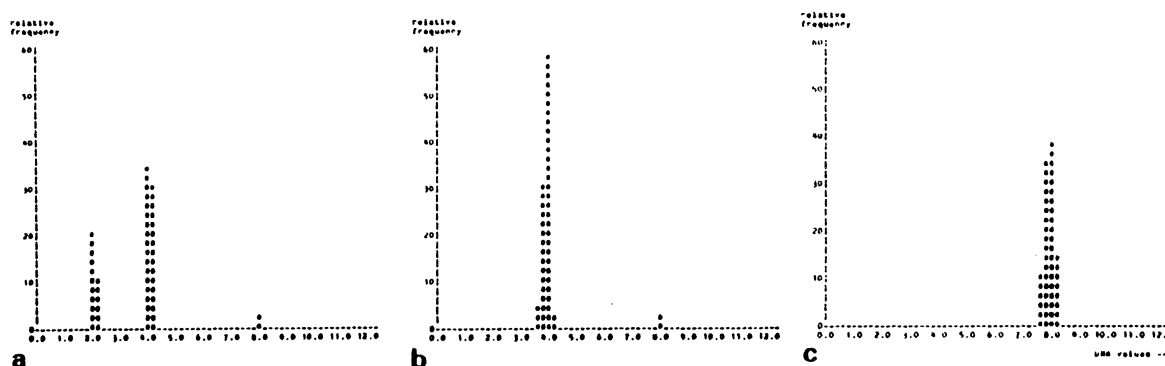


Figure 24: LEYTAS DNA histograms of rat liver cells. The histogram of figure 24a is obtained after random cell selection; diploid, tetraploid and very few octaploid cells are present. Using the LL settings for cell selection (figure 24b), no diploid cells are present, mainly tetraploid cells. Using the HL cell selection criteria (figure 24c), octaploid cells have been selected exclusively.

In figure 24a, the random distribution of the diploid, tetraploid and octaploid cells in the specimen is shown. In figure 24b, only tetraploid and octaploid cells have been selected using the LL selection criteria, whereas in fig 24c only the octaploid cell line has been selected using the HL settings.

Two things become clear in this example. First of all, DNA values which are not present or present in very low numbers in a histogram of randomly selected cells, can be visualised clearly in histograms where cells have been selected on the basis of an increased DNA content. Secondly, the 'top hat' transformation can be regarded as a threshold at a certain DNA value. As will be shown in the next part of this chapter, the cut off DNA value of the 'top hat' transformation is not as sharp as it may look in the example of the liver cells. This is due to the fact that there are very few cells with DNA values between the polyploid values (4C and 8C) in the case of liver cells. When however malignant tumors are measured, with many aneuploid cells, we will see that also some cells below the cut off value will pass the 'top hat' transformation. A rough estimate of the minimal DNA value for the LL and HL

settings of the 'top hat' transformation is 3C and 5C respectively.

In the next part of this chapter some examples will be given of the combined use of the screening program and DNA measurements. Of course, the measurement of DNA content is only one nuclear measure which can be performed on automatically selected cell populations. Other nuclear measures such as those performed on chromatin texture, are not yet available on LEYTAS, but their potential significance has been investigated with the SAMBA 200 system. Results are described in chapter 8.

Chapter 7.3 LEYTAS DNA HISTOGRAMS IN CERVICAL SCRAPES.

DNA measurements have been performed in about 50 cervical specimens that were obtained by scraping the cervix with an acryl-cotton tipped applicator. LEYTAS cell selection was performed randomly as well as by the LL settings. The histogram of randomly selected cells was almost always composed of one (near-) diploid peak. This was expected since the frequency of abnormal cells in cervical specimens is usually low (chapter 5.2). Using the LL selection criteria to enrich the histogram with elevated DNA content values, histograms from negative specimens consisted almost exclusively of diploid and tetraploid cells. In the upper tetraploid region only very few cells were found. An example of DNA histograms from a specimen with a cytological diagnosis of inflammation is given in figure 25a and b.

Measurements of cases with a cytological diagnosis of dysplasia roughly showed two types of enriched histograms (using LL settings): one type tended to form peaks at the polyploid DNA values with only very few aneuploid cells and another type showed DNA values scattering almost randomly between 2 and 8 C. In this latter type of histogram, there was no or only slight tendency towards peak formation. In some of the cases which showed the first type of histogram (including peaks in the polyploid region), the histological diagnosis showed the presence of a condyloma virus infection. An example of such a case is presented in figure 26a and b. Fig 27a and b are also histograms from a specimen diagnosed as mild dysplasia, but in this case the histograms belong to the second category; DNA values scatter randomly without peak formation. The histological diagnosis of this case was severe dysplasia.

A typical example of histograms obtained from a specimen diagnosed as 'invasive carcinoma' is given in fig 28a and b. Hardly any diploid cells are present in the histogram of the randomly selected cells. The scattering values in the peridiploid region are most probably due to the degenerative state in which also the normal cells are found in carcinoma specimens as a consequence of the necrotic activity of the tumor. In the enriched histogram, DNA values are found up to 20 C. In most cases very limited or no tendency towards peak formation was found.

Discussion.

In this chapter some typical examples have been given of DNA histograms from cervical specimens with different cytological and/or histological diagnoses. In the histograms from specimens with an abnormal cytological diagnosis (dysplasia or more serious lesion), a tendency was found towards the presence of aneuploid cells in the upper tetraploid region. Histograms from inflammatory lesions and viral infections tended to form peaks in the regions with polyploid DNA values, without many cells in the upper tetraploid region.

Although cell selection criteria as presented in this thesis ('top hat' transformation) are strongly related to the DNA content of the nucleus, some diploid cells are also selected when using the LL settings. This became evident when DNA measurements were performed on cells, selected during screening, in specimens from negative and, especially, inflammatory lesions (figure 24). The relation of nuclear size to contrast in inflammatory cells is probably such that the requirements set for the 'top hat' transformation criteria are fulfilled, whereas the DNA content is still diploid. This finding indicates once more the necessity of additional nuclear parameters (such as DNA) for a further discrimination between cells selected in positive and in negative preparations. It also explains the high decrease in false positively classified specimens which is obtained when nuclear parameters are added as is shown in chapter 8.

In some of the carcinoma specimens, the need for an extra DNA reference cell became evident, due to the heavy state of degeneration of the normal

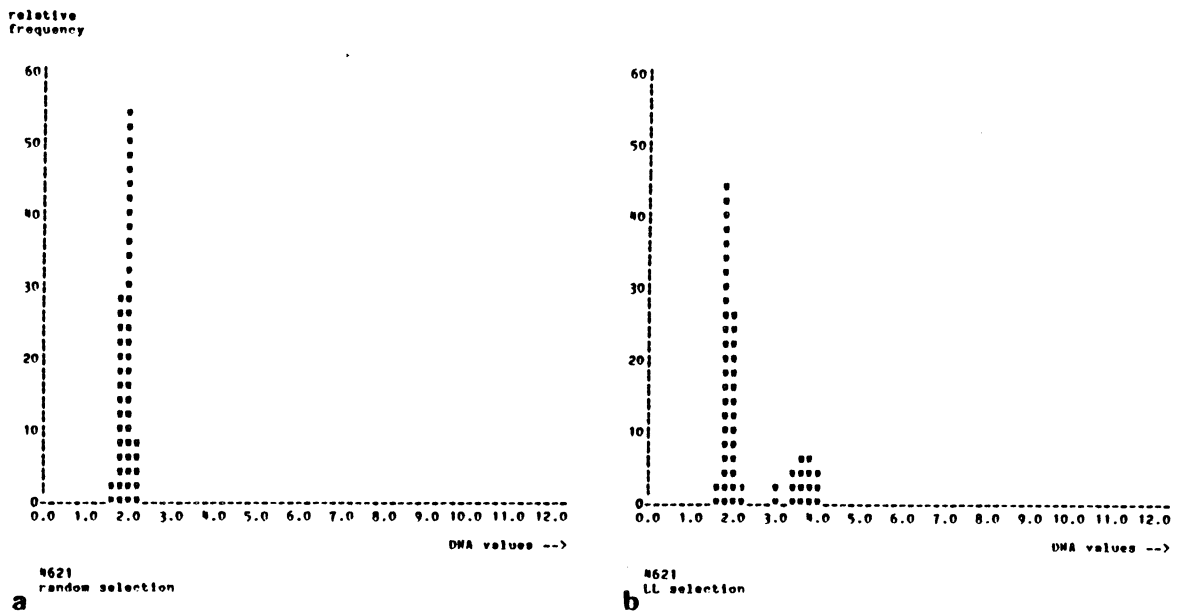


Figure 25a and b: LEYTAS DNA histograms of an inflammatory specimen, consisting of about 200 cells each. The histogram of figure 25a is obtained after random cell selection resulting in diploid cells exclusively. Figure 25b resulted from DNA measurements of cells selected by 'low level' criteria. Diploid as well as tetraploid cells have been selected.

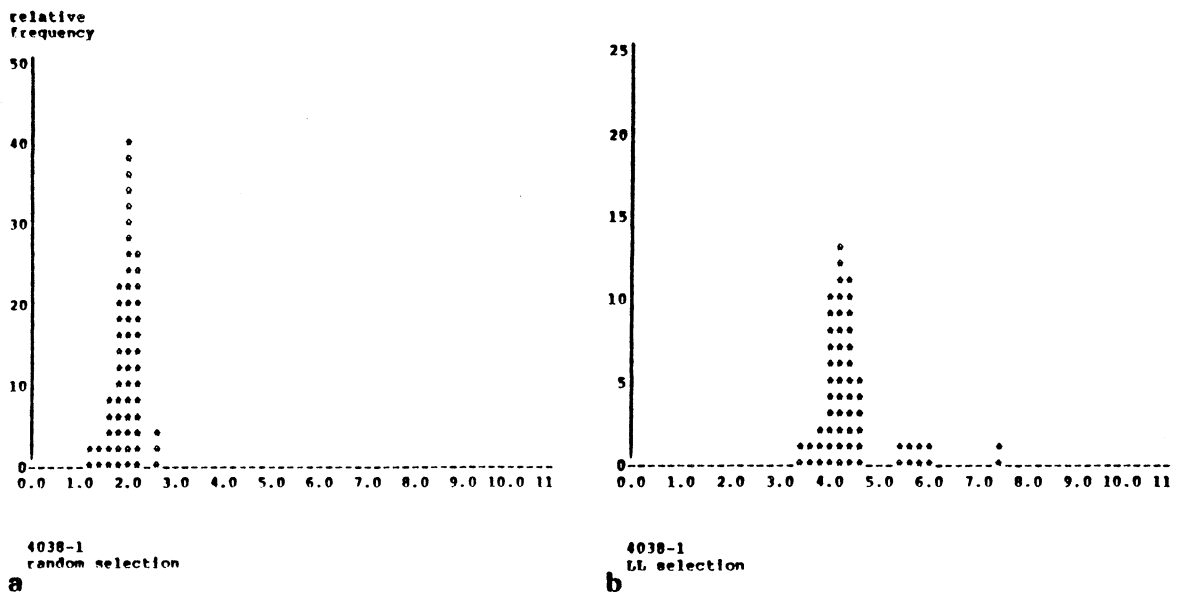


Figure 26a and b: LEYTAS DNA histograms of a mildly dysplastic specimen. Histological examination indicated the presence of a condyloma virus infection. Mainly diploid cells are found when cells are selected randomly (figure 26a), whereas 'low level' cell selection results in mainly tetraploid cells (figure 26b).

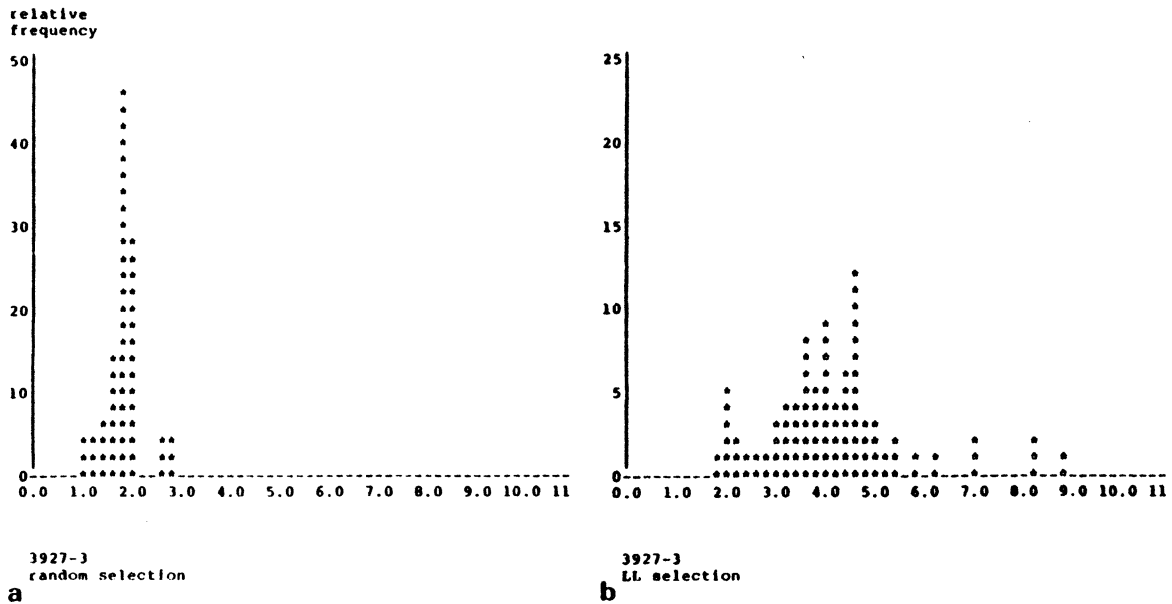


Figure 27a and b: LEYTAS DNA histograms of a specimen with a cytological diagnosis of mild dysplasia and a histological diagnosis of severe dysplasia. Although the histogram of randomly selected cells (figure 27a) shows mainly diploid cells, many aneuploid cells proved to be present in the histogram of 'low level' selected cells (figure 27b).

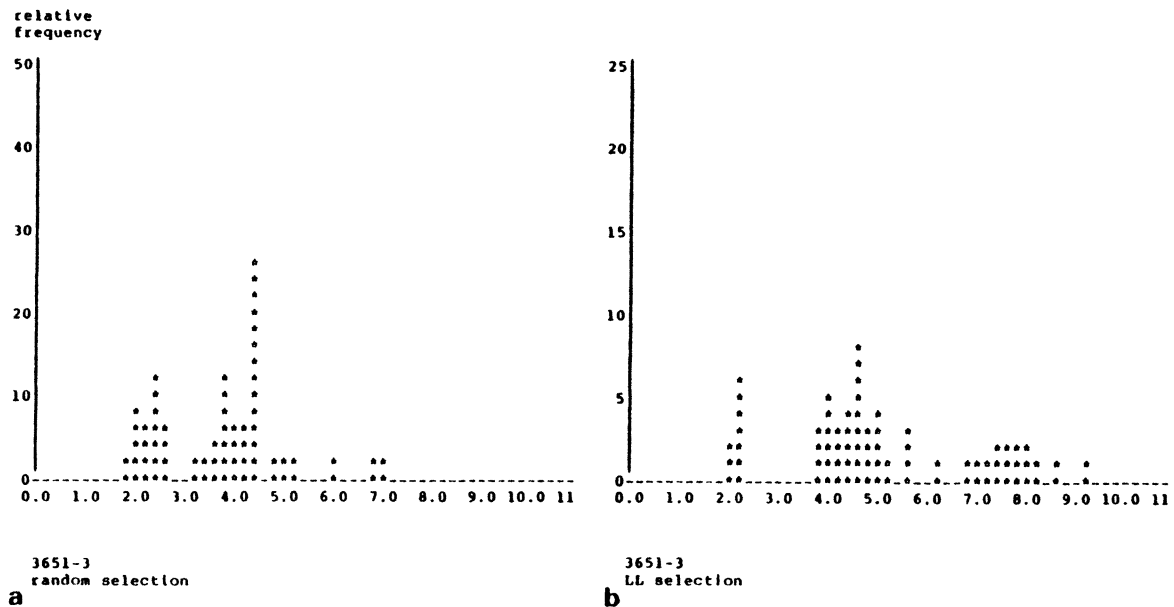


Figure 28a and b: LEYTAS DNA histograms of a carcinoma specimen. The histogram of both the random (figure 28a) and the 'low level' cell selection (figure 28b) showed the presence of many aneuploid cells up to 9 C.

cells. In most of the other cases, a clear peak was found in the histogram of randomly selected cells which could have easily been used as the diploid reference value. Nevertheless, the external trout erythrocytes have been used as the DNA reference cell in all cases.

The time for LEYTAS-2 to generate a DNA histogram of randomly selected cells will take about 5 minutes. This means that automatic measurements of large numbers of cells can now be performed with image analysis with a speed approaching that of flow cytometry. The advantage of image cytometry is the highly developed level of artefact rejection; whereas most signals in the high value region of a flow DNA histogram are caused by artefacts (mainly overlapping nuclei (van Driel-Kulker et al, 1980)), LEYTAS histograms consist predominantly of single nuclei. Furthermore, the objects can easily be displayed on a television monitor, enabling the operator to reject visually the few artefacts which have not been automatically eliminated. This opens new possibilities in the study of DNA content. Whereas DNA studies used to focuss mainly on stemline aberrations as can be accurately determined by flow cytometry, the significance of less frequent aneuploid cells with high DNA content can now be studied without extensive human interaction. In a study comparing DNA histograms obtained both by flow and by LEYTAS (Cornelisse and van Driel-Kulker, 1985), we showed that the intratumor variation in DNA content is underestimated with flow cytometry because no information can be obtained on the signals in the tail of the DNA profile unless cell sorting is applied (Tanke et al, 1983). The significance of low frequency aneuploid cells in the upper tetraploid region for diagnostic as well as prognostic purposes has been indicated by several studies (Husrovetz and Lauchlan, 1970; Ploem-Zaayer et al, 1979; Boecking et al, 1984; Bibbo et al, 1985; Rodenburg et al, in press).

Chapter 7.4 DNA AS A PARAMETER FOR SCREENING IN CERVICAL CANCER.

In this chapter the validity of DNA content as a tumor parameter is studied in relation to the sampling technique. For that reason, both the cell suspension from the cervical scrape made prior to the surgical removal of the tumor as well as the cell suspension made from the paraffin embedded tumor was investigated in 7 patients with a cytological diagnosis of (suspect for) carcinoma. Only those cases were selected that showed evidence of carcinoma and contained a high number of tumor cells in both the scrape and the histological section. The case numbers with their cytological and histological diagnoses are given in table 7.2.

Table 7.2: Histological and cytological diagnoses of patients included in the sampling study.

number	cytological diagnosis	histological diagnosis
CH001	squamous cell carcinoma	squamous cell carcinoma well differentiated
CH002	suspect for carcinoma	squamous cell carcinoma moderately differentiated
CH003	suspect for carcinoma	squamous cell carcinoma moderately differentiated
CH004	squamous cell carcinoma	adeno-squamous carcinoma moderately differentiated
CH005	suspect for carcinoma	squamous cell carcinoma moderately differentiated
CH006	suspect for adenocarcinoma	endocervical carcinoma well differentiated
CH007	carcinoma	squamous cell carcinoma

The preparation method for both the suspensions made from the scrapes and the suspensions made from the paraffin embedded tumors is given in chapter 3.3. The applied staining procedure is acriflavine-Feulgen-SITS. DNA histograms from both type of specimens are obtained using the random cell selection as well as the LL selection criteria.

Results.

Notwithstanding the different sampling procedure, a certain concurrence was found between DNA distributions in both types of specimens. Aneuploidy was diagnosed as such by the presence of a non-diploid peak in the histogram obtained by the random cell selection criteria. The DNA indices of these tumor stemlines varied from 1.3 to 1.9 and were similar in both the cell sample from the scrape and the tumor tissue block. An example is given in figure 29a en c. The histograms obtained by the LL selection criteria, of which an example is displayed in fig 29b and d, all showed cells in the upper tetraploid region. The absolute numbers of these cells are relatively high in all cases (see table 7.3), although they vary to a certain extent, especially

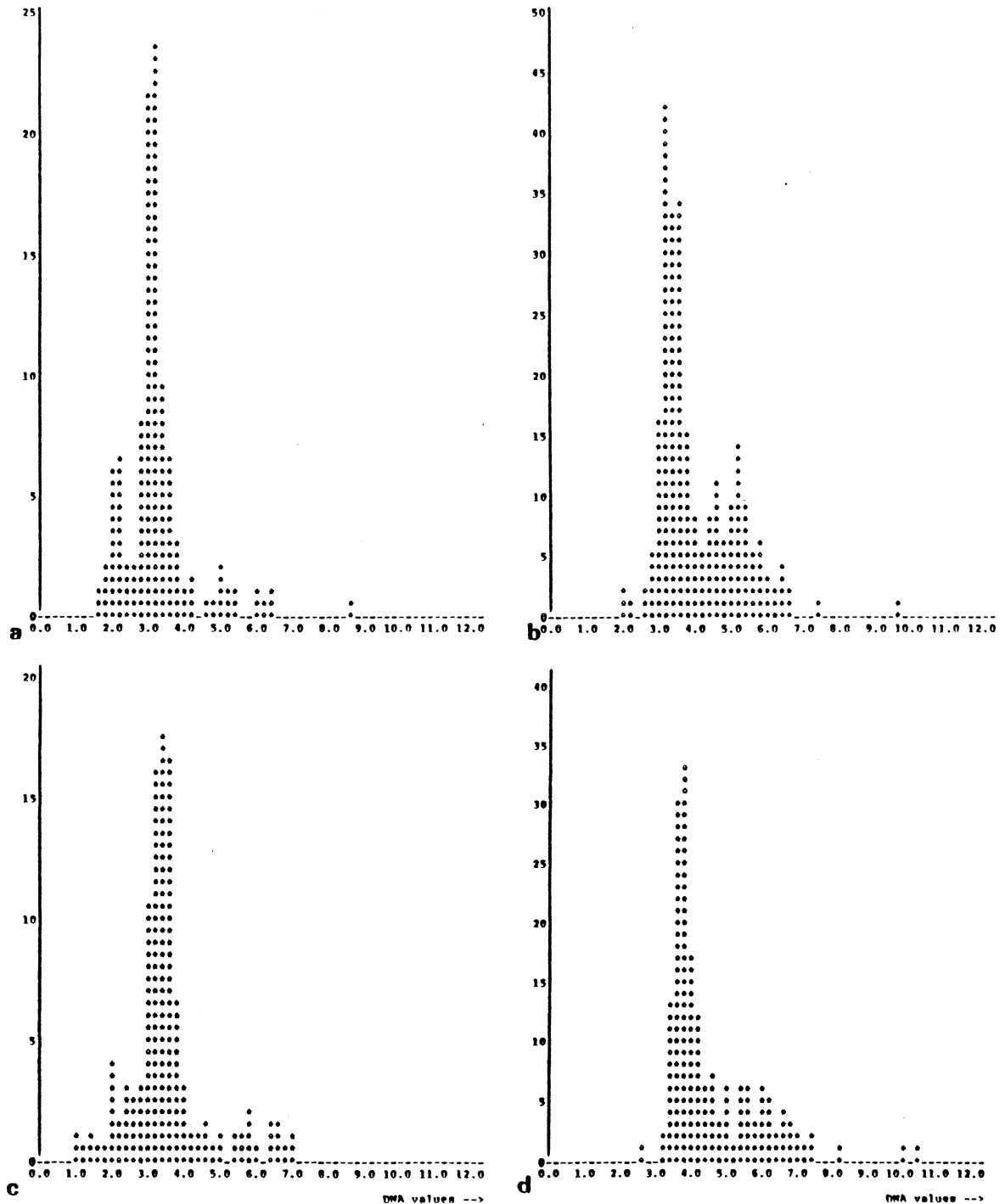


Figure 29a, b, c and d: LEYTAS DNA histograms of patient with invasive cervical carcinoma. Figure 29a and b represent the random and 'low level' histogram of the suspension specimen made from the cervical scrape. Figure 29c and d represent the random and 'low level' histogram of the suspension specimen made from a thick section of the paraffin embedded tumor of the same patient. The x axis represents the DNA value; the y axis represents the relative frequency of cells in figure a and c, and the absolute number of cells in figure b and d. Notwithstanding the different sampling procedures, similar histograms are found with regard to the DNA index of the tumor (≈ 1.6 and 1.65 , to be extracted from the random histogram) as well as to the number of cells exceeding 5C DNA (see table 7.3, to be extracted from the LL histogram).

in case nr 7. The relative numbers of high DNA content cells, expressed as a percentage of the total number of epithelial cells analyzed, differ in the same order of magnitude; higher absolute numbers are usually accompanied by higher percentages. The only exception is case nr 2, where the relatively low number of cells is attended by a relatively high percentage.

Table 7.3: Numbers and ratios of cells exceeding 5C DNA in the two types of specimens.

case number	sampling technique	number of cells >5C DNA	ratio of cells >5C DNA
CH001	scrape	567	6.9%
CH001	tumor block	455	5.4%
CH002	scrape	43	8.3%
CH002	tumor block	110	2.0%
CH003	scrape	188	2.3%
CH003	tumor block	320	6.8%
CH004	scrape	341	4.6%
CH004	tumor block	533	5.6%
CH005	scrape	67	2.5%
CH005	tumor block	136	6.5%
CH006	scrape	61	3.0%
CH006	tumor block	23	1.2%
CH007	scrape	1353	7.0%
CH007	tumor block	47	2.0%

* the number is given as the percentage of epithelial cells counted by LEYTAS.

Discussion.

This study was undertaken to investigate whether the presence of high DNA content cells in cervical scrapes was paralleled by the presence of these cells in the tumor tissue. Based on the obtained results it can be concluded that the finding of high DNA content cells in cervical scrapes is not caused by e.g. preparation artefacts or degeneration due to exfoliation. It is on the contrary, based on a biological phenomenon, that could be demonstrated in all seven investigated carcinoma cases. Similarity in stemline position as well as relatively high numbers of cells exceeding 5C DNA were observed in both the cervical scrape as well as the tumor block preparation of the seven investigated carcinoma cases. This was facilitated by the fact that these cases were selected such that both the suspension smear from the cervical scrape and the diagnostic section from the tumor tissue had to contain a high proportion of tumor cells, which was verified visually. These prerequisites were necessary because the detection of a tumor stemline in a histogram of randomly selected cells is highly dependent on the ratio of tumor cells versus abnormal cells. As can be seen in table 7.3, both well differentiated and moderately differentiated squamous carcinomas contain large numbers of cells exceeding 5C DNA. Generally more of such cells are found in the preparation from the tumor block than in the cervical scrape specimen. However, the

difference in frequency never amounted to more than 2.5x. Even in the case of the well differentiated endocervical carcinoma, cells with increased DNA values were found.

The study as it has been presented here lacks the investigation of benign lesions, due to practical problems in obtaining tissue blocks from normal epithelium. However, in some of the investigated positive cases, parts of the tissue block contained visually normal squamous epithelium. Using the selection technique as described in chapter 3.3, these normal appearing areas have been punched out and prepared. In the few cases that have been analyzed uptil now, no cells were found with a DNA content higher than 5C.

We have as yet not performed any studies on the relation of DNA content and prognosis in cervical cancer. The seven presented cases, although differing in their differentiation and type, all showed aneuploid cell lines. Future investigations will certainly include prognostic studies. In the scope of this thesis however, only the significance of high DNA content cells was investigated in relation to the diagnosis of cervical cancer in general and in the LEYTAS performance in particular.

CHAPTER 8

NUCLEAR TEXTURE INFORMATION IN AUTOMATICALLY SELECTED CERVICAL CELLS

Chapter 8.1 INTRODUCTION.

The present false positive rate (FPR) of LEYTAS is 16% as shown in chapter 6.2. Using a rapid interactive procedure to eliminate 'false' alarms, this FPR can be reduced to 11%. This means that 11% of all negative specimens cannot be discriminated from positive specimens on the basis of absolute or relative numbers of selected cells. A study was performed to try to distinguish LEYTAS detected cells in false positively classified specimens from LEYTAS detected cells in true positively classified specimens on the basis of nuclear texture. To study nuclear texture of cells, the SAMBA (System for Analytical Microscopy in Biomedical Applications, TITN, Grenoble, France) system was chosen since this system incorporates a large variety of texture parameters. For this study, the cell selection was also performed on SAMBA, by creating a program which resembled LEYTAS selection as much as possible. Artefacts were eliminated visually. Specimen classification was performed using the SAMBA software package.

Chapter 8.2 HARDWARE OF SAMBA.

All specimens were processed by the SAMBA 200 cell image processor. This commercially available instrument (TITN, Grenoble, France) is the result of a cooperative project between the Quantitative Microscopy Group of the TIM3 laboratory of the University of Grenoble, France and Thomson-TITN, Paris, France. An excellent and detailed description of the instrument is given by Brugal et al (Brugal et al, 1978; Brugal, 1984). In short, the system consists of an automated microscope with a scanning stage and autofocus equipment. The light source which was used for this study was a 100 Watt halogen lamp. Using separating prisms, the system can either use the low-resolution detector or the high-resolution scanner.

Low resolution.

The detection and location of potentially interesting objects at low magnification is performed by means of a linear photodiode array. Using a 100x objective, as was done in this study, a spatial resolution is reached of 2.5 μm , in a microscope field of 160x160 μm . The photodiode array is also used as the detector for the autofocus which is followed by an algorithm optimizing the contrast between objects and background. During the low resolution analysis, the area, perimeter and integrated extinction are measured after image thresholding. Of each of these 3 parameters, the operator can demand certain predetermined specifications which will result in the identification of interesting cells. Their x,y coordinates are stored to enable relocation of cells for high resolution analysis after finishing the low resolution detection.

High resolution.

A photomultiplier tube combined with a double mirror scanner and rotating filters serves as the input device for the high resolution analysis. The photometric signal is digitized in 8 bits of grey levels. Using a 100x objective, a spatial resolution of 0.4 μm is obtained at a microscope field of 25 x 25 μm . The same autofocus algorithm is used as for low resolution analysis; this time the photomultiplier is used for the detection of the image.

Besides the automated microscope, the hardware of SAMBA includes 2 internal processors, one processor for control of the system and the microscope and one image analyzing processor, and 1 external processor (VICTOR, California). The latter processor handles the entire software package for data processing and classification and operator/system interfacing.

Chapter 8.3 SOFTWARE OF SAMBA.

The SAMBA software which runs on the external computer, includes supervised and unsupervised classification and data analysis procedures, data storage and management and enables the operator to create new programs and alter existing programs in a user friendly language.

The graphical representation of the data as well as the statistical methods which will be presented in this chapter, are part of the standard software package of SAMBA. The following methods are available:

- histogram (program: HISTO)

This method permits the visualization of the distribution of a cell population as a function of one parameter.

- scattergram (program: NUAGE)

This method permits the visualization of the distribution of a cell population as a function of 2 parameters. Each cell is characterized by a point.

- linear discriminant analysis (program: DISCRI)

Discriminant analysis is a method which uses supervised classification to discriminate between different types of objects. It uses an intermediate step during the classification: the learning phase. During this phase an 'a priori' label is assigned to each cell. In our case this label depends on the cytology class where the cell is derived from. The cells used for the learning phase serve as the calculation basis for the analysis. The program operates step for step for so many steps as there are parameters (in this case 18). At each step a new parameter is added to the parameters which have been selected as being the most discriminating ones during the preceding steps. A non discriminating parameter is automatically removed from the analysis. The discrimination between more or less effective parameters is based on the number of well classified cells. The most discriminating parameter is the one that shows the highest constancy in classifying different cells from the same class. After the extraction of the parameters of importance, they will be used to classify all objects during the test phase.

The performance of the obtained classification is compared with the 'a priori' classification. Results are presented as a confusion matrix. After the discriminant analysis each cell can be represented by a point in a n dimensional space; n corresponding to the number of discriminating parameters. This correlation can be visualized after a canonical analysis. The canonical analysis defines a projection plane (factorial plane) by which the different classes of the population show the highest dispersion.

The statistical strategy involved in the DISCRI program highly resembles the BMD07 reference multivariate analysis (University of California). However, the ergonomics is different concerning the following points:

1. the type of analysis (principal component analysis, factorial discriminant analysis and decisional discriminant analysis) can be easily selected.
2. the program constitutes a high level of integration with graphical representation tools which can be interactively selected.
3. Since the program is compatible with the SAMBA file formats, the x and y coordinates of the cells are not lost during the analysis. Therefore, marking of a dot (by pointing) on the computer terminal during the graphical representation, triggers the immediate relocation of the corresponding cell in the center of the microscope field.

Chapter 8.4 SELECTION OF CELLS.

Thirty cases were selected, all of them being positively classified by LEYTAS. Ten of these cases had a negative cytological diagnosis, ten cases had a cytological diagnosis of dysplasia (mild or moderate) and 10 cases were positively diagnosed (severe dysplasia, carcinoma in situ or invasive carcinoma). The cytological diagnosis of all dysplasia and positive cases had been confirmed by histopathological examination to exclude potential cytodiagnostic errors. In those cases where a histological examination was performed, it confirmed the cytological diagnosis. At this point, it should be noted that the 10 cases with dysplasia and the 10 positive cases represent a more or less random selection from these categories. On the other hand, the negative cases are selected from those cases which were false positively classified by LEYTAS, and consequently, they cannot be considered as an average sample of all negative cases.

Staining procedure.

The routinely used staining procedure on centrifugation specimens for LEYTAS is AFS. Although SAMBA is equipped for analysis with blue light, as is necessary for this staining, the AFS stained cells gave low quality images with SAMBA. It was assumed that the input device was not sufficiently sensitive for blue light. Therefore parallel slides of those analyzed by LEYTAS, were stained with gallocyanine, having its absorption maximum around 573 nm (green light). This resulted in a considerable improvement of the nuclear images. The protocol for the gallocyanine staining procedure is given in chapter 3.4.

Low resolution; selection of cells.

Nuclear area and grey value density can be used as selection parameters at low magnification. A combination of these two parameters was found which resulted in roughly the same number of selected cells as was found with LEYTAS. Therefore it was assumed that these cells represented the LEYTAS selected cells fairly well. This was found necessary because potential implementation of texture parameters with LEYTAS would most probably be carried out on automatically selected cells, since it was shown in chapter 5.1 that this cell population correlates well with the disease. Either a maximum number of 600 objects were selected or the maximum area of the slide was analyzed. The total number of single cells detected by both LEYTAS and SAMBA on parallel slides from the same specimen are given in table 8.1.

One negative specimen did not contain sufficient epithelial cells and was therefore rejected from the series. Consequently, 29 specimens remained for analysis. The two absolute numbers selected by the different systems can be compared in all but 3 cases because they represent the number found after analysis of the entire slide. Because of the suspend and count procedures during the preparation technique, two parallel slides from the same patient can be considered to be similar (as discussed in chapter 6.3). In three of the positive preparations however, SAMBA selected 600 objects (its maximum for one run) prior to analyzing the entire slide; in those cases the numbers cannot be compared. For all other cases, as shown in table 8.1, the numbers of cells selected by SAMBA on a gallocyanine stained preparation correlate fairly well with those selected by LEYTAS on a parallel AFS stained preparation. The difference between the numbers of cells selected by the two systems is mainly due to 2 reasons, being:

- a. Both machines have analysed different microscope slides with different staining procedures. Although the two slides are made from the same cell sample, a slight difference cannot be excluded as is found when different slides from the same sample are analyzed by LEYTAS (chapter 6.3).

b. The selection of cells is based on DNA-related criteria by both systems. Both use a combination of greyvalue density and nuclear area. However, whereas LEYTAS compares different combinations (as is explained in chapter 4.3.1), SAMBA uses one combination. Furthermore, SAMBA measures nuclear area by counting the number of pixel points, whereas LEYTAS uses mathematical morphology (size estimation by erosions).

Table 8.1: Overview of slides selected for investigation with SAMBA.

specimen number	cytological diagnosis	number of * LEYTAS cells	number of * SAMBA cells
1	negative	26	53
2	negative	26	26
3	negative	66	300
4	negative	48	20
5	negative	57	87
6	negative	44	100
7	negative	41	40
8	negative	39	59
9	negative	62	45
10	moderate dysplasia	121	88
11	mild dysplasia	87	105
12	moderate dysplasia	56	41
13	moderate dysplasia	50	28
14	moderate dysplasia	29	29
15	moderate dysplasia	154	91
16	mild dysplasia	78	169
17	moderate dysplasia	40	41
18	mild dysplasia	104	98
19	mild dysplasia	100	91
20	severe dysplasia	222	129
21	severe dysplasia	276	374
22	severe dysplasia	61	163
23	severe dysplasia	104	172
24	invasive carcinoma	1227	436**
25	severe dysplasia	430	284**
26	invasive carcinoma	209	200
27	invasive carcinoma	123	230
28	invasive carcinoma	75	57
29	severe dysplasia	768	312**

* This number represents all objects automatically selected by the machine minus all visually recognized artefacts (=non-single nuclei).

** The maximum number of selected objects in one run (=600) was reached before the entire slide was analyzed. As a result, the number of LEYTAS selected cells cannot be compared with the number of SAMBA detected cells.

Chapter 8.5 APPLIED NUCLEAR PARAMETERS.

Each object is relocated in the center of the microscope field and an analogue image as well as a segmented and digitized image is shown at high magnification on the monitor. The operator decides whether or not the object will be entered in the data file. In this way, all objects other than well-segmented single nuclei were interactively eliminated. Of all remaining cells, the nuclear parameters were measured as mentioned in table 8.2.

Table 8.2: Nuclear parameters investigated with SAMBA.

GEOMETRY		
1.	NUS	nuclear area
2.	PER	perimeter
3.	P2/A	form factor
4.	NUS	nuclear area (=1)
DENSITOMETRY		
5.	IOD	integrated optical density
6.	MOD	mean optical density
7.	SKE	skewness of IOD histogram
8.	SOD	standard deviation of IOD histogram
9.	KUR	kurtosis of IOD histogram
TEXTURE		
computed from co-occurrence matrix		
10.	LME	local mean of grey value densities
11.	SMC	second moment of the matrix coefficients
12.	CVC	CV of the matrix coefficients
13.	COT	contrast
TEXTURE		
computed from run length section matrix		
14.	SRE	short run emphasis
15.	LRE	long run emphasis
16.	GLD	grey level distribution
17.	RLD	run length distribution
18.	RPC	run percentage

The previously mentioned SAMBA literature (Brugal et al, 1978; Brugal, 1984) gives a description of how these parameters are measured and what their potential significance might be. It should be noted that from the cytomorphological point of view, most texture parameters could not be easily interpreted. Due to the highly interactive set up of SAMBA, cells can be relocated in the microscope once the nuclear parameters have been measured and consequently the correlation between visual interpretation and parameter value can easily be established. Using this facility it was found that, except parameter 13 (contrast derived from the co-occurrence matrix), the value of the nuclear texture parameters were difficult to predict cytomorphologically. Contrast as it is defined by the co-occurrence matrix, proved to correlate fairly well with the definition of intra nuclear contrast as observed by the

human eye. Concerning the values of the geometrical parameters 1 and 4 and of the densitometrical parameters 5 and 6, they proved to be reasonably predictable. Minor segmentation errors had serious consequences on the perimeter value and the form factor (parameter 2 and 3) and those were therefore of little use for the classification of cells.

To serve as a DNA reference value and to correct for minor changes in staining intensity, about 20 intermediate cell nuclei were measured from each specimen. The IOD as well as all other density-dependent parameters were then corrected using the mean values found for the 20 intermediate cell nuclei. This was done using the special SAMBA program called 'RECAL' (recaller = rescaling).

Chapter 8.6 EFFECT OF NUCLEAR PARAMETERS ON SPECIMEN CLASSIFICATION.

After cell selection and measurement of all 29 slides, all parameter values of cell nuclei from the specimens within the three diagnostic groups are combined in three sets of cells:

1. TNR (Total Negative after Rescaling). A total of 731 cells have been selected in the 9 negative specimens.
2. TDR (Total Dysplasia after Rescaling). A total of 781 cells have been selected in the 10 cases with mild or moderate dysplasia.
3. TPR (Total Positive after Rescaling). A total of 2092 cells have been selected in the 10 positive specimens.

Since the specimen classification can be used as the 'a priori' classification of the selected cells, a supervised classification scheme (stepwise linear discriminant analysis using the Fisher-Snedecor test) can be used to differentiate the different sets of cells.

Table 8.3: Classification results between different sets of cells and selected parameters in ranking order obtained by linear discriminant analysis using the Fisher-Snedecor test.

Discriminating subgroups	ranking of parameters	class result using 1 param.	class result using all param.
TNR - TPR	6-18-15-9-10-3	75 %	85 %
TNR - TDR	6-16-10-13-9-7-15-2-3	79 %	89 %
TNR - TDPR	6-14-9-7-10-11-3	77 %	85 %
TNDR- TPR	10-15-9-5-8-3-7	64 %	68 %
TDR - TPR	7-6-16-4-10-9-3	63 %	80 %

It is evident (and was expected) that the best results are obtained when cells in negative preparations are discriminated from cells in other specimens, either dysplasia or positive or a combination of both. The parameter with main discriminatory power is number 6 (mean IOD) in all three cases. Hyperchromasia (being the cytomorphological translation of 'mean IOD') is a known important parameter to discriminate cytomorphologically between inflammatory cells found in benign lesions and abnormal cells found in malignant or premalignant lesions (Koss, 1979). Therefore the top ranking of mean optical density can easily be confirmed by cytomorphology. The most apparent reason that IOD itself is not mentioned as a parameter in this discrimination is caused by the fact that cell selection was already based on an increased IOD. An additional reason might be the correlation between parameter 6 and the IOD (parameter 5) which is 0.55 (see correlation matrix, figure 30).

Striking is the fact that the discrimination between cells in negative and cells in dysplastic specimens shows better classification results than between cells in negative and in positive preparations. This might be caused by the fact that positive specimens (especially those with a diagnosis of invasive carcinoma) often show necrosis and degeneration which can easily negatively influence the nuclear structure.

From the screening point of view, the most appropriate partitioning is between the cells found in negative slides on one side and between the cells found in the dysplastic and positive slides on the other side (TNR versus TDPR). In this study, dysplasia is considered a lesion to be detected by the system, because only those specimens have been selected where the histopathological examination confirmed the presence of a lesion classified as moderate dysplasia or as a more severe lesion.

Discrimination of TNR cells versus TDPR (a fusion of TDR and TPR) cells leads to a classification result of 85% using all 7 parameters and already to 77% using only the first one (parameter number 6 = mean IOD) (table 8.4).

Table 8.4: Confusion matrix of TNR cells and TDPR cells after linear discriminant analysis (test set = learning set).

1 parameter (no 6) used for classification			optimized parameter set used for classification		
cytology	SAMBA		cytology	SAMBA	
	TNR	TDPR		TNR	TDPR
TNR	591	140	TNR	584	147
TDPR	751	2129	TDPR	463	2417
good class. rate	77%		good class. rate	85%	

The addition of parameters does not change the classification rate for TNR cells as shown in table 8.4. The TDPR cells however, are much better classified using the additional texture and densitometric features.

If we classify the cells of the individual specimens according to TNR and TDPR using all selected parameters, results are achieved as presented in table 8.5.

	1	2	3	4	5	6	7	8	9	10	11	12	13	14	15	16	17	18
1	1.00																	
2	.96	1.00																
3	.05	.28	1.00															
4	1.00	.96	.05	1.00														
5	.70	.68	.06	.70	1.00													
6	-.17	-.16	.04	-.17	.55	1.00												
7	.21	.20	.00	.21	-.25	-.58	1.00											
8	-.17	-.15	.10	-.17	.47	.89	-.40	1.00										
9	.08	.06	-.10	.08	-.01	-.11	.21	-.30	1.00									
10	.12	.11	-.01	.12	-.30	-.53	.52	-.44	.33	1.00								
11	.16	.16	.03	.16	.65	.67	-.57	.59	.03	-.21	1.00							
12	.15	.15	.03	.15	.65	.67	-.57	.60	.03	-.21	1.00	1.00						
13	-.34	-.32	.06	-.34	.26	.80	-.61	.78	-.13	-.41	.71	.72	1.00					
14	.72	.68	.01	.72	.14	-.61	.60	-.56	.08	.26	-.52	-.53	-.77	1.00				
15	.17	.17	.03	.17	.66	.66	-.56	.60	.02	-.19	.96	.96	.70	-.51	1.00			
16	.67	.63	-.01	.67	.07	-.64	.57	-.69	.33	.48	-.45	-.46	-.76	.87	-.46	1.00		
17	.69	.66	.01	.69	.13	-.59	.61	-.54	.07	.25	-.52	-.53	-.75	1.00	-.50	.84	1.00	
18	.74	.71	.01	.74	.15	-.61	.59	-.58	.09	.28	-.51	-.52	.79	1.00	-.50	.90	.98	1.00

Correlation matrix

Figure 30: Correlation matrix of the investigated parameters. The numbers correspond with the parameters given in table 8.2

Table 8.5: Classification results of cells per specimen according to percentages of TNR and TDPR cells, automatically assigned to these classes.

negative slides	% TNR	% TDPR	dysplasia slides	% TNR	% TDPR	positive slides	% TNR	% TDPR
1	73.6	26.4	10	18.2	81.8	20	30.2	69.8
2	57.7	42.3	11	21.0	79.0	21	20.1	79.9
3	99.3	0.7	12	31.7	68.3	22	6.8	93.2
4	78.9	21.1	13	17.9	82.1	23	29.1	70.9
5	62.1	37.9	14	13.8	86.2	24	3.7	96.3
6	88.3	11.7	15	8.8	91.2	25	18.7	81.3
7	47.5	52.5	16	8.3	91.7	26	20.0	80.0
8	55.9	44.1	17	14.6	85.4	27	30.1	69.9
9	48.8	51.2	18	10.2	89.8	28	3.5	96.5
			19	3.3	96.7	29	8.3	91.7

The parameters which have been used for the partitioning in table 8.5, have already been given in table 8.3; mean IOD was ranked first. The average frequency of positively classified cells (classified as TDPR) for the negative specimens is 32.0 ± 1.71 (table 8.6). The average frequencies found in the dysplasia and the positive cases are 85.3 ± 0.76 and 83.0 ± 10.3 respectively.

Table 8.6: Average values of the ratio of positively classified cells per group of specimens.

cytology	average ratio of positively classified cells (\pm sd)	intervals	
		min	max
negative	32.0 ± 1.71	0.7	52.5
dysplasia	85.3 ± 0.76	68.3	96.7
positive	83.0 ± 10.3	69.8	96.5

As shown in table 8.6, no overlap exists between the the confidence ranges and the absolute values of the percentages of positively classified cells between the negative specimens on one hand and the dysplasia and positive specimens on the other hand. This categorizes the partitioning as highly significant.

If we use the ratio of cells classified in one of the two groups (either

TNR or TDPR, since both are complementarily dependent) as a parameter to classify the individual specimens into positive or negative, we find a complete separation between the group of negative specimens and the dysplasia/positive specimens. The lowest ratio of negatively classified cells (classified as TNR) in the negative specimens is 47.5% (no: 7), whereas the highest ratio of negatively classified cells in the positive specimens is 31.7% (specimen no: 12). Thus an absolute separation between negative and dysplasia/positive specimens can be obtained by an Bayesian frontier.

To evaluate the predictive value of the test on this limited number of specimens, a Jack Knifed classification has been performed. For this purpose, five learning subsets of increasing size (6, 9, 15, 21 and 24 cases) have been constructed, each of them containing equal numbers of randomly selected negative, dysplasia and positive specimens. Each of the subsets have been analyzed 3 or 4 times. Each time the total number of specimens in that subset was the same, but contained different specimens of the 9 or 10 available in each of the 3 categories. Results are given in figure 31.

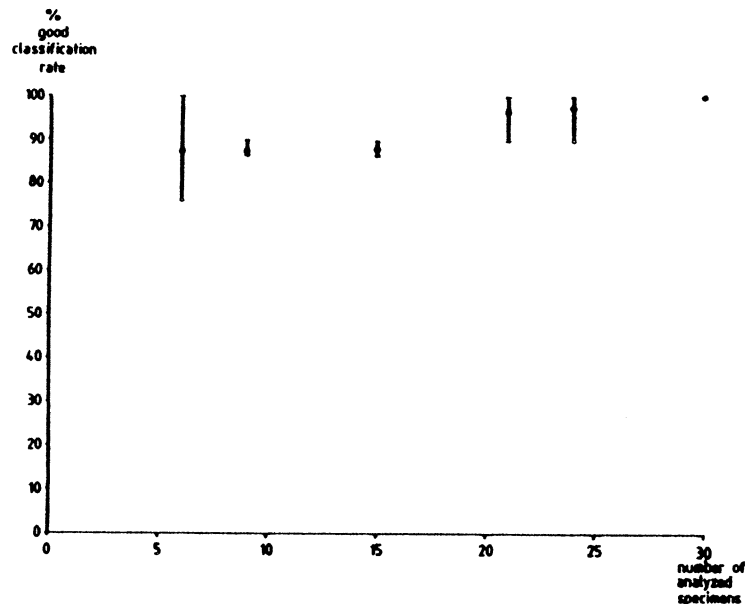


Figure 32: Results of the Jack Knifed classification, using random subsets of the analyzed specimens as the learning set. The average good classification rate is given, with the maximum and the minimum results obtained with the different subsets.

Each of the points given in figure 31, represents the average good classification rate obtained using a given number of learning specimens. The combination of specimens changed, resulting in different classification rates. The variation is given between the lowest and the highest obtained classification rate. From the results presented in figure 31, the following conclusions can be drawn:

1. even with small sets of learning specimens, good classification results can be obtained (varying from 75.9 to 100%).
2. this finding (mentioned under 1) demonstrates the fact that the intragroup variance is considerably lower than the intergroup variance.
3. the distribution of specimens within each class is rather homogeneous with respect to cell type differences.

4. the analysis of about 100 cells which have passed the alarm threshold of LEYTAS, as done in this study, is sufficient to obtain a further discrimination between positive and negative specimens.

Conclusion.

Based on this study, we conclude that the results obtained on this limited number of specimens justify the hypothesis that extension of the study to larger numbers of specimens will not drastically change the good classification results as presented here.

Execution of the applied densitometric and textural parameters on a microprocessor, in principle takes less than a second and, in the case of LEYTAS-2, can be executed in parallel to the screening program using the slave processors; this means that the negative versus positive decision on selected cells is being made while the screening procedure continues. Furthermore the use of a discriminant function to assign cells to a certain class is also a very rapid procedure of a few basic operations once the discriminant analysis is performed on the learning set. Thus it can be expected that the application of relatively sophisticated densitometric and textural parameters will result in a significant decrease in the number of false positively classified specimens, as presently detected by LEYTAS, without inducing a vital delay in the total screening time.

LITERATURE

- Abmayr, W., Burger, G., Soost, H.J.
Progress report of the TUDAB project for automated cancer cell detection.
J. Histochem. Cytochem. 27:604-612, 1979
- Al, I., Ploem, J.S.
Detection of suspicious cells and rejection of artefacts in cervical cytology using LEYTAS.
J. Histochem. Cytochem. 27:629-634, 1979
- Atkin, N.B., Richards, B.M.
Deoxyribonucleic acid in human tumours as measured by microspectrophotometry of Feulgen stain. A comparison of tumours arising at different sites.
Cancer 10:769-786, 1956
- Atkin, N.B., Richards, B.M., Ross, A.J.,
The deoxyribonucleic acid content of carcinoma of the uterus: An assessment of its possible significance in relation to histopathology and clinical course based on data from 165 cases.
Br. J. Cancer 13:773-787, 1959
- Auer, G., Eriksson, E., Azavedo, E., Caspersson, T., Wallgren, A.S.
Prognostic significance of nuclear DNA content in mammary adenocarcinomas in humans.
Cancer research 44: 394-396, 1984
- Bacus, J.W.
Application of digital image processing techniques to cytology automation.
Draft prepared for the National Cancer Institute, September 1982
- Bahr, G.F.
Frontiers of quantitative cytochemistry. A review of recent developments and potentials.
Anal. Quant. Cytol. 1:1-19, 1979
- Bahr, G.F., Bibbo, M., Oehme, M., Puls, J.H., Reale, F.R., Wied, G.L.
An automated device for the production of cell preparations suitable for automatic assessment.
Acta Cytol. 22:243-249, 1978
- Barrett, D.L., Jensen, R.H., King, E.B., Dean, P.N., Mayall, B.H.
Flow cytometry of human gynecologic specimens using log chromomycin A3 fluorescence and log 90 light scatter signals.
J. Histochem. Cytochem. 27:573-578, 1979
- Bartels, P.H., Bahr, G.F., Bibbo, M., Richards, D.L., Sonek, M.G., Wied, G.L.
Analysis of variance of the Papanicolaou staining reaction.
Acta Cytol. 18:522-531, 1974
- Bartels, P.H., Wied, G.L.
Computer analysis and biomedical interpretation of microscopic images: current problems and future directions.
Proceedings IEEE 65:252-262, 1977

- Beer, A.-C., Ostheimer, E.
Vorbereitende Untersuchungen zur Qualitaetspruefung von Zytoautomaten im Routinebetrieb.
Report nr B-SZ 1366/02 Industrieanlagen-Betriebsgesellschaft mbH, 1984
- Bengtsson, E., Eriksson, O., Holmquist, J., Nordin, B., Stenkvist, B.
High resolution segmentation of cervical cells.
J. Histochem. Cytochem. 27:621-628, 1979
- Bibbo, M., Bartels, P.H., Chen, M., Harris, M.J., Truttmann, B., Wied, G.L.
The numerical composition of cellular samples from the female reproductive tract. I. Carcinoma in situ.
Acta Cytol. 19: 438-447, 1975
- Bibbo, M., Bartels, P.H., Chen, M., Harris, M.J., Truttmann, B., Wied, G.L.
The numerical composition of cellular samples from the female reproductive tract. II. Cases with invasive squamous carcinoma of uterine cervix.
Acta Cytol. 20: 249-254, 1976
- Bibbo, M., Bartels, P.H., Chen, M., Harris, M.J., Truttmann, B., Wied, G.L.
The numerical composition of cellular samples from the female reproductive tract. III. Cases with mild and moderate dysplasia of uterine cervix.
Acta Cytol. 20:565-572, 1976.
- Bibbo, M., Bartels, P.H., Dytch, H.E., Wied, G.L.
Ploidy measurements by high-resolution cytometry.
Analyt. Quant. Cytol. Histol. 7:81-88, 1985
- Bibbo, M., Bartels, P.H., Dytch, H.E., Wied, G.L.
Ploidy patterns in cervical dysplasia.
Analyt. Quant. Cytol. Histol. 7:213-217, 1985
- Blomberg, A., Koenig, D., Oberhofer, F., Ostheimer, E., Rehkopf, M.
Einsatzmoeglichkeiten automatisierter Screeningtechniken auf dem Gebiet der Krebsfrueherkennung bei Frauen in der Bundesrepublik Deutschland.
Report nr. B-SZ 1171/01 Industrieanlagen-Betriebsgesellschaft mbH, 1979
- Boddington, M.M.
Scanning area required for screening cervical smears.
In: Proceedings 2nd Tumours Symposium Cytology Automation (ed. D.M.D. Evans) 1968, pp. 14-23
- Boecking, A., Adler, C.P., Common, H.H., Hilgarth, M., Granzen, B., Auffermann, W.
Algorithm for DNA cytophotometric diagnosis and grading of malignancy.
Analyt. Quant. Cytol. 6:1-8, 1984
- Boehm, N., Sandritter, W.
DNA in human tumors: A cytophotometric study.
Current Topics in Pathology nr. 60, 1975 Springer Verlag.
- Boehm, N., Sprenger, E., Sandritter, W.
Fluorescence cytophotometric Feulgen-DNA measurements of benign and malignant human tumors.
Beitr. Path. Bd. 142:210-220, 1971

- Bowie, J.E., Young, I.T.
An analysis technique for biological shape. II.
Acta Cytol. 21:455-464, 1977
- Bowie, J.E., Young, I.T.
An analysis technique for biological shape. III.
Acta Cytol. 21:739-746, 1977
- Brugal, G.
Image analysis of microscopic preparations. Methods and achievements in experimental pathology.
(G. Jasmin and L. Proschek eds.) Karger Medical and Scientific Publishers, Montreal, Quebec, 1984, pp 1-33
- Brugal, G., Adelh, D.
SAMBA 200: an industrial prototype for high-resolution analysis of colored cell images.
Intern. Conf. on High-Resolution Cell Image Analysis, Los Angeles, USA, 24-26 January 1982. (abstract).
- Brugal, G., Chassery, J.M.
Un nouveau système d'analyse densitométrique et morphologique des préparations microscopiques. Application à la reconnaissance et au comptage automatique des cellules dans les différentes phases du cycle mitotique.
Histochemistry 52:241-258, 1977
- Brugal, G., Garbay, C., Giroud, F., Adelh, D.
A double scanning microphotometer for image analysis: hardware, software and biomedical applications.
J. Histochem. Cytochem. 27:144-152, 1979
- Brugal, G., Quirion, C., Vassilakos, P.
Detection of bladder cancers using a SAMBA 200 cell image processor.
Anal. Quant. Cytol. Histol. In Press
- Burger, G., Juetting, U., Rodenacker, K.
Changes in benign cell populations in cases of cervical cancer and its precursors.
Anal. Quant. Cytol. 3:261-271, 1981
- Caspersson, T.
Ueber den chemischen Aufbau der Strukturen des Zellkernes. mikorchemische Methode.
Skand. Arch. Physiol. 73 (suppl.8):1-151, 1936
- Castleman, K.R. (Ed.)
Digital Image Processing.
Prentice-Hall, Inc., Englewood Cliffs, New Jersey, 1979
- Castleman, K.R., White, B.S.
The tradeoff of cell classifier error rates.
Cytometry 1: 156-160, 1980
- Castleman, K.R., White, B.S.
The effect of abnormal cell proportion on specimen classifier performance.
Cytometry 2: 155-158, 1981

Chassery, J.M.
Texture analysis of biological images using a computerized scanning microphotometer: SAMBA.
3rd Intern. Conf. on Automation of Diagnostic Cytology and Cell Image Analysis. Munich, West-Germany, 23-24 May 1980 (abstract)

Chassery, J.M., Cinquin, P., Garbay, C.
Segmentation d'images cytologiques. Etude de méthodes.
AFCET, 4th Congress: Reconnaissance des Formes et Intelligence Artificielle.
Ed. INRIA, 1: 51-69, 1984

Cornelisse, C.J., Driel-Kulker, A.M.J. van
DNA image cytometry on machine-selected breast cancer cells and a comparison between flow cytometry and scanning cytometry.
Cytometry 6:471-477, 1985

Cornelisse, C.J., Driel-Kulker, A.M.J. van, Meyer, F., Ploem, J.S.
Automated recognition of atypical nuclei in breast cancer cytology specimens by iterative image transformations.
J. Microsc. 137:101-110, 1985.

Driel-Kulker, A.M.J. van, Mesker, W.E., Velzen, I. van, Tanke, H.J., Feichtinger, J., Ploem, J.S.
Préparation of monolayer smears from paraffin-embedded tissue for image cytometry.
Cytometry 6:268-272, 1985

Driel-Kulker, A.M.J., van, Ploem, J.S.
The use of LEYTAS in analytical and quantitative cytology.
IEEE Transactions on Biomedical Engineering, vol. BME-29, no 2:92-100, 1982

Driel-Kulker, A.M.J. van, Ploem-Zaaijer, J.J., Zwanvan der Zwan, M. van der, Tanke, H.J.
A preparation technique for exfoliated and aspirated cells allowing different staining procedures.
Anal. Quant. Cytol. 2:243-246, 1980

Driel-Kulker, A.M.J. van, Stoehr, M., Goerttler, K., Tanke, H.J.
Analysis by image processing of cells sorted by two parameter flow cytometry.
In: Flow Cytometry. Proceedings of the IVth International Symposium on Flow Cytometry (Pulse Cytophotometry) (O.D. Laerum, T. Lindmo and E. Thorud eds.) Universitetsforlaget Bergen, 1980, pp. 453-457

Duijndam, W.A.L.
Cytochemical investigations on the Feulgen-Schiff reaction for DNA.
Thesis, University of Leiden, Leiden, The Netherlands, 1975

Eason, P.J., Tucker, J.H.
The preparation of cervical scrape material for automated cytology using Gallocyanin chrome-alum stain.
J. Histochem. Cytochem. 27:25-31, 1979

Evans, A.S., Monaghan, J.M.
Nuclear DNA content of normal, neoplastic and 'wart-affected' cervical biopsies.
Analyt. Quant. Cytol. 5:112-116, 1983

Evans, D.M.D., Shelley, G., Cleary, B., Baldwin, Y.
Observer variation and quality control of cytodiagnosis.
J. Clin. Path. 27:945-950, 1974.

Feldman, M., Poulsen, R., Shepherd, L., Marshall, K.G.
The occurrence of isolated dysplastic and carcinoma in situ type cells in
cervical smears from patients with dysplasia and carcinoma in situ:
significance to prescreening using image processing techniques.
Acta Cytol. 17: 395-400, 1973

Feulgen, R., Rossenbeck, H.
Mikroskopisch-chemischer Nachweis einer Nucleinsaeure vom Typus der
Thymonucleinsaeure und die darauf beruhende elektive Faerbung von Zellkernen
in mikroskopische Praeparaten.
Hoppe-Seylers Z. Physiol. Chem. 135:203-248, 1924

Fowlkes, B.J., Herman, C.J., Cassidy, M.
Flow microfluorometric system for screening gynecologic cytology specimens
using propidium iodide-fluorescein isothiocyanate.
J. Histochem. Cytochem. 24:322-331, 1976

Fu, Y.S., Hall, T.L.
DNA ploidy measurements in tissue sections.
Analyt. Quant. Cytol. Histol. 7:90-95, 1985

Garbay, C., Chassery, J.M., Brugal, G.
An iterative region-growing process for cell image segmentation based on local
color similarity and global shape criteria.
Analyt. Quant. Cytol. Histol. 8:25-34, 1986

Gay, D., Danos, L.M., Goellner, J.R.
Analysis of false-negative cervical cytology at the Mayo Clinic during a
four-year period.
Acta Cytol. 28:652, 1984

Golay, M.J.E.
Hexagonal pattern transforms.
IEEE Trans. on Comp., vol. C18, no. 8, 1969

Hedley, D.W., Friedlander, M.L., Taylor, I.W., Rugg, C.A., Musgrove, E.A.
Method for analysis of cellular DNA content of paraffin embedded pathological
material using flow cytometry.
J.Histochem. Cytochem. 31:1333-1335, 1983

Herman, C.J., Bunnag, B.
Goals of the cytology automation program of the National Cancer Institute.
J. Histochem. Cytochem. 24:2-5, 1976

Hiddemann, W., Schumann, J., Andreeff, M., Barlogie, B., Herman, C.J., Leif,
R.C., Mayall, B.H., Murphy, R.F., Sandberg, A.A.
Convention on nomenclature for DNA cytometry.
Cytometry 5:445-446, 1984

Holmquist, J., Bengtsson, E., Eriksson, O., Nordin, B., Stenkvist, B.
Computer analysis of cervical cells, automatic feature extraction and
classification.
J. Histochem. Cytochem. 26:1000-1017, 1978

- Hrushovetz, S.B., Lauchlan, S.C.
Comparative DNA content of cells in the intermediate and parabasal layers of cervical intraepithelial neoplasia studied by two-wavelength Feulgen cytophotometry.
Acta Cytol. 14:68-77, 1970
- Husain, O.A.N., Blanche Butler, E., Evans, D.M.D., MacGregor, J.E., Yule, R.
Quality control in cervical cytology.
J. Clin. Path. 27: 935-944, 1974
- Husain, O.A.N., Page-Roberts, B.A., Millet, J.A.
A sample preparation for automated cervical cancer screening.
Acta Cytol. 22:15-21, 1978
- Husain, O.A.N., Watts, K.C.
The rapid demonstration of nucleic acids using 'oxidised' gallocyanin and chromic potassium sulphate: Methods and applications.
J. Clin. Pathol. 37:99-101, 1984
- Ingen, E.M. van, Tanke, H.J., Ploem, J.S.
Model studies on the acriflavine-Feulgen reaction.
J. Histochem. Cytochem. 27:80-83, 1979
- Jakobsen, A., Bichel, P., Sell, A.
DNA distribution in biopsy specimens from human cervical carcinoma investigated by flow cytometry.
Virchows Arch B Cell Path. 29:337-342, 1979
- Jensen, R.H., Mayall, B.H., King, E.B.
Multiparameter flow cytometry applied toward diagnosis of cervical carcinoma. In: The automation of cancer cytology and cell image analysis (N.J. Pressmann and G.L. Wied, eds.) Tutorials of Cytology, Chicago, 1979, pp. 95-102
- Kishigami, Y., Noda, S., Morishita, T., Hashimoto, Y.
Improvement of the preparation method for vaginal smears for the auto-cyto-screener.
Anal. Quant. Cytol. 3:43-48, 1981
- Kolmogorov, A.
Confidence limits for an unknown distribution function.
Ann. Math. Statist. 12:461-463, 1941
- Koss, L.G.
Diagnostic cytology and its histopathologic bases.
Two volumes, J.B. Lippincott comp., Philadelphia 3rd ed. 1979
- Kunze, K.D., Hermann, W.R., Meyer, W.
The ZYPAB imageprocessing system for cytologic prescreening for cervical cancer.
Anal. Quant. Cytol. 2:252-263, 1980
- Leif, R.C., Gall, S., Dunlap, L.A., Ratley, C., Zucker, R.M., and Leif, S.B.
Centrifugation cytology: IV. The preparation of fixed stained dispersions of gynecologic cells.
Acta Cytol. 19:159-168, 1975

- Louis, C., Poulsen, R., Marshall, K.G., Johnston, R. de B.
The occurrence of isolated dysplastic, carcinoma in situ, and invasive type cells in cervical smears from patients with invasive squamous cell carcinoma: significance to prescreening using image processing techniques.
Acta Cytol. 20:158-161, 1976
- Mayall, B.H.
Deoxyribonucleic acid cytophotometry of stained human leukocytes. I. Differences among cell types.
J. Histochem. Cytochem. 17:249-259, 1969
- Mayall, B.H.
System operating characteristic and cost analysis in automated cytodiagnosis of gynecologic specimens.
J. Histochem. Cytochem. 27:584-590, 1979
- Matheron, G.
Eléments pour une théorie des milieux poreux.
Masson, Paris, 1967.
- Matheron, G.
Random sets and integral geometry.
Wiley, New York, 1975.
- Mazia, D., Schatten, G., Sale, W.
Adhesion of cells to surfaces coated with polylysine. Applications to electron microscopy.
J. Cell Biology 66:198-200, 1975
- Meyer, F.
Contrast feature extraction.
In: Quantitative analysis of microstructures in material sciences, biology and medicine. Special issue of Practical Metallography (Chermant, J.L., Ed). Riederer Verlag, Stuttgart, pp 374-380, 1978.
- Meyer, F.
Iterative image transformations for automatic screening of cervical smears.
J. Histochem. Cytochem. 27:128-135, 1979
- Meyer, F.
Cytologie quantitative et morphologie mathématique.
Thesis, l'Ecole Nationale Supérieure des Mines de Paris, France, 1979
- Meyer, F.
Empiricism or idealism ...
In: Pattern Recognition in Practice (E.S. Gelsema, L.N. Kanal, eds.) North-Holland Publ. Company, Amsterdam, 1980
- Meyer, F., Driel-Kulker, A.M.J. van
Automatic screening of Papanicolaou stained cervical smears with the TAS.
Acta Microscopica, suppl. 4:82-95, 1980
- Meyer F., van Driel, A.
The application of mathematical morphology in cervical cancer screening.
In: Quantitative image analysis in cancer cytology and histology (Mary, J.Y., Rigaut, J.P., Eds). Elsevier, Amsterdam, pp 33-49, 1986.

Mikuz, G., Hofstaedter, F., Delgado, R.
Extraction of cells from paraffin-embedded tissue sections for single-cell DNA cytophotometry.
Anal. Quant. Cytol. Histol. 7:343-346, 1985

Montana, J., Tolles, W.E., Garcia, G.L., Bennett, M., Willis, B.B.
Cytologic cell collection suspension and preservation for automated screening procedures.
Anal. Quant. Cytol. 4:55-59, 1982

Mukawa, A., Kamitsuma, Y., Jisaki, F., Tanaka, N., Ikeda, H., Ueno, T., Tsunekawa, S.
Progress report on experimental use of CYBEST model 2 for practical gynecologic mass screening. Alterations of the specimen rejection threshold and specimen preparation.
Anal. Quant. Cytol. 5:31-35, 1983

Nasiell, K., Auer, G., Nasiell, M., Zetterberg, A.
Retrospective DNA analysis in cervical dysplasia as related to neoplastic progression or regression.
Anal. Quant. Cytol. 1:103-106, 1979

Neugebauer, D., Otto, K., Soost, H.-J.
Numerical analysis of cell populations in smear and monolayer preparations from the uterine cervix. I. The proportions of isolated, abnormal epithelial cells in slides from one applicator.
Anal. Quant. Cytol. 3: 91-95, 1981

Otto, K., Hoeffken, H., Soost, H.-J.
Components and results of a new preparation technique for automated analysis of cervical samples.
Anal. Quant. Cytol. 1:127-135, 1979

Otto, K., Hoeffken, H., Soost, H.-J.
Sedimentation velocity separation: a preparation method for cervical samples.
J. Histochem. Cytochem. 27:14-18, 1979

Oud, P.S., Zahniser, D.J., Haag, D.J., Boekel, M.C.G. van, Hermkens, H.G., Herman, C.J., Vooijs, G.P.
A new disaggregation device for cytology specimens.
Cytometry 5:509-514, 1984

Papanicolaou, G.N.
Diagnosis of uterine cancer by the vaginal smear.
New York St. J. Med. 45: 1336-1338, 1945

Pearse, A.G.E.
Histochemistry. Theoretical and Applied. Volume one: Preparative and optical technology. Churchill Livingstone, Edinburgh, London and New York, fourth edition, 1980

Ploeg, M. van der, Broek, K. van den, Smeulders, A.W.M., Vossepoel, A.M., Duijn, P. van
HIDACSYS: computer programs for interactive scanning cytophotometry.
Histochemistry 54:273-288, 1977

Ploeg, M. van der, Duijn, P. van, Ploem, J.S.
High-resolution scanning-densitometry of photographic negatives of human metaphase chromosomes. I. Instrumentation.
Histochemistry 42:9-29, 1974

Ploem, J.S.
New instrumentation for sensitive image analysis of fluorescence in cells and tissues.
In: Fluorescence in the Biological Sciences (D. Lansing Taylor, A.S. Waggoner, F. Lanni, R.F. Murphy, R.R. Birge, eds.) Alan R. Liss Inc. New York, 1986, pp. 289-300

Ploem, J.S., Driel-Kulker, A.M.J. van, Goyarts-Veldstra, L., Ploem-Zaaijer, J.J., Verwoerd, N.P., Zwan, M. van der
Image analysis combined with quantitative cytometry: results and instrumental developments for cancer diagnosis.
Histochemistry 84:549-555, 1986

Ploem, J.S., Verwoerd, N., Bonnet, J., Koper, G.
An automated microscope for quantitative cytology combining television image analysis and stage scanning microphotometry.
J. Histochem. Cytochem. 27:136-143, 1979

Ploem-Zaaijer, J.J., Beyer-Boon, M.E., Leyte-Veldstra, L., Ploem, J.S.
Cytofluorometric and cytophotometric DNA measurements of cervical smears stained using a new bi-color method.
In: The automation of cancer cytology and cell image analysis (N.J. Pressmann and G.L. Wied, eds.) Tutorials of Cytology, Chicago, 1979, pp. 225-235

Pycok, D., Taylor, C.J.
Use of the MAGISCAN image analyzer in automated uterine cancer cytology.
Anal. Quant. Cytol. 2:195-202, 1980

Pycok, D., Taylor, J.
The magiscan image analyser as a diagnostic aid in cytology.
Anal. Quant. Cytol. 3: 49-54, 1981

Reinhardt, E.R., Erhardt, R., Schwarzmnn, P., Bloss, W.H., Ott, R.
Structure analysis and classification of cervical cells using a processing system based on TV.
Anal. Quant. Cytol. 1:143-150, 1979

Ringsted, J., Amtrup, F., Asklund, C., Baunsgaard, P., Christensen, H.E., Hansen, I., Jakobsen, C., Jensen, N.K., Moesner, J., Rasmussen, J., Reintoft, I., Rolschau, J.
Reliability of histo-pathological diagnosis of squamous epithelial changes of the uterine cervix.
Acta Path. Microbiol. Scand. Sect. A. 86:273-278, 1978

Rodenburg, C.J., Cornelisse, C.J., Heintz, A.P.M., Hermans, J., Fleuren, G.J.
Tumor ploidy as a major prognostic factor for survival in advanced ovarian cancer.
Cancer (in press)

Rodenburg, C.J., Ploem-Zaaijer, J.J., Cornelisse, C.J., Mesker, W.E., Hermans, J., Heintz, A.P.M., Ploem, J.S., Fleuren, G.J.

DNA image cytometry additional to flow cytometry in advanced ovarian cancer; an improvement in predicting the clinical outcome.

Submitted for publication.

Rosenthal, D.L., Stern, E., McLatchie, C., Wu, A., Lagasse, L.D., Wall, R., Castleman, K.R.

A simple method of producing a monolayer of cervical cells for digital image processing.

Anal. Quant. Cytol. 1:84-88, 1979

Specifications for automated cytodiagnostic systems proposed by the International Academy of Cytology.

Acta Cytol. 28:352, 1984

Sandritter, W., Carl, M., Ritter, W.

Cytophotometric measurements of the DNA content of human malignant tumors by means of the Feulgen reaction.

Acta Cytol. 10:26-30, 1966

Schenck, U., Neugebauer, D., Otto, K., Soost, H.-J., Wagner, D.

Monolayer preparation of cervical samples.

Anal. Quant. Cytol. 3:285-287, 1981

Sedlis, A., Walters, A.T., Balin, H., Hontz, A., Sciuto, L.

Evaluation of two simultaneously obtained cervical cytological smears, a comparison study.

Acta Cytol. 18:291-296, 1974

Serra, J.

Image Analysis and Mathematical Morphology.

Academic Press Inc. London, 1982

Smeulders, A.W.M.

Pattern analysis of cervical specimens.

Thesis, University of Leiden, The Netherlands, 1983

Smeulders, A.W.M., Leyte-Veldstra, L., Ploem, J.S., Cornelisse, C.J.

Texture analysis of cervical cell nuclei by segmentation of chromatin patterns.

J. Histochem. Cytochem. 27:32-35, 1979

Soost, H.-J., Falter, E.W., Otto, K.

Comparison of two Papanicolaou staining procedures for automated prescreening.

Anal. Quant. Cytol. 1:37-42, 1979

Sprenger, E., Witte, S.

The diagnostic significance of nuclear deoxyribonucleic measurements in automated cytology.

J. Histochem. Cytochem. 27:520-521, 1979

Stephenson, R.A., Gay, H., Fair, W.R., Melamed, M.R.

Effect of tissue thickness on quality of flow cytometric DNA content determinations in paraffin-embedded tissues.

Cytometry 7:41-44, 1986

Sturmans, F., Haes, W.F.M. de, Mulder, P.G.H.

De betekenis van de betrouwbaarheid en validiteit van de testmethode en de prevalentie van de ziekte bij de beslissing al of niet tot screening over te gaan.

Huisarts en wetenschap 19:87-93, 1976

Tanaka, N., Ikeda, H., Ueno, T., Mukawa, A., Kamitsuma, K.

Field test and experimental use of CYBEST Model 2 for practical gynecologic mass screening.

Analyt. Quant. Cytol. 1:122-126, 1979

Tanaka, N., Ikeda, H., Ueno, T., Okamoto, Y., Hosoi, S.

CYBEST-CDMS Automated cell dispersion and monolayer smearing device for CYBEST.

Anal. Quant. Cytol. 3:96-102, 1981

Tanke, H.J.

Cytochemical staining of DNA and RNA for analytical cytology. Development of methods for image and flow cytometry and their diagnostic application.

Thesis, University of Leiden, Leiden, The Netherlands, 1982

Tanke, H.J., Ingen, E.M. van

A reliable Feulgen-Acriflavine-SO₂ staining procedure for quantitative DNA measurements.

J. Histochem. Cytochem. 28:1007-1013, 1980

Tanke, H.J., Ingen, E.M., van, Ploem, J.S.

Acriflavine-Feulgen stilbene staining: a procedure for automated cervical cytology with a television based system (LEYTAS)

J. Histochem. Cytochem. 27:84-86, 1979

Tanke, H.J., Ploem, J.S., Jonas, U.

Kombinierte Durchflusszytometrie und Bildanalyse zur automatisierten Zytologie von Blasenepithel und Prostata

Akt. Urol. 13:109-115, 1982

Taylor, J., Puls, J., Sychra, J.J., Bartels, P.H., Bibbo, M., Wied, G.L.

A system for scanning biological cells in three colors.

Acta Cytol. 22:29-35, 1978

Timmers, T., Gelsema, E.S.

A model for the classification of specimens containing random proportions of abnormal cells.

Cytometry 6:22-25, 1985

Tucker, J.H.

An image analysis system for cervical cytology automation using nuclear DNA content.

J. Histochem. Cytochem. 27:613-620, 1979

Tucker, J.H., Gresham, G.A.

Preparation of cervical scrape material for automatic screening.

J. Obstetrics and Gynaecol. 78:947-953, 1971

- Tucker, J.H., Husain, O.A.N.
Trials with the cerviscan experimental prescreening device on
polylysine-prepared slides.
Anal. Quant. Cytol. 3: 117-120, 1981
- Tucker, J.H., Shippey, G.F.
Basic performance tests on the CERVIFIP linear array prescreener
Anal. Quant. Cytol. 5:129-137, 1983
- Vindelov, L.L., Christensen, I.J., Nissen, N.I.
Standardization of high-resolution flow cytometric DNA analysis by the
simultaneous use of chicken and trout red blood cells as internal reference
standards.
Cytometry 3: 328-331, 1983
- Vrolijk, J., Pearson, P.L., Ploem, J.S.
"LEYTAS", A system for the processing of microscopic images.
Anal. Quant. Cytol. 2:41-49, 1980
- Wagner, D., Sprenger, E., Merkle, D.
Cytophotometric studies in suspicious cervical smears.
Acta Cytol. 20:366-371, 1976
- Watts, K.C., Husain, O.A.N., Tucker, J.H., Stark, M., Eason, P., Shippey, G.,
Rutovitz, D., Frost, G.T.B.
The use of cationic polyelectrolytes in the preparation of cell monolayers for
automated cell scanning and diagnostic cytopathology.
Anal. Quant. Cytol. 6:272-278, 1984
- Weber, J.E., Baldessari, B.A., Bartels, P.H.
Test statistics for detecting aneuploidy and hyperdiploidy.
Anal. Quant. Cytol. Histol. 7:131-139, 1985
- Wheless, L.L., Onderdonk, M.A.
Preparation of clinical gynecologic specimens for automated analysis. An
overview.
J. Histochem. Cytochem. 22:522-525, 1974
- Wied, G.L., Bibbo, M., Pishotta, F.T., Bartels, P.H.
Intermediate cell markers for malignancy. Consistency of expression.
Anal. Quant. Cytol. 6:243-246, 1984
- Wittekind, D.
Standardization of dyes and stains for automated cell pattern recognition.
Anal. Quant. Cytol. Histol. 7:6-31, 1985
- Wittekind, D., Hilgarth, M., Kretschmer, V.
Die einfache und reproduzierbare Papanicolaou-Faerbung.
Geburtsh. u. Frauenheilk. 39:969-973, 1979
- Zahniser, D.J.
The development of a fully automatic system for the prescreening of cervical
smears: BIOPEPR.
Thesis, University of Nijmegen 1979

Zahniser, D.J., Oud, P.S., Raaijmakers, M.C.T., Vooys, G.P., Walle, R.T. van
de
Field test results using the BioPEPR cervical smear prescreening system.
Cytometry 1:200-203, 1980

SUMMARY.

In this thesis, a method will be presented to diagnose premalignant and malignant lesions of the cervix uteri on cervical scrape specimens using an automatic screening device.

About 15 years ago, the desire to detect and treat all precancerous and cancerous lesions of the cervix uteri, was initiated by the western civilized world and stimulated by the upcoming women liberation societies. The execution of a mass screening program was however, hampered by the lack of sufficiently trained cytotechnicians. Since at that time unemployment was not yet considered a major economical problem, the solution was sought in an automated screening system.

The quality of visual screening was not as well investigated as nowadays and the only demand was the development of a system which could do the screening with an equivalent accuracy as a cytotechnician but much faster. It was only 5 to 10 years later that the requirements for automated cytology systems became more exactly defined. During these years the false negative errors of conventional screening of certified cytology laboratories (up to 25% false negative diagnoses) were published and related to the incidence of cervical carcinoma (5 per 1000) in the female population. These numbers caused a shift in the machine requirements; accuracy became more important than speed. In a report published in 1983 with support of the German government, the maximum false negative error for severe dysplasia and more serious lesions of any machine should be restricted to 2%. The International Academy of Cytology even describes the false negative limits as: "the system shall not pass as negative any sample which contains malignant tumor cells". In other words, the system should be much better than visual screening. These severe restrictions have played a major role in the development of the Leyden Television Analysis System (LEYTAS) as will be discussed in this thesis.

The main aim of the investigation reported in this thesis is the diagnosis of malignant and premalignant lesions of the cervix uteri with a high sensitivity (low false negative rate (FNR)), higher than the sensitivity in most of the cytological laboratories using conventional diagnostics. A higher specificity (lower false positive rate (FPR)) than conventional cytodiagnosis is hardly possible since the FPR of the visual performance is below 1%. However, the number of false positively classified specimens should not be so high that it is no longer economically attractive to use a system since a cytotechnologist has to rescreen all these slides. The time needed for an automated classification should be similar to the time needed for a visual diagnosis.

One of the drawbacks of automated image analysis for the classification of cervical specimens is the complexity of the traditionally used cervical smear as was introduced by Papanicolaou. Since the presently available machines are not as capable in the recognition of different cellular constituents as the human eye, automated analysis of cells demands additional preparation procedures as compared to techniques used in conventional cytology. Therefore a procedure has been developed to reduce the number of overlapping cells and the varying thickness of the preparations. This procedure together with its rationales and applied staining procedures are presented in chapter 3. Two types of material have been discussed separately: fresh and paraffin embedded material.

The preparation procedure for fresh material starts with the sampling of cervical cells using a cotton-wool tipped applicator, after which the applicator is immersed in a preservative solution with ethanol in a final concentration of 25%. In this solution the cells can be kept for several days at room temperature which enables mailing. Further preparation includes fixation in carbowax, cell dissociation by syringing and cell concentration

estimation by light scatter measurements. If necessary the cells are further diluted. The fixed cells are deposited onto the glass using a newly developed centrifugation bucket. To enhance attachment of cells to the glass, centrifugation is performed at high centrifugal force and microscope slides are coated with poly-L-lysine. Subsequently the slides are left to dry and kept in the refrigerator until staining.

Preparation of paraffin embedded material starts with thick (50 μ m) sections. These are dewaxed using xylene and rehydrated in a sequence of aqueous solutions with decreasing ethanol concentrations, finishing with PBS. Incubation in a 0.05% pronase solution at 37°C with intermittent vortex mixing activates cellular isolation. After thorough washing with cold PBS, the sample is filtrated to remove remaining cell clumps. Cells which pass the filter are deposited onto a microscope glass by means of the centrifugation technique.

To enable the determination of the DNA content during the automated analysis, a reference cell is needed with a fixed and known DNA content. For this purpose, erythrocytes of rainbow trouts, containing 80% of the human diploid DNA value, are centrifuged simultaneously with the patients cell suspension. Deposition takes place onto the same microscope preparation but on a different fixed location.

Since several preparations can be made from one cell sample, different staining procedures can be used as described in chapter 3.4. The routine protocol includes the staining of one preparation with the conventional Papanicolaou and one with the acriflavine-Feulgen-SITS (AFS) procedure. The AFS staining procedure has been developed to match machine requirements while also enabling cytomorphologic examination. The method contains 2 different dyes; one dye (acriflavine) which stains DNA quantitatively according the Feulgen reaction, and a second dye (SITS) for demonstrating cellular protein. In the AFS the two dyes can be visualized separately using the different spectral properties. (absorption maximum of acriflavine is 466 nm and of SITS 365 nm). With LEYTAS (the system for which this staining has been developed) only the absorption image of acriflavine is analysed at its optimal wavelength of 466 nm. At this wavelength SITS absorbs no light and the quantitative properties of acriflavine can be fully explored. The use of SITS is mainly for cytomorphological reasons (recognition of amount and shape of cytoplasm, nucleoli). The blue fluorescence of SITS can be visualized using UV exciting light. To control the reproducibility of the PAP and the AFS procedure on centrifugation preparations during a long period, microdensitometry measurements were carried out on slides from 42 routinely executed staining series. The average CV per slide (intraslide variation) was 9.4% for the Papanicolaou and 4.7% for the AFS procedure whereas the interslide variation (CV of average IOD's per slide) amounted to 9.2 and 5.8% respectively. It can be concluded that the high reproducibility of the AFS procedure makes it highly suitable for automated image analysis.

Another staining procedure is described to be used for automated analysis of conventional smears. Although this thesis mainly deals with the analysis of suspension preparations, a preliminary investigation of the automated analysis of conventional smears is also discussed. In the case of conventional smears, no parallel slides can be made and thus cytomorphology and image analysis have to be performed on the same preparation. First the specimen is stained according to gallocyanine and analyzed with the machine. Following automated analysis, the slides are counterstained using the normal Papanicolaou dyes as eosin and orange G. Resulting images are hardly distinguishable from Pap images using hematoxylin as the nuclear stain, whereas the machine could analyze nuclear densities without disturbance from varying cytoplasmic staining intensities.

In chapter 4, a description is given of the system used for automated

image analysis: the Leyden Television Analysis System (LEYTAS). Two versions of LEYTAS have been developed during the investigation, being distinctive both in the optical system as well as in the structure of the image analysis computer.

Concerning the optical system, LEYTAS-1 is composed of a, although completely automated, conventional microscope, whereas the microscope system for LEYTAS-2 is specially constructed for image analysis. A super wide field objective has been used which results in microscope fields of $500 \times 500 \mu\text{m}$ with a $1 \mu\text{m}$ pixel separation at low magnification. Both systems use Plumbicon high quality measuring cameras as input devices. Automatic change in magnification in the LEYTAS-1 microscope has been realized by a computer controlled rotor in front of the camera including two projectives with a different magnification. The LEYTAS-2 microscope is equipped with two cameras working at a different magnification. For instance, rapid cell selection can be done with the low magnification TV camera; once an object is detected and centered, the image of the high magnification camera can be analyzed at high resolution. Automated focusing is provided via movement of the microscope stage in LEYTAS-1 and via movement of the objective in LEYTAS-2. Concerning the image analysis part of the systems, the TAS (Texture Analysis System) and the MIAC (Modular Image Analysis Computer) - both from Leitz - are used in the old and the new version respectively.

Both versions have been constructed in such a way that the user has easy insight in the performance of the image analysis routines. The TAS by itself offers the possibility to follow each image analysis transformation on the television monitor, which is of considerable advantage during development of new programs. Furthermore, the grey value buffer memory (containing 4 bit greyvalue information for LEYTAS-1 and 8 bit for LEYTAS-2) in which selected objects can be stored, allows direct visualization of the results of the cell selection during and after the entire screening procedure. Visual inspection of one TV screen displaying 16 alarms takes less than a minute and offers possibilities to add rapid human interaction to automated screening. This facility can be used to eliminate visually the few remaining artefacts and to investigate quickly whether possibly abnormal cells are present. Besides this way to interact with the screening results, a relocation of alarms in the microscope is also possible. This is executed with the computer operated stage using the stored x and y coordinates.

Most of the image analysis used for this study is based on iterative transformations. An overview of the applied transformations is given in chapter 4.3; the programs have been written by Meyer from the Centre of Mathematical Morphology in Fontainebleau, France (Meyer, 1979; Meyer, 1982). A nuclear segmentation algorithm has been implemented which is based on the detection of zones with high gradient. The 'top hat' transformation is applied to select cells on parameters which are highly related to DNA content. This transformation combines different greyvalue thresholds with size estimations in order to select cells on the basis of nuclear contrast and size. Two fixed combinations are used at present differing both in contrast and size requirements.

The variable settings of sizes and grey value thresholds used in the 'top hat' transformation were determined on a learning set of about 150 preparations, using a sequential method of testing. The learning set consisted exclusively of negative (normal and inflammation) and positive (severe dysplasia and more serious lesions) specimens. No specimens with a cytological diagnosis of mild or moderate dysplasia entered the trial during the learning phase, because of the known uncertainty of the cytological diagnosis as well as its high potential to regress. Two settings were selected: 'high level' (HL) and 'low level' (LL). HL settings were optimized to detect no or almost no nuclei in negative specimens but to detect single

nuclei in most positive specimens. Although the HL criteria appeared to be a highly sensitive parameter, the number of selected nuclei generally was low. Thus, the chance of missing these nuclei would be high. Therefore the LL criteria were added to detect more cells in the positive specimens, accepting the detection of few cells in the negative cases.

Only those objects which pass the 'top hat' transformation are tested with several artefact rejection routines using a hierarchical tree structure. This means that objects continue into the tree only when previous artefact rejection algorithms accepted the objects as potential single nuclei. First two 'top hat' transformations are performed for rapid elimination of artefacts on the basis of contrast and size, followed by transformations measuring nuclear shape. All these transformations are carried out on entire microscope fields. Finally, a parameter derived from the bending energy and from the most concave and convex parts of the object is measured from individual nuclear contours of all selected cells.

In chapter 4.3.3 the performance of the different image analysis transformations on the object level is discussed. It is shown that about 67% of all visually abnormal cells in the specimen are selected. Regarding all objects selected by the 'top hat' transformation, the number of relevant objects (single cells) constitutes 46% of these. Artefact rejection algorithms based on image transformations proved to eliminate 79% of all selected artefacts (non-single nuclei) whereas also 10% of all single nuclei were rejected. The transformations which perform best are those based on the conditional bisectrix. After the artefact elimination transformations, single nuclei constitute 79% of all selected, remaining objects. The contours of these objects are tested individually for a parameter strongly related to the bending energy. This parameter eliminates 38% of remaining non-single nuclei and 3% of remaining single nuclei.

In the last part of chapter 4, the Total Cell Population Analysis (TCPA) program is described which characterizes all individual cells concerning nuclear size and absorption, in contrast to the screening program that is focused on object selection and cell counting.

In chapter 5, the frequency of HL and LL selected cells (chapter 5.1) and alarms (cells + artefacts) (chapter 5.2) are discussed in a series of 972 specimens. It is shown that the number of selected LL cells as well as HL cells is significantly different between the group of negative specimens (NOR), the specimens with a cytological diagnosis of mild or moderate dysplasia (DYS) and the specimens with a cytological diagnosis of severe dysplasia and more serious lesions (POS). The number of LL cells proved to provide a more significant distinction between the three groups than the number of HL cells.

Furthermore a comparison was made between numbers of visually counted abnormal cells in the literature and the numbers of HL and LL cells selected by the machine. Although the different counting methods reported in the literature varied, which contributed to the variance in the number of counted cells, it appeared that the number of LEYTAS selected cells was in the same order of magnitude and showed the same trend.

In the last part of this chapter, absolute and relative alarm numbers are given as they are obtained using the LL settings. In this case no visual discrimination is made between LEYTAS selected single nuclei and non-single nuclei. Again, differences found between the three diagnostic groups of specimens proved to be significant at the 99% level using the Kolmogorov Smirnov test for comparison of cumulative histograms. A decision threshold based on the absolute and relative alarm numbers was selected which results in as few missed positive classifications as possible, whereas the false positive rate is still within limits.

In chapter 6, the classification results of a series of 1459 specimens is

given using the decision thresholds as determined in chapter 5 (minimal absolute number is 10 and minimal relative number is 0.3%). This results in a false positive rate of 13% for the negative specimens and 49.3% for the inflammatory specimens. The missed positive rate varies from 15.8% in the specimens diagnosed as mild dysplasia, 8.5% in the moderate dysplasia and 0.3% (1 out of 321) in the positive specimens. The negative and the inflammatory specimens have been evaluated separately in this series because of the high proportion of inflammatory specimens, caused by the fact that these samples were obtained in gynecologic clinics from patients with complaints. To estimate the false positive rate in a population screening program, a series of 563 cervical samples from a birth control center have been analyzed. The false positive rate (FPR) for this group of specimens including both negative and inflammatory specimens is 16%. Reduction of the FPR to 11% can be obtained easily by a rapid interactive procedure during which detected non-single nuclei are visually recognized on the basis of stored greyvalue images and subsequently eliminated.

The missed positive rate in morphologically positive specimens is thus very low (0.3%) and fulfills the demands formulated by Blomberg et al (1979). Missed positive rates in the mild and moderate dysplasias are higher; they are partly caused by problems in cellular preservation (in cases where no exact cytological diagnosis can be given, but atypia is seen), and in ambiguity in the cytological diagnosis (especially in the cases of mild dysplasia). The T CPA program proved to be more sensitive to detect dysplasia specimens. On the other hand, regarding the high potential of dysplastic lesions to regress combined with the uncertainty of the cytological diagnosis of dysplasia, a high detection of dysplastic cases should not be necessary or even desired.

Reproducibility tests of the screening program showed that none of the specimens in the presented series ever changed classification after re-analysis. Re-analysis has been carried out on every positive specimen of which the criteria fell close to the decision threshold. It was also found that rescreening could be performed until at least one year after staining without consequences for the slide classification, provided the specimens were stored in the dark at 4°C. When comparing different preparations from one cell sample, only small variations occurred as can be expected from different aliquots from a well dispersed cell sample. A change in the slide classification occurred only once when a parallel preparation from the only missed positive preparation from the series was screened. The classification changed into positive. Parallel preparations of other positive samples which fell very close to the cut-off value, were also positively classified.

The relatively elaborate preparation procedure which is needed for the presented LEYTAS classification, is considered by us as a limitation of its applicability in a population screening. Therefore an investigation has started to analyze conventional smears. For this purpose the galloxyanine staining procedure has been used. In chapter 6.4, a pilot study of 32 negative smears, 4 smears with a diagnosis of dysplasia and 1 carcinoma in situ is presented. No overlap was found in the absolute and/or relative numbers of alarms when comparing the negative smears with the positive smear. One of the smears diagnosed as mild dysplasia showed numbers in the same range as the negative smears. The program for analyzing conventional smears will be further optimized and tested on larger series.

Results of the Total Cell Population Analysis (T CPA) program are presented in chapter 6.5 with regard to its potential to classify centrifugation preparations. In a pilot study of 109 specimens, where the results of the T CPA program have been compared with the results of the already existing screening program, a higher detection rate of specimens diagnosed as mild and moderate dysplasia was obtained with T CPA. At the same time, the false positive rate was also improved. At present, the applicability of the T CPA

program is limited only by its speed (several hours for the analysis of 1 square cm). Implementation on LEYTAS-2 and execution on a limited number of microscope fields as an addition to the screening program, will probably result in an acceptable screening time.

In chapter 7, potentialities of LEYTAS are given with regard to DNA measurements. These can be carried out on cells in clinical samples which have been selected automatically using the LEYTAS screening facilities. The stored greyvalue images of the alarms are used to visually recognize all remaining artefacts which have not been eliminated automatically. Each cell is measured and its IOD value is correlated to the reference cell value. In the case of LEYTAS-2, DNA measurements can be performed simultaneously with the screening program in one of the slave processors. Relocation will then no longer be necessary.

This measurement procedure can be applied to the different cell selection facilities of the screening program (e.g. 'low level' and 'high level' criteria). Random cell selection can also be carried out by adjusting the 'top hat' settings such that most epithelial cells will be selected. It is indicated that high DNA (e.g. $>5C$) values that are not present or present in very low frequencies in a histogram of randomly selected cells, can be visualized clearly in histograms where cells have been selected on the basis of the LL or HL criterium. It also becomes clear that the 'top hat' transformation can be regarded as a rough threshold for DNA values. A rough estimate of the DNA threshold for the LL and HL settings of the 'top hat' transformation proves to be $3C$ and $5C$ respectively.

In chapter 7.3 some typical examples have been given of DNA histograms from cervical specimens with different cytological and/or histological diagnosis. In the histograms from specimens with an abnormal cytological diagnosis (dysplasia or more serious lesion), a tendency was found towards the presence of aneuploid cells in the upper tetraploid region. Histograms from inflammatory lesions and viral infections tended to form peaks in the regions with polyploid DNA values, without many cells in the upper tetraploid region. In principle the time to generate a DNA histogram using LEYTAS-2 takes less than 5 minutes. This means that automatic measurements of large numbers of cells can now be performed with image analysis with speed approaching the speed of flow cytometry. The advantage of image cytometry is the highly developed level of artefact rejection; whereas most signals in the high value region of a flow DNA histogram are caused by artefacts (mainly overlapping nuclei), LEYTAS histograms consist predominantly (or exclusively if visually recognized artefacts are eliminated) of single nuclei. This opens new possibilities in the study of DNA content. To the DNA studies mainly focused on stemline aberrations, as can be accurately determined by flow cytometry, the information on the occurrence of less frequent aneuploid cells can now be added without extensive human interaction.

In chapter 7.4 a limited study was undertaken to investigate whether the presence of high DNA content cells ($>5C$) in cervical scrapes was paralleled by the presence of these cells in the tumor tissue. As this hypothesis could be confirmed in this investigation, it can be concluded that the finding of high DNA content cells in cervical scrapes is indeed a biological phenomenon and not an artefact due to sample preparation or to degeneration caused by exfoliation.

The measurement of DNA content is only one example of a nuclear measure which can be performed on automatically selected cell populations. Other nuclear measures such as those performed on chromatin texture, are not available yet on LEYTAS. Their potential significance has been investigated with the SAMBA 200 (SAMBA = System for Analytical Microscopy in Biomedical Applications) system as described in chapter 8. With this system a study was undertaken to distinguish LEYTAS detected cells in false positively classified

specimens from LEYTAS detected cells in true positively classified specimens on the basis of nuclear texture. For this purpose, 30 cases were selected, all of them being positively classified by LEYTAS. Ten of these cases had a negative cytological diagnosis (false positive cases), ten cases had a cytological diagnosis of dysplasia (mild or moderate) and 10 cases were positively diagnosed. Cell selection was also performed on SAMBA, by creating a program which resembled LEYTAS selection. Artefacts were eliminated visually. Nuclei of selected cells were analyzed using some of the SAMBA nuclear parameters. These included 4 geometrical parameters, 5 densitometrical parameters, 4 texture parameters computed from the co-occurrence matrix and 5 texture parameters computed from the run length section matrix. About 20 intermediate cell nuclei per specimen were also measured to serve as reference cells.

All cells selected in the negative specimens were combined in one set of cells named TNR (Total cells in Negative specimens after Rescaling), cells from the dysplasia and positive specimens were combined in TDPR (Total cells in Dysplasia and Positive specimens after Rescaling). A supervised classification is applied (linear discriminant analysis) to discriminate between the different cell types. Using TNR versus TDPR as the learning set, all cells from the different specimens were classified according the extracted parameters. The most important parameter proved to be the mean IOD (Integrated Optical Density). Using only this parameter, 8 of the 9 negative specimens could be discriminated from all 20 dysplasia and positive specimens. The best discrimination was obtained using a combination of 7 parameters (including texture and densitometry parameters). All negative specimens could be discriminated from all dysplasia and positive specimens. This discrimination proved to be statistically significant.

From these results, although obtained on a limited set of specimens, it can be concluded that the present false positive rate of LEYTAS can be reduced significantly when other nuclear parameters such as the mean IOD and parameters computed from the run length matrix (the second important parameter) are used on the automatically selected cell population.

Conclusion.

Based on the investigations and results described in this thesis, we are of the opinion that automated image analysis will be a realizable entity in a clinical setting for the near future. Speed and cell selection efficiency are presently within acceptable limits. Furthermore it is to be expected that the price versus performance ratio of automated systems will continue to drop. The main drawbacks at present are the elaborate procedures that are necessary for sample preparation and the extreme demands that are put to a diagnostic machine as defined by the International Academy of Cytology.

In contrast to what was expected from automated diagnosis, automation will not promote unemployment but it will stimulate the education of well trained cytotechnologists, who must be able to evaluate the machine selected cases. Their work will be more interesting, as the large number of negative specimens will no longer require monotonous visual screening. Only the specimens with a machine positive classification will have to be further evaluated, which, using LEYTAS as the screening system, will be a highly interactive procedure due to its display and relocation facilities.

Résumé.

Ce mémoire de thèse présente une méthode de diagnostic des lésions pré-malignes et malignes du col de l'utérus, fondée sur l'utilisation d'un système automatique d'analyse des frottis cervico-vaginaux. Il y a quinze ans environ, l'intention de détecter et de traiter toutes les lésions précancéreuses et cancéreuses du col de l'utérus s'est manifestée dans les pays occidentaux, et a été soutenue par les mouvements de libération de la femme. La réalisation d'un programme de dépistage de masse était cependant gêné par le manque de cytotechniciens suffisamment entraînés. A cette époque, les problèmes de l'emploi n'étaient pas considérés comme une difficulté économique majeure, si bien que la solution envisagée pour pallier le manque de cytotechniciens avait conduit au développement de méthodes automatiques de dépistage. En outre, la qualité du dépistage visuel n'était pas aussi bien étudiée qu'elle ne l'est aujourd'hui, c'est pourquoi l'instrument envisagé était un système pouvant réaliser le dépistage avec une précision équivalente à celle des cytotechniciens mais de façon plus rapide. Il n'y a que 5 ou 10 ans que les spécifications de l'analyse automatique et des systèmes correspondant ont été définies avec plus de précision. Pendant cette dernière décennie le taux de faux négatifs commis sur les préparations conventionnelles, dans les laboratoires de cytologie, a été évalué à environ 25% et a été publiés en relation avec le taux d'incidence des cancers du cervix. Ce pourcentage de faux négatifs a provoqué un changement des qualités requises pour un système de dépistage: la précision est devenue plus importante que la rapidité. Dans un rapport publié en 1983, à la demande du gouvernement allemand, le taux maximum de faux négatifs acceptable de la part d'une machine pour la diagnostic des dysplasies sévères et des lésions malignes a été fixé à 2%. L'Académie Internationale de Cytologie a même défini le taux de faux négatifs de la façon suivante: le système ne doit pas marquer quelque spécimen négatif que se soit qui contienne des cellules malignes. En d'autres termes, le système doit être plus performante que le dépistage visuel. Ces restrictions très sévères ont joué un rôle majeur dans le développement et l'évolution du système d'analyse LEYTAS comme le montre ce mémoire.

L'objectif principal des travaux décrits dans ce mémoire a été le diagnostic des lésions malignes et pré-malignes du col utérin avec une haute sensibilité, c'est-à-dire un taux très bas de faux négatifs, par comparaison avec les résultats obtenus dans les laboratoires pratiquant les diagnostics conventionnels. Par contre, une spécificité meilleure que celle obtenue dans les laboratoires conventionnels est difficile à atteindre puisque le taux de faux positifs, commis dans les diagnostics visuels, est inférieur à 1%. Cependant, le nombre de faux positifs, commis par un système automatique ne doit pas être élevé au point de rendre cet instrument économiquement injustifiable par rapport à un cytotechnicien. De plus, le temps nécessaire pour la classification automatique doit être du même ordre de grandeur que le temps nécessaire pour le diagnostic visuel.

Une difficulté en analyse automatique des images pour le diagnostic des spécimens cervico-vaginaux réside dans la complexité des frottis utilisés de façon conventionnelle selon la coloration de Papanicolaou. Puisque les systèmes disponibles actuellement ne sont pas capables de reconnaître les différents constituants cellulaires de la même façon que l'oeil humain, l'analyse automatique des cellules requiert des méthodes préparatives originales par rapport aux méthodes conventionnelles utilisées en cytologie. A cette fin, une méthode a été développée pour réduire le nombre de cellules chevauchantes, et pour réduire la variation de l'épaisseur des préparations. Cette procédure est présentée dans le chapitre 3. Deux types de matériel cytologique ont été utilisés séparément: d'une part du matériel fraîchement recueilli; d'autre part des frottis confectionnés à partir de matériel inclus

dans la paraffine. La préparation du matériel frais commence avec l'échantillonnage des cellules cervicales prélevées à l'aide d'un applicateur. Cet applicateur est ensuite immergé dans une solution conservatrice contenant de l'éthanol à concentration finale de 25%. Dans cette solution, les cellules peuvent être conservées plusieurs jours à la température ordinaire ce qui permet leur transmission par la poste. L'étape suivante de la préparation comporte la dissociation de l'échantillon à l'aide de seringues et l'estimation de la concentration en cellules par un dispositif de mesure néphélométrique. Si nécessaire, la suspension de cellules est diluée, puis les cellules sont déposées sur une lame microscopique au moyen d'une centrifugeuse développée à cet effet. Afin d'augmenter l'adhérence des cellules sur le verre, la centrifugation est réalisée avec une force centrifuge élevée sur des lames préalablement recouvertes de polylysine. Enfin les préparations sont séchées à l'air et conservées au réfrigérateur jusqu'au moment de la coloration. La préparation de frottis à partir de matériel inclus dans la paraffine consiste à découper des tranches épaisses (50 μ m) qui sont déparaffinées dans le xylène puis réhydratées et recueillies dans du PBS. Les tissus sont incubés dans une solution à 0.05% de pronase à 37 °C et la dissociation est favorisée par des remises en suspension intermittentes. Après lavage avec du PBS froid, l'échantillon est filtré afin d'éliminer les agrégats et les cellules qui passent à travers le filtre sont déposées par centrifugation sur une lame de microscope.

Afin de permettre la mesure du contenu en ADN cellulaire par l'analyse automatique, une référence est nécessaire; à cet effet, des érythrocytes de truite contenant 80% du taux diploïde d'ADN chez l'homme, sont centrifugés en même temps que les cellules de l'échantillon sur la même préparation mais à un endroit différent.

Plusieurs préparations peuvent être faites à partir d'un seul prélèvement, de sorte que différentes techniques de coloration peuvent être utilisées (voir chapitre 3.3). Le protocole habituel consiste à colorer une préparation par la méthode conventionnelle de Papanicolaou et une autre par l'acridine Feulgen SITS (AFS). La coloration AFS a été développée pour respecter les contraintes de contraste du système tout en permettant l'observation visuelle. La méthode est fondée sur l'utilisation de deux colorants: l'un quantitatif (acridine qui colore l'ADN comme la réaction de Feulgen), l'autre qualitatif (SITS) qui colore les protéines cellulaires de façon non stoechiométrique. Dans la coloration AFS les deux colorants peuvent être visualisés séparément en raison de la différence de leurs propriétés spectrales: l'absorption maximale de l'acridine est à 466 nm et celle du SITS est à 365 nm. Avec le système LEYTAS pour lequel cette coloration a été mise au point, seule l'image colorée à l'acridine est analysée à la longueur d'onde d'absorption maximale de 466 nm. A cette longueur d'onde le SITS n'absorbe pas la lumière et le caractère quantitatif de l'acridine peut être exploité correctement. L'utilisation du SITS est intéressante pour l'observation complémentaire de la morphologie cellulaire et en particulier l'évaluation de la quantité de cytoplasme, l'observation des nucléoles, le degré de différenciation. La fluorescence bleue du SITS peut être visualisée en utilisant un faisceau excitateur UV. Pour contrôler la stabilité du Papanicolaou et de la coloration AFS pendant une longue période, des mesures microdensitométriques ont été réalisées sur 42 séries de colorations. Le coefficient de variation moyen par lame était de 9.4% pour le Papanicolaou et 4.7% pour la coloration AFS, alors que la variation entre lames (ou coefficient de variation de la densité optique moyenne par lames) atteignait 9.2% et 5.8% respectivement. Il a été conclu que la bonne reproductibilité de la coloration AFS la rendait utilisable pour l'analyse d'images automatique. Nous avons décrit une troisième méthode de coloration

pouvant être utilisée à la fois pour l'analyse automatique et pour l'analyse conventionnelle. Bien que ce mémoire de thèse concerne principalement l'analyse de préparations confectionnées à partir de suspensions de cellules, une étude préliminaire a cependant été réalisée sur des frottis conventionnels. Dans ce cas, l'analyse ne requiert qu'une seule lame sur laquelle sont réalisées à la fois l'analyse d'images et l'analyse visuelle. Dans un premier temps, le spécimen est coloré par la gallocyanine et analysé par le système. Après cette analyse, les frottis sont contre-colorés par la méthode de Papanicolaou en n'utilisant que l'éosine et l'orangé G qui entrent dans la composition des colorants cytoplasmiques. Les images qui en résultent combinent donc la coloration bleutée de la gallocyanine avec la coloration habituelle des cytoplasmes; ces images sont difficilement distinguables de celles obtenues par la coloration de Papanicolaou à base d'hématoxyline comme colorant nucléaire. Par ailleurs, le système peut analyser la densité nucléaire sans être gêné par la variabilité éventuelle de la coloration cytoplasmique.

Le chapitre 4 décrit le système d'analyse d'images automatique utilisé: LEYTAS. Deux versions du LEYTAS ont été développées au cours de ce travail et se distinguent à la fois par leurs caractéristiques optiques et par le système informatique associé. En ce qui concerne le système optique, LEYTAS 1 comporte un microscope conventionnel (bien que presque complètement automatisé) alors que le microscope du système LEYTAS 2 a été spécifiquement construit pour l'analyse d'image. Dans ce dernier, un objectif à faible grandissement et grande ouverture permet d'obtenir des champs microscopiques de $500 \times 500 \mu\text{m}$, avec une résolution de $1 \mu\text{m}$ par pixel à basse résolution. Les systèmes LEYTAS 1 et LEYTAS 2 utilisent une caméra plumbicon de haute qualité comme capteur. Les changements automatiques de grandissement dans le système LEYTAS 1 sont réalisés, sous commande logique, par la rotation d'un projectif disposé entre caméra et objectif. Au contraire le système LEYTAS 2 dispose de 2 caméras qui acquièrent des images à deux grandissements différents. Ainsi, la détection rapide des cellules peut être réalisée à faible grossissement et chaque objet détecté peut être centré dans le champ du microscope pour que son image soit acquise à haute résolution par la seconde caméra. La mise au point automatique est réalisée grâce au déplacement de la platine du microscope dans le système LEYTAS 1, et grâce au mouvement de l'objectif dans le système LEYTAS 2. En ce qui concerne le système d'analyse d'image, LEYTAS 1 est connecté à un analyseur TAS (Texture Analysis System, Leitz), et le LEYTAS 2 est associé à un MIAC (Modular Image Analysis Computer, Leitz). Les deux versions, LEYTAS 1 et LEYTAS 2, ont été construites de telle façon que l'utilisateur puisse obtenir des informations précises sur le déroulement du traitement et de l'analyse des images réalisées en routine. Les logiques du TAS offrent elles-mêmes la possibilité de suivre chacune des transformations qui constituent l'analyse, ce qui présente un avantage certain et une aide au développement et à la mise au point des programmes. De plus, une mémoire image en niveau de gris, de 4 bits par point dans la version LEYTAS 1, et 8 bits par point dans la version LEYTAS 2, permet le stockage des images des objets ou cellules sélectionnés et permet ainsi leur visualisation en fin d'analyse. L'inspection visuelle sur le moniteur de contrôle, qui peut afficher en même temps 16 images d'objets considérés comme des alarmes, offre la possibilité d'une interaction rapide entre l'opérateur et le système.

Cette interaction peut être exploitée pour éliminer, parmi les objets retenus, ceux qui correspondent à des artefacts, et pour examiner rapidement si les objets retenus comme anormaux correspondent effectivement à des cellules pathologiques. En dehors de cette méthode d'utilisation interactive des systèmes, un re-positionnement des alarmes dans le champ du microscope est possible. Ce re-positionnement est commandé automatiquement par les

logiques du système sur la base des adresses x et y des objets sélectionnés.

La plupart des méthodes d'analyse d'image utilisées dans cette étude sont fondées sur des transformations itératives. Une revue des transformations utilisées est donnée dans le chapitre 4.3; les programmes correspondants ont été écrits par Meyer (Centre de Morphologie Mathématique de Fontainebleau). Un algorithme de segmentation des images nucléaires a été implémenté, et se fonde sur la détection des zones de gradient. La transformation 'chapeau haut de forme' a été appliquée pour sélectionner, parmi les cellules, celles dont les paramètres correspondent à une quantité élevée d'ADN. Cette transformation combine différents seuils de niveaux de gris avec une estimation de la surface des zones seuillées afin de sélectionner les cellules sur la base de leur taille et du contraste nucléaire par rapport au fond. Deux combinaisons de seuils sont utilisées actuellement et diffèrent à l'égard du contraste et des tailles retenues. Les variables de taille et de niveau de gris correspondant à ces seuils ont été déterminées à partir d'un lot d'apprentissage de 150 frottis environ et en utilisant une méthode séquentielle de test. Le lot d'apprentissage comportait exclusivement des spécimens négatifs et positifs (dysplasie sévère et lésions plus malignes). Aucun spécimen avec un diagnostic cytologique de dysplasie légère ou modérée n'a été retenu dans ce lot d'apprentissage en raison du peu de fiabilité de tels diagnostics et en raison de la réversibilité potentielle de ces dysplasies. Deux combinaisons de seuils ont été utilisées, l'une dite à haut niveau (HL) et l'autre dite à bas niveau (LL). Les seuils à haut niveau ont été optimisés afin de ne détecter aucun noyau ou presque aucun noyau dans les frottis négatifs, mais pour détecter des noyaux isolés dans la plupart des frottis positifs. Bien que la combinaison HL apparaisse hautement sensible aux artefacts, le nombre de noyaux sélectionnés par ces seuils est généralement faible. Ainsi la probabilité de manquer des noyaux anormaux reste élevée. Pour cette raison la combinaison de seuils à bas niveau a été ajoutée pour sélectionner plus de cellules dans les spécimens positifs, les seuils LL acceptant en effet plus de cellules isolées dans les spécimens positifs mais également dans les spécimens négatifs. Seuls les objets ayant résisté à la transformation 'chapeau de haut forme' sont soumis à différentes procédures de rejet automatique des artefacts en utilisant une structure hiérarchique de décision. Ainsi, les objets détectés ne parcourent l'arbre que lorsque les étapes de rejet des artefacts ont accepté ces objets comme des noyaux isolés possibles. Les deux premières transformations 'chapeau de haut de forme' sont réalisées pour une élimination rapide des artefacts sur la base de la taille et du niveau de densité des noyaux; elles sont suivies par des transformations évaluant la forme des noyaux. Toutes ces transformations sont réalisées sur la totalité du champ du microscope. Finalement, un paramètre dérivé de 'l'énergie de courbure' et d'un calcul des concavités et des convexités de l'objet, est mesuré à partir du contour des objets considérés comme noyaux isolés.

Dans le chapitre 4.3.3, la performance des différentes étapes de l'analyse d'images sont présentées et discutées. Les résultats obtenus montrent que 67% des cellules visuellement anormales dans un spécimen sont effectivement sélectionnées par la succession de ces transformations. Parmi les objets sélectionnés par la transformation 'chapeau haut de forme' les noyaux isolés représentent 46%. Les algorithmes de rejet des artefacts, fondés sur des transformations successives, éliminent 79% des artefacts parmi les objets sélectionnés par la transformation 'chapeau haut de forme', alors que 10% seulement des noyaux isolés sont rejetés par cette procédure. Les transformations qui offrent le meilleur résultat dans le rejet des artefacts, sont celles qui se fondent sur le calcul de la bissectrice conditionnelle. Après la procédure de rejet des artefacts, les noyaux isolés représentent 79% de l'ensemble des objets sélectionnés. Les contours de ces objets sont

testés, noyau par noyau, sur la base d'un paramètre dérivé de l'énergie de courbure qui élimine 38% des artefacts restant et 3% des noyaux isolés.

Dans la dernière partie du chapitre 4, le programme d'analyse global des cellules est décrit; il permet de caractériser toutes les cellules sur la base de leur taille nucléaire et de leur densité optique intégrée, par opposition au programme de dépistage automatique qui ne s'intéresse qu'à la sélection et au comptage des objets considérés comme alarmes.

Dans le chapitre 5, la fréquence des noyaux détectés par les combinaisons de seuils HL et LL, et la fréquence des alarmes sont analysées sur une série de 972 frottis. Les résultats obtenus montrent que le nombre des cellules sélectionnées à bas niveau, ainsi que le nombre des cellules sélectionnées à haut niveau sont significativement différents entre les spécimens négatifs, les spécimens présentant une dysplasie légère ou modérée, et les spécimens présentant une dysplasie sévère ou une lésion maligne. Le nombre de cellules détectées à bas niveau permet une distinction plus significative que le nombre de cellules sélectionnées à haut niveau. En outre, une comparaison a été réalisée entre le nombre d'objets détectés à haut niveau et à bas niveau par le système LEYTAS et le nombre de cellules anormales comptées visuellement dans différents degrés de dysplasie. Bien que les méthodes de comptage diffèrent selon les travaux considérés, les résultats obtenus par le comptage automatique des alarmes varient dans le même sens et avec le même ordre de grandeur que les résultats obtenus visuellement.

Dans la dernière partie de ce chapitre, les nombres absolus et relatifs d'alarmes ont été analysés; dans ce cas, aucune sélection visuelle n'a été réalisée. Malgré la fréquence élevée des alarmes artefactuelles, des différences significatives (au seuil de 99%) ont été obtenues entre les histogrammes cumulatifs des échantillons négatifs et les échantillons positifs (test de Kolmogorov Smirnov). Un seuil de décision, fondé sur le nombre absolu et le nombre relatif d'alarmes, a donc été déterminé et a permis un taux de classification satisfaisant ne faisant apparaître que quelques échantillons positifs, faussement classés négatifs, tout en conservant le taux d'échantillons faussement classés positifs dans des limites acceptables.

Le chapitre 6 présente les résultats de la classification d'une série de 1459 frottis analysés en utilisant le seuil déterminé précédemment: tout échantillon ayant plus de 10 alarmes et plus de 0.3% des objets détectés classés comme alarmes est considéré comme positif. En utilisant ce seuil le taux de faux positifs obtenu était 13% pour les spécimens négatifs et de 49.3% pour les spécimens inflammatoires. Les faux négatifs variaient entre 15.8% pour les spécimens classés comme dysplasie légère, 8.5% pour les spécimens classés dysplasie modérée et 0.3% (1/321) pour les spécimens classés positifs. Les spécimens négatifs et les spécimens inflammatoires ont été analysés séparément dans cette série (frottis provenant de consultations gynécologiques de patientes symptomatiques). Pour estimer le taux de faux positifs dans un programme de dépistage au niveau de la population, une série de 563 spécimens obtenus d'un centre de contrôle de naissances ont été analysés. Le taux de faux positifs dans cette série, incluant à la fois les négatifs et les spécimens inflammatoires, était de 16%. La réduction de ce taux de faux positifs à 11% a été possible par une interaction rapide, permettant de supprimer les artefacts présentés en fin d'analyse. Le taux de faux négatifs, parmi les spécimens morphologiquement positifs, est très bas (0.3%), et remplit les critères formulés par différentes instances. Le taux de faux négatifs, dans le cas des dysplasies légères et modérées, est plus élevé et dû, en partie, à une mauvaise conservation des cellules; dans ce cas le diagnostic conventionnel de dysplasie est plutôt remplacé par un diagnostic d'atypie. Les dysplasies légères sont d'ailleurs souvent diagnostiquées de façon ambiguë. Quoi qu'il en soit, le programme d'analyse

de la totalité du spécimen s'est révélé plus sensible que le diagnostic conventionnel à l'analyse des frottis dysplasiques. Des tests de reproductibilité du programme de dépistage ont montré qu'aucun des spécimens n'a changé de classification après renouvellement des analyses. Les analyses ont été renouvelées sur tous les spécimens positifs pour lesquels les critères de décision étaient proches de la frontière de décision. Il a été montré également que l'analyse peut être renouvelée jusqu'à un an après la coloration sans conséquence sur la classification à condition que les spécimens aient été conservés à l'obscurité et à 4 C.

En comparant différentes préparations d'un même échantillon, seules de petites variations ont été observées; ces variations sont compatibles avec les différences statistiques entre aliquots provenant d'un échantillon de cellules correctement dispersées. Une seule différence de classification a été observée entre différentes préparations d'un même échantillon: il s'agissait du seul échantillon faussement classé négatif: l'une des préparations a été classée positive et l'autre négative. Toutes les préparations des autres échantillons positifs dont les critères étaient près du seuil de décision, ont toutes été classées positives.

Les travaux que nous avons réalisés montrent que les méthodes requises pour la préparation des échantillons peuvent être considérées comme limitantes de l'applicabilité dans la pratique clinique. Une étude a donc été commencée pour analyser des préparations conventionnelles. A cette fin, la méthode de coloration par la galloxyanine a été utilisée. Dans le chapitre 6.4 une étude de faisabilité concernant 32 échantillons négatifs, quatre échantillons dysplasiques et un échantillon positif de carcinome in situ a été réalisée. Nous n'avons pas obtenu de confusion concernant le nombre absolu et le nombre relatif des alarmes entre les échantillons négatifs et les échantillons positifs. Par contre l'un des échantillons diagnostiqués dysplasie légère présentait un nombre d'alarmes du même ordre de grandeur que les échantillons négatifs. Le programme permettant l'analyse des frottis conventionnels sera développé et optimisé sur des séries plus nombreuses d'échantillons.

Les résultats obtenus dans l'analyse de la totalité des cellules sont présentés dans le chapitre 6.5, en particulier pour ce qui concerne la classification des frottis centrifugés. Dans une étude de faisabilité concernant 109 échantillons les résultats de l'analyse de la totalité des cellules ont été comparés avec ceux obtenus par le programme de dépistage. Un taux de détection plus élevé a été obtenu dans le cas des dysplasies légères et modérées ainsi qu'un taux de faux positifs plus bas. Actuellement l'applicabilité du programme d'analyse de la totalité des cellules est limitée par sa vitesse (plusieurs heures pour l'analyse de 1 cm²). L'implémentation sur le LEYTAS 2 et l'analyse de la totalité des cellules dans un nombre limité de champs du microscope en plus du programme de dépistage devrait permettre d'atteindre un temps d'analyse acceptable.

Dans le chapitre 7, les performances du système LEYTAS sont données à l'égard de la mesure du contenu en ADN. Ces mesures peuvent être réalisées sur les cellules d'échantillons qui ont été automatiquement sélectionnées à l'aide du programme de dépistage. Les images en niveau de gris de toutes les alarmes sont stockées et peuvent être utilisées pour visualiser et éliminer tous les artefacts qui ne l'ont pas été automatiquement. Chaque cellule est repositionnée et son contenu en ADN (densité optique intégrée) est ajusté à l'égard d'une valeur de référence. Dans le cas de LEYTAS 2 les mesures du contenu en ADN peuvent être réalisées simultanément avec le programme de dépistage grâce à un processeur auxiliaire; grâce à ce dispositif, le repositionnement des cellules n'est plus nécessaire. Cette méthode de mesure peut naturellement être appliquée sur les cellules sélectionnées par les niveaux HL et LL du programme de dépistage. Une sélection, au hasard, des

cellules peut également être obtenue en ajustant les seuils de la transformation 'chapeau de haut forme' de telle sorte que toutes les cellules épithéliales soient sélectionnées. Les résultats obtenus montrent que les cellules ayant un contenu élevé en ADN (supérieure à 5C) sont absentes ou très peu fréquentes dans les histogrammes obtenus à partir de cellules sélectionnées au hasard. Par contre ces cellules sont présentes en plus grandes proportions lorsque les cellules à mesurer ont été sélectionnées sur la base des seuils LL ou HL. La transformation 'chapeau haut de forme' peut être utilisée pour estimer de façon grossière la quantité en ADN, cette estimation de la quantité minimale d'ADN permettant aux cellules d'être sélectionnées par les seuils LL et HL correspondent respectivement de 3C et 5C.

Dans le chapitre 7.3, quelques exemples d'histogrammes de distributions des cellules en fonction de leur contenu en ADN sont présentés pour des spécimens ayant différents types de diagnostics cytologiques. Dans les histogrammes des spécimens anormaux (dysplasie ou malignité) on peut observer une tendance vers l'augmentation de la fréquence de cellules aneuploïdes dans la région supérieure à 4C. Les histogrammes des spécimens inflammatoires ou présentant une infestation virale, présentent une tendance à fournir des pics, dans les valeurs polyploïdes, sans beaucoup de cellules dans la région supérieure à 4C. Le temps moyen pour obtenir un histogramme d'ADN, en utilisant le système LEYTAS 2, est inférieur à 5 mn. Ceci signifie que les mesures automatiques, sur de grand nombres de cellules peuvent être actuellement envisagées par l'analyse d'image avec une vitesse approchant celle obtenue en cytométrie en flux. Les avantages de la cytométrie par analyse d'image résident dans le rejet des artefacts. Alors que, le signal obtenu dans la région à contenu élevé en ADN par cytométrie en flux, est fréquemment dû à des artefacts, les histogrammes obtenus à l'aide du système LEYTAS représentent essentiellement des mesures obtenues à partir de cellules isolées. Ces résultats montrent que les études de contenu en ADN essentiellement tournées vers la détermination précise des anomalies du contenu en ADN de la population cellulaire peuvent être complétées par des informations concernant des cellules aneuploïdes moins fréquentes.

Dans le chapitre 7.4 une étude a été entreprise afin de rechercher si la présence des cellules ayant un contenu élevé en ADN (supérieur à 5C) dans les frottis cervicaux, était en relation avec la présence de telles cellules dans les tissus tumoraux. Cette corrélation a été confirmée et nous avons conclu que la présence de cellules à contenu élevé en ADN dans les frottis cervicaux est un phénomène biologique et non pas un artefact dû à l'échantillonnage ou à une dégénération cellulaire provoquée par l'exfoliation.

La mesure de la quantité d'ADN n'est qu'un exemple des différents paramètres nucléaires qui peuvent être mesurés sur des cellules sélectionnées automatiquement. D'autres mesures peuvent être réalisées concernant la texture de la chromatine et ne sont pas actuellement disponibles sur le système LEYTAS. Leur signification a été étudiée à l'aide du système SAMBA 200 (SAMBA= System for Analytical Microscopy in Biomedical Applications, TITN, Grenoble, France). Ce système est décrit dans le chapitre 8. A l'aide de cet instrument, une étude a été entreprise pour tenter de discriminer les cellules détectées par LEYTAS dans les échantillons faux positifs et les échantillons positifs sur la base des paramètres de texture. A cette fin, 30 cas ont été sélectionnés qui étaient classés positifs par le système LEYTAS; 10 de ces cas avaient un diagnostic cytologique négatif, 10 avaient un diagnostic cytologique de dysplasie légère ou modérée, et 10 cas étaient positifs. La sélection des cellules a été réalisée directement sur le système SAMBA en créant un programme du même type que le programme de sélection des alarmes utilisé dans le système LEYTAS et les artefacts ont été éliminés visuellement. Les noyaux des cellules sélectionnées ont été analysés en

utilisant quelques paramètres nucléaires calculés par le système SAMBA: quatre de ces paramètres décrivaient la géométrie, cinq décrivaient la densitométrie, quatre décrivaient la texture à partir du calcul des matrices de co-occurrence et cinq paramètres décrivaient la texture calculée à partir des matrices de longueurs de section. Environ 20 noyaux de cellules intermédiaires par échantillon ont été mesurés et utilisés comme cellules de référence. Toutes les cellules sélectionnées dans les échantillons négatifs ont été combinées en un seul lot appelé TNR (Total cells in Negative specimens after Rescaling); les cellules obtenues à partir des échantillons dysplasiques et positifs ont été réunies en un seul lot nommé TDPR (Total cells in Dysplastic and Positive specimens after Rescaling). Une classification multidimensionnelle supervisée (analyse discriminante linéaire) a été utilisée pour rechercher les différences entre les cellules négatives et les cellules positives. La discrimination entre les cellules TNR et les cellules TDPR a été réalisée à partir du paramètre moyenne de la densité optique, ce seul paramètre permet de séparer 8 échantillons négatifs (parmi 9) des vingt échantillons dysplasiques ou positifs. La meilleure discrimination entre négatifs et positifs a été obtenue en utilisant une combinaison de sept paramètres représentant la texture et la densitométrie nucléaire. A l'aide de ces sept paramètres, tous les échantillons négatifs ont pu être discriminés des échantillons dysplasiques et positifs. Cette discrimination s'est révélée hautement significative. Bien que ces résultats aient été obtenus sur un nombre limité d'échantillons, il est possible de conclure que le taux actuel de faux positifs commis par le système LEYTAS peut être réduit très fortement en utilisant des paramètres nucléaires tels que la densité optique moyenne et les paramètres calculés à partir des matrices de co-occurrence et de longueur de section.

CONCLUSION.

Les travaux présentés dans ce mémoire démontrent que l'automatisation de l'analyse de frottis cervico-vaginaux est réalisable en laboratoire clinique à court terme. La vitesse et l'efficacité de la sélection et de l'analyse des cellules sont dans des limites acceptables; de plus, il est attendu que le prix encore élevé des systèmes d'analyse d'image continue à diminuer. Le principal inconvénient actuel dans l'application de ces méthodes est la nécessité de réaliser des préparations selon un protocole complexe et standardisé. Un autre inconvénient majeur résulte des contraintes de plus en plus sévères, imposées notamment aux Etats Unis, aux systèmes de diagnostic automatique.

Enfin, l'idée peut être émise que l'analyse automatique des échantillons ne sera pas à l'origine d'un sous-emploi des cytotechniciens; au contraire, l'interaction entre l'instrument et les cytotechniciens devrait rendre leur travail plus intéressant, plus efficace, et moins fastidieux puisque déchargé de l'analyse d'un grand nombre de spécimens négatifs. Seuls les spécimens classés positifs par le système doivent être contrôlés et diagnostiqués par les cytotechniciens en utilisant (avec LEYTAS) les facilités d'affichage des cellules détectées comme alarmes.

De la lecture des rapports de :

- Monsieur C. DA LAGE

et

- Monsieur F. MEYER


il ressort que rien ne s'oppose à la soutenance de la thèse de :

Madame KULKER Anna épouse VAN DRIEL

devant un jury comprenant * :

- M. J.S. PLOEM - Professeur, Département Cytochimie et Cytométrie
Sylvius Laboratories - Leiden - Pays Bas
- M. G. BRUCAL - Professeur, USTMG
- M. J.M. CHASSERY - Chargé de Recherche, C.N.R.S., GRENOBLE
- M. P. CHIBON - Professeur, USTMG.
- M. C. DA LAGE - Professeur, Lab. Histologie, Embryologie et Cytologie
Hôpital Necker, Paris.
- M. F MEYER - Maître de Recherche - Ecole des Mines de Paris.

conforme à l'arrêté du 5 Juillet 1984


J. VALENTIN
J. J. PAYAN
Responsable

des Etudes Doctorales de l'USMG

* Indiquer grade, fonction, université.

